UNIVERSITY OF OTTAWA
FACULTY OF SCIENCE
DEPARTMENT OF CHEMISTRY
OTTAWA-CARLETON CHEMISTRY INSTITUTE

Co(II) Based Magnetic Systems

Part I Spin Crossover Systems and Dendritic Frameworks.
Part II Co(II) Single Molecule Magnets.

Ahmed M. S. Farghal
Hon. B.Sc., University of Ottawa, 2008

Thesis submitted to the Faculty of Graduate and Postdoctoral Studies
In partial fulfillment of the requirements for the M.Sc. degree in
Chemistry

Supervisor: Dr. Darrin Richeson

Abstract

This work comprises two main parts. The first part outlines our efforts to expand on the recent work of Gütlich *et.al.* by synthesizing Co(II) based spin crossover systems within a dendritic framework. We wanted to investigate the possibility of synthesizing different first generation, triazole containing dendrimers using "click" type reactions and their coordination ability with Co(II) ions. To this end we have had limited success mainly due to the numerous challenges in synthesizing a pure dendrimer product.

The second part details our efforts in the synthesis of a mononuclear Co(II) based single molecule magnet. This comes as an extension to recent reports by Chang and Long where they have successfully obtained mononuclear Fe(II) single molecule magnets by inducing structural distortions within the complexes to amplify the spin-orbit coupling. We postulated that the use of Co(II) in conjunction with a bulky ligand framework would lead to desirable magnetic properties. We chose the known bis(imino)pyridine ligand scaffold due to its rich chemistry and its interesting and unexpected coordination behaviour, as we have seen in previous research efforts by our lab. To this end we were successful in isolating and characterizing 4 compounds, and we have carried out detailed magnetic measurements on the two most magnetically interesting species.

Table of Contents

List of Tables

List of Figures

$$\chi T = \frac{Ng^2}{k}\frac{1+9e^{-2x}}{4(1+e^{-2x})} + \frac{2Ng^2\beta^2}{k}\frac{4+\frac{3}{x}(1-e^{-2x})}{4(1+e^{-2x})}$$

Where x=D/kT

Legend

M	Molar magnetization
H	Applied magnetic field
χ	Magnetic susceptibility
χ^D	Diamagnetic susceptibility
χ^P	Paramagnetic susceptibility
μ_{eff}	Effective magnetic moment
m_s	Electron spin quantum number
k_B	Boltzmann constant
S	Spin ground state
ΔE	Energy difference between m_s levels
C	Curie constant
θ	Weiss Constant
T	Temperature
$T_{1/2}$	Spin transition temperature
γ_{HS}	High spin fraction
γ_{LS}	Low spin fraction
T_c	Critical temperature
D	Zero field splitting parameter
U	Energy barrier to magnetic relaxation
T_B	Blocking temperature
E_B	Energy barrier hindering the free rotation of the magnetization.
O_h	Octahedral symmetry

χ'	In-phase magnetic susceptibility
χ''	Out-of-phase magnetic susceptibility
τ	Relaxation time
U_{eff}	Anisotropic energy barrier
g	Electron g-factor
N	Avogadro's number
B	Bohr magneton
HS	High spin
LS	Low spin
ac	Alternating current
dc	Direct current
Gn	Generation number
Dp	Degree of polymerization
ZFS	Zero field splitting
SCO	Spin crossover
NMR	Nuclear magnetic resonance
EPR	Electron paramagnetic resonance
SQUID	Superconducting quantum interference device
DFT	Density functional theory
QTM	Quantum tunnelling of magnetization
UV-Vis	Ultraviolet-visible light
MAO	Methyl alumoxane
SMM	Single molecule magnet
CuAAC	Cu(I) catalyzed alkyne-azide cycloadditions

phen	1,10-phenanthroline
tsa	salicylaldehyde thiosemicarbazone
PBE	Poly(benzyl)ether
Et-saoH_2	2-hydroxyphenylpropanone oxime
H_2pdm	2,6-pyridinedimethanol
H_3tpa^{Mes}	tris-mesityl tris(pyrrolylmethyl)amine
TPA	Tris(2-pyridylmethyl)amine
bppppa	*N*,*N*-bis[(6-phenyl-2-pyridyl)methyl]-*N*-[(6-pivaloylamido-2-pyridyl)methyl]amine
Trz	2,4,6-Tris(prop-2-ynyloxy)-1,3,5-triazine
^{t}Bu	t-Butvl Azide
Bn	Benzyl Azide

Acknowledgements

I cannot begin to describe the important role my parents and siblings have played in my life as a whole; they have always stood by me and provided me with a tremendous amount of love and support through even the toughest times. Also, my close friends who I have made during my time here, thank you for being family when family was so far away. For that I am truly grateful. Next I would like to acknowledge my supervisor Dr. Darrin Richeson and Co-supervisor Dr. Muralee Murugesu for everything that they have taught me about chemistry and life, this work would have not been possible without their help, support, advice and patience. I would also like to acknowledge all the professors, support staff and administrative staff in the Department of Chemistry, for enriching my learning experience, for always being there to lend a helping hand when I needed it and for their smiles which brightened even the darkest days. I also cannot forget my labmates, past and present. Titel, thank you for all of your help and for sharing many of your synthesis tricks. Ian, Jessica, Natalie and Dominique, you are all graduated now, but I will not forget the help, support and the great times spent. Sheila and Roger, thank you both for being great coworkers. Sarah and Nastaran, you have only recently joined our lab as a graduate student, and already you are proving yourselves to be a great addition to the Richeson group. Lastly, the undergrads and summer students, I hope your experience working with us was a great one. All the people acknowledged above, and those who I have missed, I would not be the person who I am today if it wasn't for you. Thank you.

This work is dedicated to my late grandparents. I know you are watching over me and I truly miss you.

Chapter 1

1.1 Introduction

Molecular magnetism is an area of research that deals with the magnetic properties of isolated molecules and assemblies of molecules. These molecules may contain one or more magnetic centres. Assemblies of molecules are in most cases found in molecular crystals and the assemblies arise from weak intermolecular interactions. These systems can also be built using a bottom-up approach, where larger molecules are built from smaller precursors, in a way that maximizes such intermolecular interactions and in turn yield bulk magnetic properties.

Over the last two decades, the concept of magnetism evolved from a macroscopic property of materials to a microscopic property that can be defined at the molecular level. Further, the observation of unique magnetic properties in things such as metalloprotein active sites, natural minerals and even biological organisms has garnered a great deal of attention from researchers in diverse areas such as synthetic inorganic chemistry, theoretical chemistry and physics, material science and even biology.[1]

Molecular magnetism as a field is very multidisciplinary. Firstly it involves synthetic chemistry. The main challenge that it poses for synthetic chemists lies in the synthesis of molecular systems with predictable magnetic traits. This has materialized in the form of novel inorganic compounds, coordination complexes, organic radicals as well as polymers utilizing

[1] Kahn, O.; Molecular Magnetism (1993); VCH Publishers Inc.

novel bridging groups. It is also important to realise that in order to access such systems with predictable magnetic properties, ideas from theoretical chemistry are very important. It is through theory that models to utilise and to understand the underlying mechanisms of such phenomena are constructed. In recent years, novel macroscopic and microscopic approaches have been utilized in the field of molecular magnetism, and these approaches originate from the most basic concepts of quantum mechanics. Interestingly, molecular magnetism can be one of the most straightforward applications of well known concepts of quantum mechanisms. The field has also allowed us to challenge many of these quantum mechanical concepts that are used in other fields such as the molecular orbital model, which in its simplest form cannot be used to fully understand the interaction between two magnetic centres.

Molecular and solid state physics have played a very pivotal role in the field of molecular magnetism. It would be inappropriate to deny that some of the earliest and most important discoveries in the field of molecular magnetism were in fact attributed to physicists. Names such as J. H. Van Vleck and P.W. Anderson could even be considered as the founding fathers of the field, and their contributions towards understanding the underlying principles and providing theoretical and mathematical models that explain observed magnetic properties are still in use to this day.

Molecular magnetism as a field also provides a crossing point between the areas of chemistry and biology. Many biological systems contain proteins with active sites possessing metal ions and numerous essential biological processes utilize these metalloproteins. An understanding of the magnetic properties of these systems as well as the interactions between

metal centres could bring to light the mechanisms of action of these specialized proteins in biological systems. Further, such an understanding would allow a more educated approach towards biomimetic synthesis of such systems, and their directed application for various purposes.

It is also important to mention that in the 21st century and with the emerging field of molecular electronics, the field of molecular magnetism has found its niche in terms of applicability. Molecular electronics can be defined as the use of certain molecular systems in electronic devices. The simplest example of such applicability arises from the ability of some magnetic systems to undergo spin transition. Such bistability of two magnetic states has allowed researchers to envision the potential application of such systems in devices such as data storage media.[1]

Clearly, the field of molecular magnetism still presents numerous challenges to researchers in various areas of the applied sciences. And with all of the recent progress that has been made in terms of understanding the magnetic properties of molecular systems as well as the synthesis of novel molecular systems exhibiting desirable traits as well as surpassing their predecessors in terms of performance, there is much to be learned.

This work represents some of my efforts to synthesize novel magnetic systems exhibiting both spin-crossover behaviour as well as single molecule magnet behaviour. This thesis will be divided into two major parts. The first will highlight my efforts in designing and synthesizing spin-crossover systems within a macromolecular, dendritic framework. The latter will deal with efforts to synthesize monometallic molecular complexes that exhibit single

molecule magnet behaviour. Having introduced the scope of the field as well as the focus of this thesis, it is now appropriate to explain some basic concepts that are used in the field.

1.2 Magnetization and Magnetic Susceptibility [2]

Consider 1 mol. of a molecular compound with a homogenous applied field H. The compound acquires a molar magnetization M, which is related to H by

$$\delta M/\delta H = \chi \qquad \text{(eq. 1)}$$

Where χ is defined as the molar magnetic susceptibility and has the units of cm^3mol^{-1}.

When the magnetic field is sufficiently weak, χ becomes independent of H, and we can write the relation

$$M = \chi H \qquad \text{(eq. 2)}$$

Often, the quantity of interest in molecular magnetism is χT, which is the product of the molar magnetic susceptibility and temperature, because it is an indicator of the type of magnetic interaction within a system.

[2] (a) Gatteschi, D.; Sessoli, R.; Villain, J.; Molecular Magnets (2006); Oxford University Press, Inc.; N.Y. (b) Murugesu, M.; Special Topics in Inorganic Chemistry: Molecular Magnetism (2009); Department of Chemistry; University of Ottawa

1.3 Diamagnetism, Paramagnetism and their Susceptibilities [2, 3]

Diamagnetic materials are those which possess only paired electrons. Diamagnetism is a property of all matter. This property arises from the interaction of electron pairs with the applied magnetic field, which generates a field opposing the applied field. Diamagnetic materials tend to move to areas of lowest field strength. The diamagnetic susceptibility is given by χ^D.

Paramagnetism arises from the presence of one or more unpaired electrons. The unpaired electron is essentially what makes a material exhibit magnetic properties. Paramagnetic materials are attracted to a magnetic field. Paramagnetic susceptibility is given by χ^P.

As stated above, diamagnetism is a property of all matter. It will always be present even when masked by the apparent paramagnetic nature of the material. Diamagnetic susceptibilities carry a negative sign and paramagnetic susceptibilities a positive sign. The observed magnetic susceptibility depends on the dominating contribution in a given material. For any molecular system, the observed magnetic susceptibility is given by

$$\chi = \chi^D + \chi^P \qquad \text{(Eq. 3)}$$

For a given molecular system, diamagnetic susceptibilities are essentially additive. The diamagnetic contributions for various atoms, ions and functional groups have been calculated and documented. However for modern molecular magnetism calculations, it is always assumed

[3] Morgenstern-Badarau, I.; Cocco, D.; Desideri, A.; Rotilio, G.; Jordanov, J.; Dupré, N.; J. Am. Chem. Soc. (1998); 108; 300.

that experimentally determined susceptibilities are corrected for the diamagnetic contributions. [1, 4]

1.4 Curie Paramagnetism [2]

In the early 1900's; the famous scientist Pierre Curie was able to show that in a paramagnetic substance with isolated magnetic sites, the magnetic susceptibility is inversely related to the temperature. This phenomenon has been used to explain the magnetic behaviour of many substances and is even applicable to more contemporary research efforts.

The simplest example to explain Curie paramagnetism lies in an isolated S=1/2 spin. At zero field the available m_s states (m_s=+1/2 and m_s=-1/2) are degenerate. When an external field is applied this degeneracy is lost and the energy levels split, with an energy difference between the levels denoted by ΔE. [4]

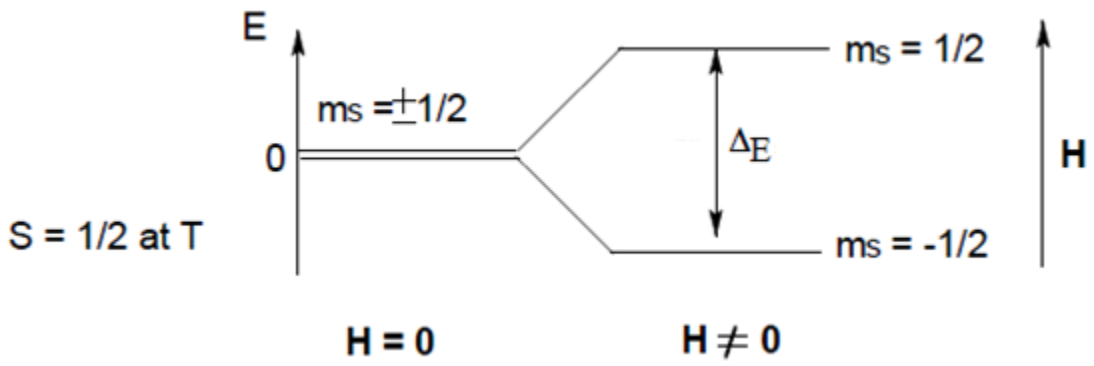

Figure 1.1. Splitting of m_s states in the presence of an applied field (H) for an isolated S=1/2 spin.

[4] (a) Bain, G. A.; Berry, J. F.; J. Chem. Ed. (2008); Vol. 85; No. 4; 532. (b) Carlin, R. L. Magnetochemistry (1986); Springer-Verlag: Berlin. (c) Drago, R. S. Physical Methods in Chemistry (1992); W. B. Saunders Company: Philadelphia.

Let us assume that the magnetization in the direction of the applied field is given by μ_n. The total molar magnetization (M) can then be defined as the sum of the individual magnetic moments in the direction of the applied field as weighted by their Boltzmann populations. As with any simple mathematical proportionality relationship, the magnetic susceptibility of the material is related to the temperature in an inversely proportional manner through a constant, known as the Curie Constant (C).

$$\chi = C/T \qquad \text{(Eq. 4)}$$

The resulting plot of χ vs. 1/T is a straight line passing through the origin. According to the Boltzmann distribution, at room temperature, there is enough thermal energy to result in a relatively equal population of the m_s states.

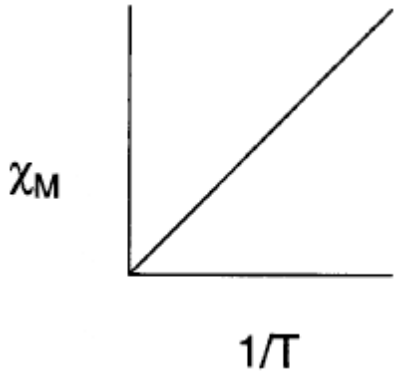

Figure 1.2. χ vs. 1/T plot showing the inversely proportional relationship between magnetic susceptibility and temperature.

The Curie law provides a good theoretical model when dealing with isolated spins. However in reality, numerous systems do not involve isolated or non-interacting spin carriers. In these cases the Curie law cannot be used to explain the observed magnetic behaviour.

1.5 Magnetic Interactions [2]

It becomes important at this point to define the differing types of magnetic interactions. As mentioned, numerous compounds exhibiting magnetic properties of interest possess two or more interacting paramagnetic metal centres.

In the absence of an applied magnetic field, most materials do not possess a net magnetic moment. However, many materials are historically known to exhibit magnetization, such as iron and cobalt, which are used in the fabrication of permanent magnets.

This magnetic behaviour is in fact a result of the interaction of paramagnetic metal centres in the bulk sample. This is an example of the first type of magnetic interaction that should be defined, and that is ferromagnetic interactions. In this type of magnetic interaction, the magnetic spins are all aligned in the direction of the magnetic field. It is this uniform alignment that gives permanent magnets their magnetic behaviour. Classically, scientists were only interested in understanding the bulk magnetic properties of materials they observed in nature such as in some minerals. However, with increased understanding of quantum mechanics as well as advances in theoretical modelling and instrumentation, interest has shifted towards molecular magnetism, which deals with the microscopic magnetic behaviour of a single molecule with more than one interacting metal centre.

The second kind of magnetic interactions is antiferromagnetic interactions. As the name suggests, antiferromagnetically coupled metal centres have their spins aligned in opposing directions. This results in a net magnetization of zero due to the spins cancelling each other out.

The third and final kind of magnetic interactions is known as ferrimagnetic interactions. Ferrimagnetic interactions, similar to antiferromagnetic interactions have the spins aligned in opposing directions. However, the interacting spins are of differing magnitudes. This results in a net magnetization in such materials.

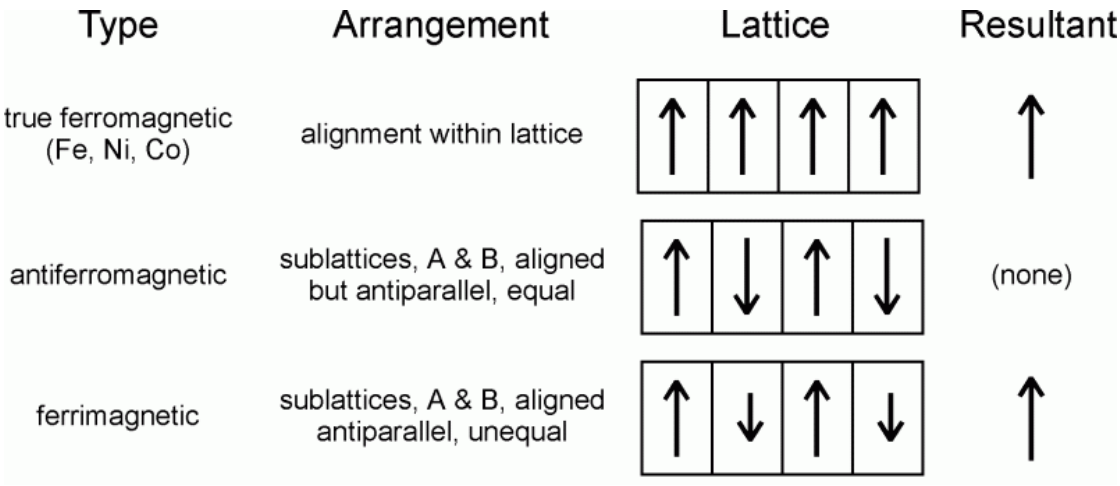

Figure 1.3. Schematic depicting the different types of magnetic interactions.[5]

1.6 Curie-Weiss Paramagnetism

Magnetic species, even if they are well separated, are rarely perfectly isolated from one another. As a result, it becomes necessary to define a theoretical model which takes into consideration the presence of interacting magnetic centres. The Curie-Weiss model was developed in order to account for these weak intermolecular interactions. The magnetic susceptibility in the case of weakly interacting magnetic species is mathematically defined as:

[5] Image retrieved from http://gravmag.ou.edu/mag_rock/mag_rock.html

$X = C/(T-\theta)$ (Eq. 5)

This is known as the Curie-Weiss Law where C is the Curie constant and θ is the Weiss constant. Plots of $1/\chi$ vs. T yield a straight line of slope C^{-1}. The intercept of this line gives both the sign and the value of the Weiss constant. The sign of the Weiss constant allows us to define graphically the type of interaction observed in the molecular system. A positive θ is indicative of a ferromagnetic interaction and a negative θ is indicative of an antiferromagnetic interaction.

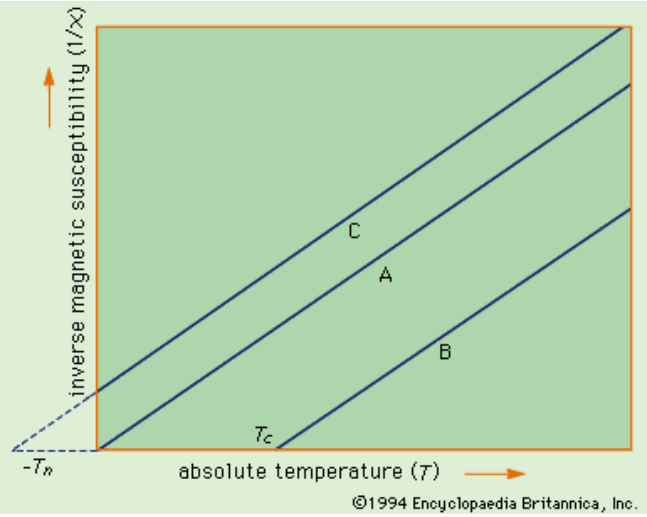

Figure 1.4. Graphical representation of the Curie-Weiss law for (A) Paramagnetic (B) Ferromagnetic and (C) Antiferromagnetic materials.[6]

In the form of a χT vs. T plot, a positive Weiss constant leads to an increase of χT on cooling and a negative Weiss constant leads to a decrease of χT on cooling. Similar to the Curie law, the magnetization is more pronounced at lower temperatures.

[6] *Curie–Weiss law: graphic representation*. Art. *Encyclopædia Britannica Online*. Web. 27 Jun. 2011. <http://www.britannica.com/EBchecked/media/1364/Plot-of-1chi>.

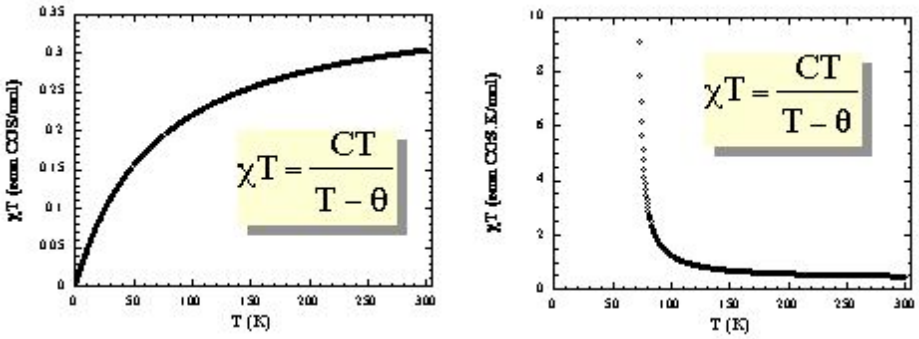

Figure 1.5. χT vs. T plots showing an antiferromagnetic interaction (left) and a ferromagnetic interaction (right).[2]

Chapter 2

Spin Crossover Systems and Dendritic Frameworks

2.1 Introduction

In terms of spin states, coordination compounds have historically been categorized into two types, exhibiting either a high spin state or a low spin state. It is this division that raised the question of whether it would be possible to transition between these two spin states. Other questions like the nature of this transition were also raised such as the nature of this transition as well as the possibility of influencing such a transition by external perturbation.[7]

Such questions were raised by Linus Pauling, during his attempts in understanding the nature of the chemical bond. He postulated that systems can exist which exhibit both types of spin states simultaneously, and that the ratios of both states would be determined by the energy difference between them.[8]

The possibility of such systems was soon realised in the pioneering work of Cambi and Szego[9]. They observed unusual magnetism of iron (III) dithiocarbamate derivatives, and recognized that there is in fact an interconversion of spin states as a result of variation in temperature. This has led to the definition of the spin crossover phenomenon and a rapid increase in the acceptance of and interest in understanding this phenomenon.

---

[7] Gütlich, P; Goodwin, H. A.; Top. Curr. Chem. (2004); Vol. 233 Spin Crossover in Transition Metal Compounds I; Springer-Verlag; Berlin Heidelberg.

[8] (a) Pauling, L.; J. Am. Chem. Soc. (1932); 54; 988. (b) Pauling, L.; The Nature of the Chemical Bond, 2nd ed. (1940); Oxford University Press.

[9] Cambi, L.; Szego, L.; Ber. Deutsch. Chem. Ges. (1931); 64; 167.

Later works on the magnetism of heme derivatives of iron (III) species and other porphyrin derivatives established that the spin crossover phenomenon does occur in natural systems. For certain species the intermediate value of the magnetic moment that was observed was attributed to a partially ionic and partially covalent nature of the bonding in these systems[10] The advent of the ligand field theory and its widespread acceptance by coordination chemists then led to attempts to define the spin crossover region for various d^4 to d^7 transition metal ions. Works by Busch and co-workers in the early 1960s attempted to define the spin crossover region for iron (II) and cobalt (II) ions and reported the first spin crossover complex for a cobalt (II) ion.[11] Similarly, Madeja and König undertook a systematic study in which they varied the anionic groups in iron (II) systems $[Fe_2(phen)_2X_2]$ ($X = Br^-$; Cl^-; SCN^-; N_3^-; OCN^-; $HCOO^-$; CN^-) in an attempt to define the spin crossover region for iron (II).[12] Simultaneously, studies on the iron (III) dithiocarbamate systems were extended and included an experiment that demonstrated the effect of pressure in influencing the spin state in spin crossover systems. This experiment was the first example of the application of pressure on the spin crossover phenomenon and predicted the favouring of the low spin state under a higher pressure.[13]

Presently, the field of spin crossover has developed beyond being an interesting chemical phenomenon that exists in biological systems to become a broad interdisciplinary field that equally attracts chemists, physicists, theoreticians, biochemists as well as material scientists. As a result the focus has shifted towards the applicability of materials exhibiting this

[10] Pauling, L.; J. Am. Chem. Soc. (1937); 59; 633.

[11] (a) Figgins, D. E.; Busch, D. H.; J. Am. Chem. Soc. (1960); 82; 820. (b) Robinson, M. A.; Curry, J. D.; Busch, D. H.; Inorg. Chem. (1963); 2; 1178.

[12] Madeja, K.; Konig, E.; J. Inorg. Nucl. Chem. (1963); 25; 377.

[13] Ewald, A. H.; Martin, R. L.; Ross, I. G.; White, A. H.; Proc. R. Soc. A. (1964); 280; 235.

property to devices.[14] This can be achieved by the exploitation of the basic changes which accompany spin transition. Triazole systems that exhibit high cooperativity have been suggested for use as contrast agents in magnetic resonance imaging as well as temperature sensors for hyperthermia treatment in tumors.[15] Other systems that are influenced by change in pressure or light irradiation have also been considered for application in molecular sensors. And lastly, systems exhibiting bistability could be applied in devices for data storage.

The field of spin crossover systems still garners great interest from scientists. The focus of current research includes defining different physical properties that influence spin state as well as the development of novel systems that can exhibit the spin crossover phenomenon with desirable physical properties which would make them useful for various applications.

2.2 Occurrence of Spin Crossover

Spin crossover can be defined as the change in spin state exhibited by certain transition metal complexes as a result of external perturbation. This phenomenon has been referred to by a number of terms: spin crossover, spin transition and sometimes the term spin equilibrium is used. The most well known external stimulus influencing spin crossover is variation in temperature. However, molecular systems responding to pressure, light irradiation and changes in magnetic field are also known (Figure 2.1).

[14] Kahn, O.; Launay, J. P.; Chemtronics (1988); 3; 140.
[15] Muller, R. N.; Elst, L. V.; Larent, S.; J. Am. Chem. Soc. (2003); 125; 8405.

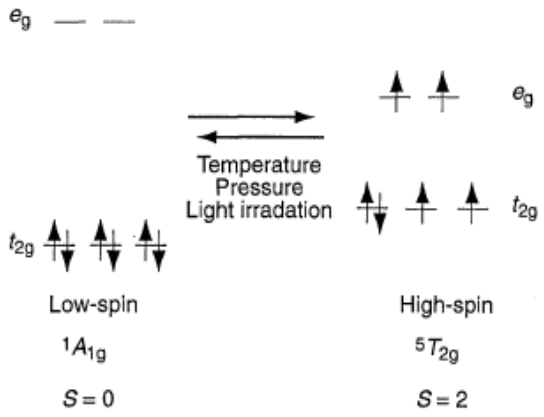

Figure 2.1. Spin transition behaviour in an octahedral Fe(II) complex.

Under the influence of a ligand field, d orbitals of transition metals lose their degeneracy. Taking the octahedral geometry as an example, ligand field splits the d orbitals into the t_{2g} and e_g sets. Octahedral complexes of certain of the transition metal ions may exist in either the high-spin or low-spin state, depending on the nature of the ligand field about the metal ion. In weak fields the ground state is HS where the spin multiplicity is a maximum, the d electrons being distributed over the t_{2g} and e_g sets whereas strong fields stabilise the low spin state with minimum multiplicity, the t_{2g} set being completely occupied before electrons are added to the e_g set. For the d^6 ion of iron(II), for example, the two states are illustrated by $[Fe(H_2O)_6]^{2+}$, which, with the configuration $t_{2g}^4 e_g^2$, has four unpaired electrons and thus is strongly paramagnetic ($^5T_{2g}$ state in octahedral symmetry), and $[Fe(CN)_6]^{4-}$ ($t_{2g}^6 e_g^0$) which has no unpaired electrons ($^1A_{1g}$ state). The magnitude of the ligand field compared to the spin pairing energy may also affect the spin state of any given compound. It may be possible to have a scenario where there is an equilibrium between both spin states, as shown in Figure 2.2.

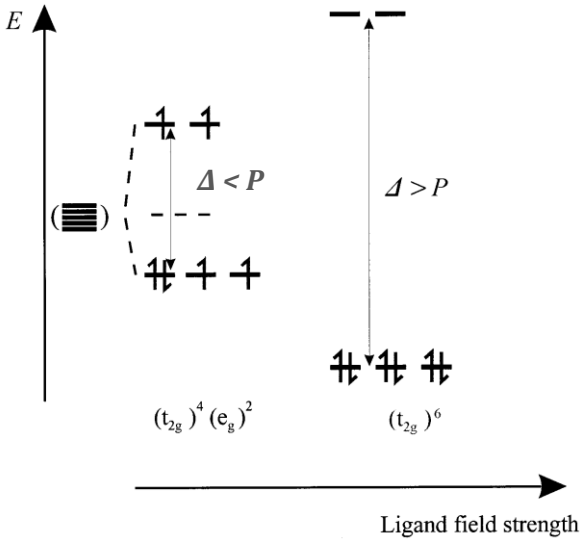

Figure 2.2. Electronic configuration for a d^6 iron(II) ion, in the LS state, in the HS state and equilibrium between these two states in the case of thermal spin crossover. Δ stands for the cubic ligand field parameter and P for the mean spin-pairing energy.

For intermediate fields the energy difference ($\Delta E°_{HL}$) between the lowest vibronic levels of the potential wells of the two states may be sufficiently small that application of some relatively minor external perturbation effects a change in the state (Figure 2.3). A spin transition will be induced thermally when $\Delta E°_{HL} \cong k_B T$ and when this criterion is met pressure- and light induced transitions may also be observed.[16]

[16] Gütlich, P.; Garcia, Y.; Goodwin, H. A.; Chem. Soc. Rev. (2000); 29; 419.

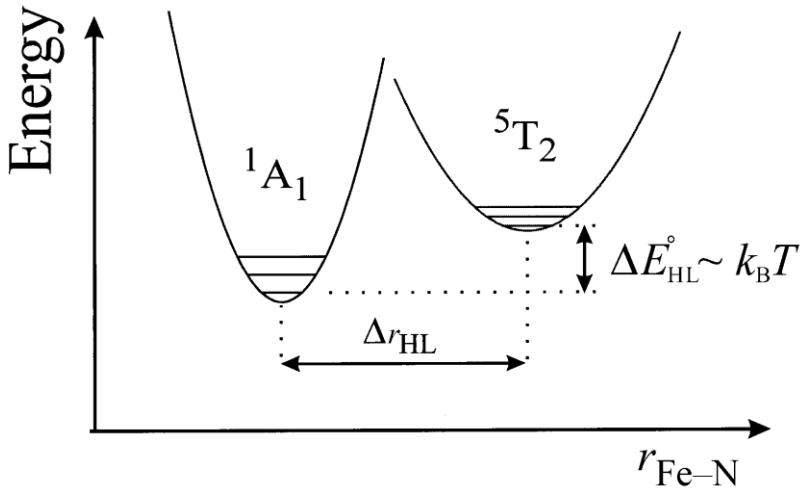

Figure 2.3. Representation of the potential wells for the $^1A_1$ and $^5T_2$ states of an iron(II) SC system, the nuclear coordinate being the metal–donor atom distance.

The origin of the term "spin crossover" lies in the crossover of the energy versus field strength curves for the possible ground state terms for ions in a particular d^n configuration in a Tanabe-Sunago diagram. Spin crossover is possible in ions with a d^4, d^5, d^6 and d^7 configuration. Most examples in the literature are of complexes of these configurations. There are isolated examples of complexes exhibiting spin crossover in the second transition series. However, due to the lower spin pairing energy coupled with the stronger ligand field, it is less likely that there will be many examples of such compounds that will be found.[7]

The most common ion exhibiting spin crossover is of the configuration d^6 and iron (II) represents the vast majority of examples presented in the literature.[17] Cobalt (III) compounds also exhibit ions with a d^6 configuration; however the numbers of examples available in the literature are more limited. This is due to the fact that cobalt (III) produces a stronger ligand field. This ligand field stabilization, coupled with a lower spin pairing energy results in

[17] (a) Lindoy, L.F.; Livingstone, S.E.; Coord. Chem. Rev. (1967); 2; 173. (b) Barefield, E. K.; Busch, D. H.; Nelson, Q.; Rev. Chem. Soc. (1968); 22; 457. (c) Martin, R. L.; White, A. H.; Transition Met. Chem. (1968); 4; 113.

complexes adopting a low spin configuration in most cases.[18] A similar situation is observed for the smaller d^5 iron (III), where the low spin configuration is relatively favoured, but not to the extent of cobalt (III). This, however, is due to the fact that iron (III) possesses a relatively low spin pairing energy and a higher ligand field stabilization energy than cobalt (III). Therefore examples of spin crossover systems of iron (III) are more widespread than cobalt (III). It is also worth mentioning that the conditions for spin crossover systems for iron (III) are less favourable than iron (II), partly due to the fact that high spin complexes of iron (III) tend to be readily hydrolysed.[7]

Cobalt (II) with a d^7 electronic configuration, is the second most commonly reported transition metal ion exhibiting spin crossover. Systems based on cobalt (II) are well characterized, albeit less common than iron (II) based systems. This could be due to the higher spin pairing energy, coupled with the destabilizing effect of a single electron in the e_g orbital in low spin octahedral complexes.[7] The only other d^7 ion showing spin crossover is nickel (III), however this phenomenon is observed in only one instance – in the salts of $[NiF_6]^{3-}$.[19]

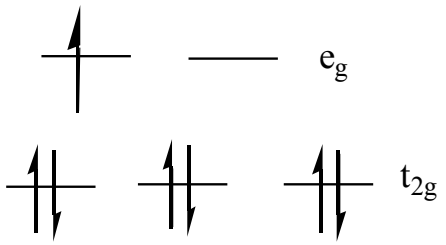

Figure 2.4. Electron configuration of a d^7 transition metal ion in an octahedral ligand field.

[18] Konig, E.; Kremers, S.; Theor. Chim. Acta (1971); 23; 12.
[19] Reinen, D.; Friebel, C.; Propach, V.; Z. Anorg. Allg. Chem. (1974); 408; 187.

2.3 Detection of Spin Transition

Consequent to spin transition are other physical and electronic changes within the complex. The two most important changes that are observed accompanying spin transition are changes in the metal-donor atom distance (Figure 2.3), which arise as a result of the change in occupancy of t_{2g} and e_g orbital sets, and changes in the magnetic properties of the complex. While the physical changes accompanying spin transition can be monitored by observation of a colour change, using X-ray diffraction and other techniques, changes in the magnetism of the complexes can now be quantitatively measured, and this is a result of the significant advances in the field of magnetochemistry and in SQUID magnetometry.

The change from a low spin to a high spin configuration results in a pronounced increase in the paramagnetism of the complex. Hence, measurement of this change as a function of temperature, was the method initially applied for detection and monitoring of spin crossover, and remains the most widely used method.

Mössbauer spectroscopy offers another way of monitoring the spin transition in iron-based spin crossover complexes. This is a more direct way of determining the relative concentrations of the spin states within a spin crossover system, and this is a result of the fact that the different spin states give separate and well defined characteristics in the overall spectrum (isomer shift and quadrupole splitting), which are easily identifiable provided the lifetimes of the spin states are greater than the timescale of the Mossbauer effect (10^{-7}s). This is generally the case for iron (II) systems, with one known exception for six-coordinate systems of

this ion.[20] This is not the case, however, for iron (III) systems, as the rates of interconversion of spin states are generally too rapid to enable their identification in a Mössbauer spectrum[21,22,23,24], but when the contributions of the spin states are seen in the spectrum, their area fractions can usually be determined with reasonable accuracy.[7,]

Our efforts will aim to design spin crossover systems based on cobalt (II). Therefore the measurements with greatest value would be structural elucidation and those methods using SQUID magnetometry. The Mossbauer methods described above would be of great importance for iron based systems, and unfortunately are not applicable for the purposes of our current efforts.

2.4 Spin transition Curves

The phenomenon of spin crossover can be observed from a spin transition curve. A spin transition curve is defined as the plot of the high spin fraction (γ_{HS}) versus the temperature (T). Spin transition manifests itself in many forms, and some of these are shown in Figure 2.5.

These curves can be very informative. The most important parameter that these graphs give us is the spin transition temperature. For a simple, complete change in spin states, the spin transition temperature is defined as the temperature where the two spin states are present in the ratio 1:1 ($\gamma_{HS} = \gamma_{LS} = 0.5$) and is denoted by $T_{1/2}$.

---

[20] Chang, H-R; McCusker, J. K.; Toftlund, H.; Wilson, S. R.; Trautwein, A. X.; Winkler, H.; Hendrickson, D. N.; J. Am. Chem. Soc. (1990); 112; 6814.

[21] Nihei, M.; Shiga, T.; Maeda, Y.; Oshio, H.; Coord. Chem. Rev. (2007); 251; 2606

[22] (a) Timken, M. D.; Abdel-Mawgoud, A. M.; Hendrickson, D.N.; Inorg. Chem. (1986); 25; 160; (b) Nishida, Y.; Oshio, S.; Kida, S.; Bull. Chem. Soc. Jpn. (1977); 50; 199. (c) Kennedy, B. J.; McGrath, A. C.; Murray, K. S.; Skelton, B. W.; White, A. H.; Inorg. Chem. (1987); 26; 483. (d) Oshio, H.; Maeda, Y.; Takashima, Y.; Inorg. Chem. (1983); 22; 2684. (e) Oshio, H.; Kitazaki, K.; Mishiro, K. J.; Kato, N.; Maeda, Y.; Takashima, Y.; J. Chem. Soc. Dalton Trans. (1987); 1341. (f) Maeda, Y.; Tsutsumi, N.; Takashima, Y.; Inorg. Chem. (1984); 23; 2440.

[23] Merrithew, P. B.; Rasmussen, P. G; Inorg. Chem. (1972); 11; 325.

[24] Kunze, K. R.; Perry, D. L.; Wilson, L. J.; Inorg. Chem. (1977); 16; 594.

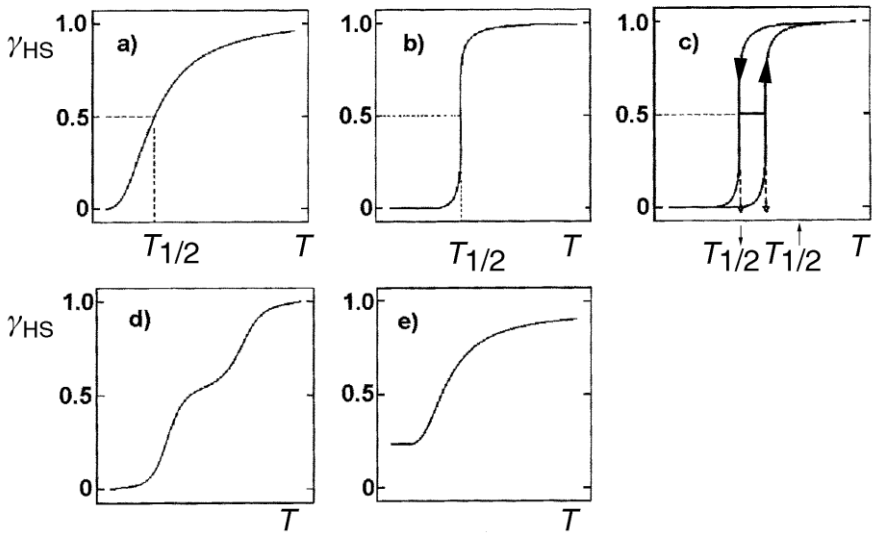

Figure 2.5. The nature of ST curves for SC systems in the solid state: (a) gradual; (b) abrupt; (c) with hysteresis; (d) with steps; (e) incomplete.[16]

The variety of mechanisms in which spin transition can occur are evident from the shapes of the curves shown. This variation arises from a number of sources, but the most important is the degree of intermolecular cooperativity. This can be thought of as the extent to which the effects associated with spin change (such as metal-donor atom distances) are propagated throughout the solid, which is determined by the lattice properties.[7]

Materials in the solution phase show very little cooperativity. The metal centres are well separated, and if there is spin crossover, no cooperativity is associated with the transition. In this case, a gradual spin transition occurs and follows a curve similar to that of Figure 2.5.(a). This may be interpreted in terms of a simple thermal equilibrium involving a Boltzmann distribution over all energy levels of the two spin states. In this instance the transition occurs essentially at the molecular level without the constraints of lattice interactions. For solid

systems lattice effects assume importance, however, continuous spin transitions may still be observed.[16]

In neat spin-crossover compounds, transition curves tend to be more abrupt (Figure 2.5.(b)) and may occur as first order phase transitions with a hysteresis (Figure 2.5.(c)). Two transition temperatures are defined for spin transitions with hysteresis, one for increasing ($\uparrow T_{1/2}$) and one for decreasing temperature ($\downarrow T_{1/2}$). Such a cooperative behaviour is due to elastic interactions between the spin-crossover complexes, which result from the comparatively large differences in molecular geometry between the two states.[25] The presence of hysteresis in a system is one of the most significant aspects of the spin crossover phenomenon. The presence of hysteresis can be used as a measure of the bistability of the system. Bistability means the ability of a system to be observed in two differing electronic states over a certain range of some external perturbation.[14] The prospect of exploiting these desirable spin crossover properties has driven much of recent research, and an understanding of the factors favouring such behaviour is continuing.[26]

The presence of hysteresis in a system can be explained in terms of the structural phase changes in the lattice that may accompany the spin transition. The second origin of hysteresis lies in the intramolecular structural changes that may occur during spin transition, and that may be communicated to neighbouring molecules by a cooperative interaction. The mechanism of this communication is not known, but some strategies have been developed in order to generate it including: (i) linkage of transition metal centres by covalent bond, such as in

[25] (a) Spiering, H.; Top. Curr. Chem. (2004); 235; 171; (b) Spiering, H.; Boukheddaden, K.; Linares, J.; Varret, F.; Phys. Rev. B (2004); 70; 184. (c) Spiering, H.; Meissner, E.; Koppen, H.; Muller, E.W.; Gütlich, P.; Chem. Phys. (1982); 68; 65.

[26] Kahn, O.; Martinez, C. J.; Science (1998); 279;44.

polymeric systems[27], (ii) incorporating hydrogen bond donors and acceptors in the organometallic structure, allowing for cooperativity directly between metal centres or through anions or solvent molecules[16], (iii) incorporation of aromatic moieties in the ligand framework, promoting π-π interactions and thus favouring cooperative behaviour[28]. The number of examples exhibiting transitions of this type is on the rise.[7]

Transitions that are stepped (Figure 2.5(d)) are more rare and the first report was in 1981 for the iron (III) complex $NH_4[Fe(5\text{-}Br\text{-}tsa)_2]$ (tsa = salicylaldehyde thiosemicarbazone).[29] Examples of the last type of transition, which involves the retention of a high spin fraction at low temperatures (Figure 2.5(e)) or an incomplete transition, are also known for a number of compounds.[30,31,32,33]

2.5 Dendrimers

Dendrimers are one type of macromolecular architecture which is defined by its polymeric, hyperbranched, monodispersed structures. Dendrimers are large spherical molecules, which are made by addition of pendant groups to a symmetrical dendritic core. From a conceptual point of view, dendrimers have been of great interest and have been attracting research from different fields of chemistry and biochemistry.

---

[27] Kahn, O.; Codjovi, E.; Garcia, Y.; van Koningsbruggen, P. J.; Lapuoyadi, R.; Sommier, L.; Molecule Based Magneic Materials; ACS Symposium Series (1996); 644; 44.

[28] Juhász, G.; Hayami, S.; Sato, O.; Maeda, Y.; Chem. Phys. Lett. (2002); 364; 164.

[29] Ryabova, N. A.; Ponomarev, V. I; Zelentsov, V. V.; Shipilov, V. I.; Atovmyan, L. O.; J. Struc. Chem. (1981); 22; 234

[30] Ritter, G.; Konig, E.; Irler, W.; Goodwin, H. A.; Inorg. Chem. (1978); 17; 224.

[31] (a)Buchen, T.; Gütlich, P.; Inorg. Chem. (1994); 33; 4573. (b) Buchen, T.; Gütlich, P.; Sugiyarto, K. H.; Goodwin, H. A.; Chem. Eur. J. (1996); 2; 1134.

[32] Hayami, S.; Maeda, Y.; Inorg. Chim. Acta (1997); 255; 181.

[33] Moliner, N.; Gaspar, A. B.; Munoz, M. C.; Niel, V.; Cano, J.; Real, J. A.; Inorg. Chem. (2001); 40; 3986.

Self-assembly of dendritic macromolecules is an interesting subject from a fundamental viewpoint[34] and has also been studied in relation to certain events in biological systems. To develop novel functional soft materials with a nanometric structural precision, recent studies have focused on self-assembly of molecularly engineered dendritic macromolecules to form large hierarchical structures with enhanced complexities.[35] The literature provides a wealth of examples of such complex architectures as well as their applications. Some of these examples include columnar and nanotubular assemblies,[36] hollow architectures,[37] self-assembled synthetic proton channels,[38] and template-directed dendrisilica nanocomposites.[39]

Metallodendrimers are also known and have been studied and reviewed in the literature. [40,41] The most well studied metallodendrimers are those which incorporate metallocenes in their core structure or their peripheries (Figure 2.6). They were found to have electron transport properties, and can be stable in both the oxidized and reduced forms (chemical reversibility). Electrochemical studies reveal that electron transfer within the dendrimers and between the dendrimers and electrodes are both very fast processes when the

---

[34] (a) Fréchet, J. M. J.; Tomalia, D. A.; Dendrimers and Other Dendritic Polymers (2000); VCH-Wiley: New York. (b) Narayanan, V. N.; Newkome, G. R.; Top. Curr. Chem. (1998); 197; 19. (c) Bosman, A. W.; Janssen, H. M.; Meijer, E. W.; Chem. Rev. (1999); 99; 1665. (d) Tomalia, D. A.; Aldrichimica Acta (2004); 37; 39.

[35] Serrette, A. G.; Swager, T. M.; J. Am. Chem. Soc. (1993); 115; 8879. (b) Lehmann, M.; Sierra, T.; Barber, J.; Serrano, J. L.; Parker, R.; J. Mater. Chem. (2002); 12; 1342. (c) Percec, V.; Johansson, G.; Heck, J.; Ungar, G.; Batty, S. V.; J. Chem. Soc., Perkin Trans. 1 (1993); 1411. (d) Percec, V.; Johansson, G.; Ungar, G.; Zhou, J.; J. Am. Chem. Soc. (1996); 118; 9855. (e) Percec, V.; Cho, W.-D.; Ungar, G.; Yeardley, D. J. P.; Chem. Eur. J. (2002); 8; 2011. (f) Percec, V.; Holerca, M. N.; Uchida, S.; Cho, W. D.; Ungar, G.; Lee, Y.; Yeardley, D. J. P.; Chem. Eur. J. (2002); 8; 1106.

[36] (a) Percec, V.; Glodde, M.; Bera, T. K.; Miura, Y.; Shiyanovskaya, I.; Singer, K. D.; Balagurusamy, V. S. K.; Heiney, P. A.; Schnell, I.; Rapp, A.; Spiess, H.-W.; Hudson, S. D.; Duan, H.; Nature (2002); 417; 384. (b) Yamaguchi, T.; Ishii, N.; Tashiro, K.; Aida, T.; J. Am. Chem. Soc. (2003); 125; 13934.

[37] (a)Schultz, L. G.; Zhao, Y.; Zimmerman, S. C.; Angew. Chem., Int. Ed. (2001); 40; 1962. (b) Kim, Y.; Mayer, M. F.; Zimmerman, S. C.; Angew. Chem., Int. Ed. (2003); 42; 1121.

[38] Percec, V.; Dulcey, A. E.; Balagurusamy, V. S. K.; Miura, Y.; Smidrkal, J.; Peterca, M.; Nummelin, S.; Edlund, U.; Hudson, S. D.; Heiney, P. A.; Duan, H.; Magonov, S. N.; Vinogradov, S. A.; Nature (2004); 430; 764.

[39] Landskron, K.; Ozin, G. A.; Science (2004); 306; 1529.

[40] Newkome, G. R.; He, E.; Moorefield, C. N.; Chem. Rev. (1999); 99; 1689.

[41]Hwang, S. H.; Shreiner, C. D.; Moorefield, C. N.; Newkome, G. R.; New J. Chem. (2007); 31; 1192.

branches are flexible (electrochemical reversibility). When the dendrimer branches are sufficiently long, the redox events at the many termini of the metallodendrimer are independent, appearing as a single wave in the cyclic voltammogram, because of very weak electrostatic effects.[42] These properties have made them suitable for applications such as molecular electronics,[43] energy conversion,[44] sensing,[45]and catalysis.[46]

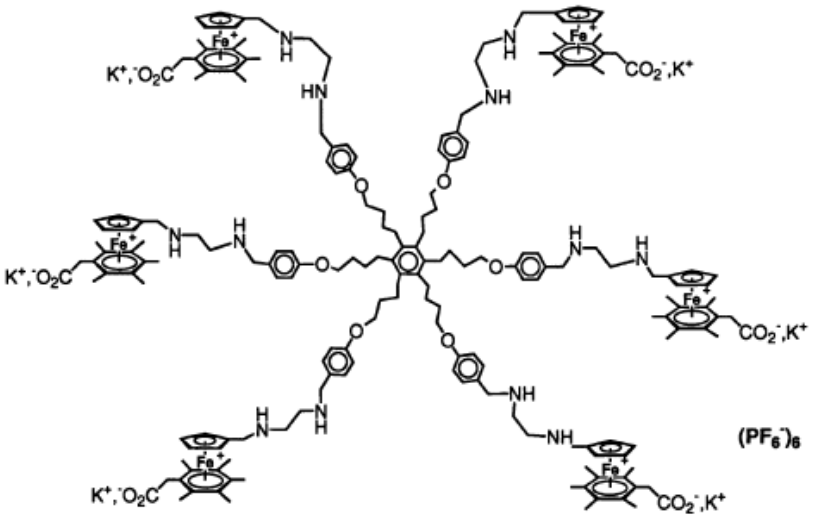

Figure 2.6. Star-shaped water-soluble organometallic redox catalyst for the cathodic reduction of NO_2^- and NO_3^- to NH_3.

Current research on spin crossover systems aims to design systems that are stable, undergo spin transition at the room temperature range, and also exhibit a great degree of

[42] Astruc, D.; Ornelas, C.; Ruiz, J.; Acc. Chem. Res. (2008); 41; 841.

[43] (a)Balzani, V.; Ceroni, P.; Juris, A.; Venturi, M.; Campagna, S.; Puntoriero, F.; Serroni, S.; Coord. Chem. Rev. (2001); 219; 545. (b) Gorman, C. B.; Smith, J. C.; Acc. Chem. Res. (2001); 34; 60. (c) Casado, C. M.; Cuadrado, I.; Moran, M.; Alonso, B.; Garcia, B.; Gonzalez, B.; Losada, J.; Coord. Chem. Rev. (1999); 185-6; 53.

[44] Balzani, V.; Campagna, S.; Denti, G.; Juris, A.; Serroni, S.; Venturi, M.; Acc. Chem. Res. (1998); 31; 26.

[45] (a)Cuadrado, I.; Moran, M.; Casado, C. M.; Alonso, B.; Losada, J.; Coord. Chem. Rev. (1999); 193-5; 395. (b) Ong, W.; Gomez-Kaifer, M.; Kaifer, A. E.; Chem. Commun. (2004); 1677. (c) Kaifer, A. E.; Eur. J. Inorg. Chem. (2007); 5015.

[46] (a) Oosterom, G. E.; Reek, J. N. H.; Kamer, P. C. J.; van Leeuwen, P. W. N. M.; Angew. Chem., Int. Ed. (2001); 40; 1828. (b) van Heerbeek, R.; Kamer, P. C. J.; van Leeuwen, P. W. N. M.; Reek, J. N. H.; Chem. Rev. (2002); 102; 3717. (c) Kreiter, R.; Kleij, A. W.; Gebbink, R. J. M. K.; van Koten, G.; Top. Curr. Chem. (2001); 217; 163. (d) Astruc, D.; Chardac, F.; Chem. Rev. (2001); 101; 2991.

cooperative interactions. Our attention was turned to dendrimers as a suitable ligand framework due to its desirable properties. The dendritic architecture is extremely variable, and can be engineered to accommodate a number of functional groups, coordination sites, as well as various branching hierarchies. The chemical properties, such as solubility and processability, can also be fine tuned by alteration of peripheral groups. Also, considering the aforementioned conditions that would be expected to increase cooperative interactions in spin crossover systems, the dendritic framework has the potential to provide the necessary structural features that would promote these conditions, and thus could promote cooperative interactions between metal centres.

The first attempt at synthesizing spin crossover dendrimers was by Fujigaya and coworkers.[47] Fujigaya's work presented dendronized iron(II) complexes of the kind iron(II)-tris[Gn-poly(benzyl ether)dendron] methyl sulfonic acid (Gn, n = 0, 1, 2). These dendronized coordination polymers were magnetically active, and underwent a thermal spin transition. However, when the generation number of the dendritic unit was larger (n = 0, 1, 2), the average degree of polymerization (Dp = 20, 10, 3) and spin crossover temperature ($T_{1/2}$ = 335, 315, 300 K) of the resulting polymer were lower. It was also found that the conversion of low to high spin states was irreversible due to an irreversible loss of water during the first heating process leading to the spin change.

More recently, the group of Philip Gütlich attempted to synthesize the first- (G1) and second generation (G2) Fréchet/Hawker-type dendronized triazole complexes of the kind [Fe(G1,2-PBE)]A2·*x*H2O where G1- PBE denotes 4-[3,5-bis(benzyloxy)benzyl]-4*H*-1,2,4-triazole

[47] Fujigaya, T.; Jiang, D.-L.; Aida, T.; J. Am. Chem. Soc. (2005); 127; 5484.

and G2-PBE represents 4-{3,5-bis[3,5-bis(benzyloxy)benzyloxy] benzyl}-4*H*-1,2,4-triazole as ligands, with toluenesulfonate and trifluorosulfonate as counter ions. All the compounds studied by Gütlich showed spin transition temperatures below 200K. The spin transitions were gradual and incomplete. Further, the abrupt decrease of χMT observed below 50 K originates from zero-field-splitting, which was proven by ^{57}Fe-Mössbauer spectroscopy.[48]

In this thesis, we discuss our attempts in the synthesis of cobalt(II) containing spin crossover systems, encapsulated in a dendritic framework. We adopted a divergent synthesis using the click reaction for the dendritic frameworks in order to incorporate 1,2,3-triazole groups within the architecture.

[48] (a) Sonar, P.; Grunert, C. M.; Wei, Y-L.; Kusz, J.; Gütlich, P.; Schlüter, A. D.; Eur. J. Inorg. Chem. (2008); 1613. (b) Wei, Y-L.; Sonar, P.; Grunert, M.; Kusz, J.; Schlüter, A. D.; Gütlich, P.; Eur. J. Inorg. Chem. (2010); 3930.

Chapter 3.

Co(II) Single Molecule Magnets

3.1 Introduction

Single molecule magnets are a class of molecules that exhibit superparamagnetic type behaviour, or undergo slow magnetic relaxation, below a characteristic blocking temperature. The barrier to magnetic relaxation results from an inherent negative molecular magnetic anisotropy (*D*) and a nonzero spin ground state (*S*), producing the barrier given by the expression $U = S^2|D|$ for integer spin values and $U = |D|(S\text{-}1/2)^2$ for half-integer spin values (Figure 3.1).[49] However, most importantly, the magnetic hysteresis shown by these materials is of purely molecular origin, thus they behave as "tiny magnets", and may also exhibit quantum effects such as quantum tunneling of the magnetization.[50]

[49]Aromí, G.; Brechin, E. K.; Struct. Bond. (2006); 122; 1.

[50]Wang, X-Y.; Avendaño, C.; Dunbar, K. R.; *Chem. Soc. Rev.* (2011); **40**; 3213.

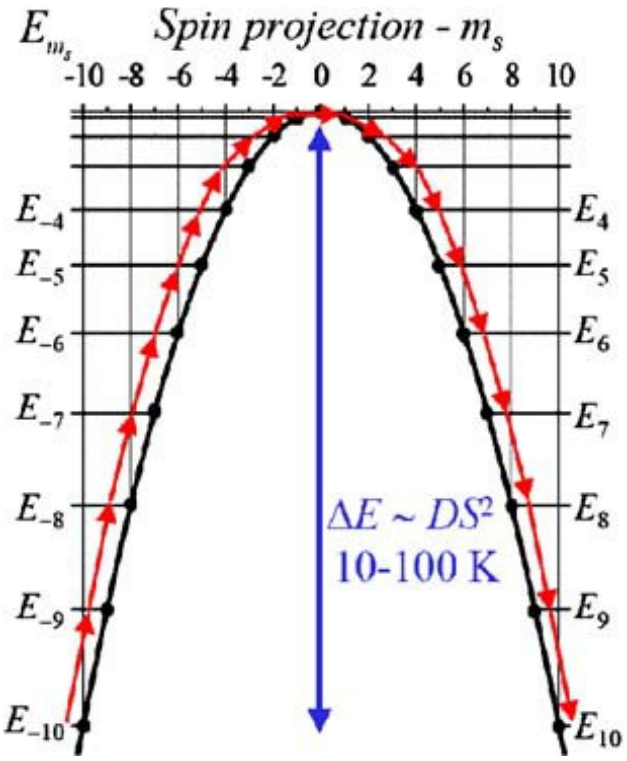

Figure 3.1. Energy diagram showing the relative positions of the zero-field split M_S levels of an S = 10 system, and the barrier mediating between the M_S =+ 10 and the M_S =– 10 states.

The first observation of a single molecule magnet was two decades ago[51], for a mixed-valence manganese cluster $[Mn_{12}O_{12}(CH_3COO)_{16}(H_2O)_4].2CH_3COOH.4H_2O$, or Mn_{12}acetate (Figure 3.2), first synthesized and characterized in 1980.[47,52] The term single molecule magnet was coined by George Christou and David N. Hendrickson in 1996.[53] Most known examples are polynuclear complexes, with the Mn-based clusters accounting for the majority of known single molecule magnets (SMMs), and Fe based complexes being the second most abundant. Mixed-valence Mn complexes of the family $[Mn_{12}O_{12}(O_2CR)_{16}(H_2O)_x]^{n-}$ (n=0, 1, 2; x = 3, 4) are the 'prototype' SMMs and are the most well studied.

[51] Caneschi, A.; Gatteschi, D.; Sessoli, R.; Barra, A. L.; Brunel, L. C.; Guillot, M.; J. Am. Chem. Soc. (1991); 113; 5873.
[52] Lis, T.; Acta Cryst. Section B (1980); 36; 2042.
[53] Aubin, S. M. J.; Wemple, M. W.; Adams, D. M.; Tsai, H-L.; Christou, G.; Hendrickson, D. N.; J. Am. Chem. Soc. (1996); 118; 7746.

A variety of metal ions can be used to yield SMMs and there are, in addition to Mn and Fe complexes, a number of known homometallic and heterometallic complexes of Co, Ni, lanthanides and even V, showing SMM behaviour.[54] However, Mn -based clusters still hold the record for the highest blocking temperature. Mn_{12}acetate has a blocking temperature (T_B; the temperature where the apparent magnetization is zero) of 2.1 K, while the current best SMM $[Mn_6O_2(Etsao)_6(O_2CPh)_2(EtOH)_6]$ {Et-saoH$_2$ = 2-hydroxyphenylpropanone oxime} has an S = 12 ground state and an energy barrier to magnetisation reversal of 86 K ($T_B \approx 4.5$ K). [55]

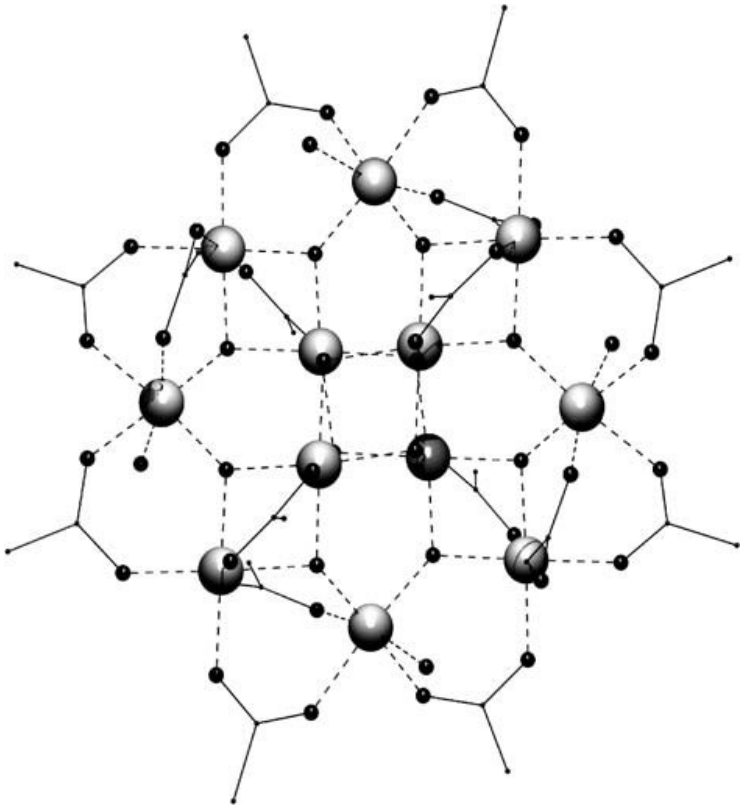

Figure 3.2. PovRay representation of $[Mn_{12}O_{12}(O_2CMe)_{16}(H_2O)_4]$. Hydrogen atoms are omitted for clarity. (*large grey*, Mn; *medium black*, O; *rest*, C)[49]

[54](a) Zhang, Y-Z.; Wernsdorfer, W.; Pan, F.; Wanga Z-M.; Gao, S.; Chem. Commun. (2006); 3302. (b) Jia, Q-X.; Tian, H.; Zhang, J-Y.; Gao, E-Q.; Chem. Eur. J. (2011); 17; 1040. (c) Tang, J.; Hewitt, I.; Madhu, N. T.; Chastanet, G.; Wernsdorfer, W.; Anson, C. E.; Benelli, C.; Sessoli, R.; Powell, A. K.; Angew. Chem. Int. Ed. (2006); 45; 1729

[55] Milios, C. J.; Vinslava, A.; Wernsdorfer, W.; Moggach, S.; Parsons, S.; Perlepes, S. P.; Christou, G.; Brechin, E. K.; J. Am. Chem. Soc. (2007); 129; 2754.

Generally SMMs are based around large transition metal ion clusters, having a high total spin ground state. All such known complexes are synthesized (at least initially) by the serendipitous addition of metal and ligand, or by reaction of a preformed cluster with a solvent, reductant/oxidant, and/or flexible organic bridging ligand to yield a large polynuclear organometallic complex. This approach has led to the largest isolated SMM $[Mn_{84}O_{72}(O_2CMe)_{78}(OMe)_{24}(OH)_6(MeOH)_{12}]$ [56]and complexes with spin ground states as high as 51/2 in the complex $[Mn_{25}O_{18}(OH)_{2(}N_3)_{12}(pdm)_6(pdmH)_6](Cl)_2]$ (H_2pdm = 2,6-pyridinedimethanol)[57]. Although this approach to the synthesis of SMMs has resulted in numerous, well studied examples of such materials, as well as allowed us to gain a greater understanding of the dynamics of relaxation of the magnetic moment[58] and led to the experimental observation of quantum tunnelling of the magnetisation[59], the final structures are quite difficult to predict. This problem is especially prominent when using multidentate ligands possessing many binding sites and differing binding modes. The unpredictability of such large structures gives chemists little synthetic control. In order to be able to predict the magnetic properties of a compound, control over many aspects of the composition and structure of polynuclear complexes is required, however, it is clear that much work is needed in order to be able to exert such a level of structural control.

[56] Tasiopoulos, A. T.; Vinslava, A.; Wernsdorfer, W.; Abboud, K. A.; Christou, G.; Angew. Chem. Int. Ed. (2004); 43; 2117.
[57] Murugesu, M.; Habrych, M.; Wernsdorfer, W.; Abboud, K. A.; Christou, G.; J. Am. Chem. Soc. (2004); 126; 4766.
[58] (a) Fernandez, J. F.; Luis, F.; Bartolome, J.; Phys. Rev. Lett. (1998); 80; 5659. (b) Bokacheva, L.; Kent, A. D.; Walters, M. A.; Polyhedron (2001); 20; 1717. (c) Wernsdorfer, W.; Bhaduri, S.; Tiron, R.; Hendrickson, D. N.; Christou, G.; Phys. Rev. Lett. (2002); 89; 197201.
[59] Hendrickson, D. N.; Christou, G.; Ishimoto, H.; Yoo, J.; Brechin, E. K.; Yamaguchi, A.; Rumberger, E. M.; Aubin, S. M. J.; Sun, Z. M.; Aromí, G.; Polyhedron (2001); 20; 1479.

On the other hand, it can be argued that smaller complexes may allow for a better ability to predict final molecular structure. Further, the insight gained from studying these smaller magnetic systems could then be applied to increasingly larger systems in an effort to overcome their unpredictability. Mononuclear lanthanide or actinide systems have been shown to exhibit slow magnetic relaxation at low temperatures.[60] This barrier to relaxation results from a high magnetic anisotropy which is attributed to the high degree of spin-orbit coupling observed in f-block elements. Also, recent reports from Chang and Long have shown that mononuclear Fe(II) SMMs are attainable and one example is shown in Figure 3.3.[61] Here, the SMM behaviour arises due to a highly anisotropic ground state resulting from a spin orbit coupling induced by the ligand scaffold. In both these cases, the exploitation of the magnetic anisotropy in the system to make up for the lack of a large spin ground state, has proved to be an effective strategy in the design of materials that exhibit slow magnetic relaxation.

[60] (a) Ishikawa, N.; Sugita, M.; Wernsdorfer, W.; J. Am. Chem. Soc. (2005); 127; 3650. (b) Jiang, S.-D.; Wang, B.-W.; Sun, H.-L.; Wang, Z.-M.; Gao, S.; J. Am. Chem. Soc. (2011); 133; 4730. (c) Li, D. P.; Wang, T. W.; Li, C. H.; Liu, D. S.; Li, Y. Z.; You, X. Z.; Chem. Commun. (2010); 46; 2929. (d) AlDamen, M. A.; Clemente-Juan, J. M.; Coronado, E.; Marti-Gastaldo, C.; Gaita-Arino, A.; J. Am. Chem. Soc. (2008); 130; 8874. (e) Rinehart, J. D.; Long, J. R.; J. Am. Chem. Soc. (2009); 131; 12558. (f) Jiang, S. D.; Wang, B. W.; Su, G.; Wang, Z. M.; Gao, S. Angew. Chem. Int. Ed. (2010); 49; 7448. (g) Magnani, N.; Apostolidis, C.; Morgenstern, A.; Colineau, E.; Griveau, J.-C.; Bolvin, H.; Walter, O.; Caciuffo, R.; Angew. Chem. Int. Ed. (2011); 50; 1696. (h) Rinehart, J. D.; Meihaus, K. R.; Long J. R.; J. Am. Chem. Soc. (2010); 132; 7572.

[61](a) Harman, W. H.; Harris, T. D.; Freedman, D. E.; Fong, H.; Chang, A; Rinehart, J. D.; Ozarowski, A.; Sougrati, M. T.; Grandjean, F.; Long, G. J.; Long, J. R.; Chang, C. J.; J. Am. Chem. Soc. (2010); 132; 18115. (b) Freedman, D. E.; Harman, W. H.; Harris, T. D.; Long, G. J.; Chang, C. J.; Long, J. R.; J. Am. Chem. Soc. (2010); 132; 1224.

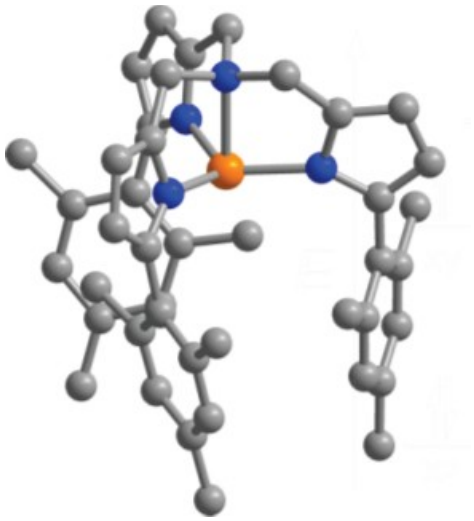

Figure 3.3. Structure of the trigonal pyramidal complex $[(tpa^{Mes})Fe]^-$ (H_3tpa^{Mes} = tris-mesityl tris(pyrrolylmethyl)amine). Orange, blue, and gray spheres represent Fe, N, and C atoms, respectively; H atoms have been omitted for clarity.

The use of highly anisotropic metal centres has provided another approach to the design of SMMs. Also, it is clear that smaller compounds allow for better synthetic control, producing structures with more predictable properties. Inspired by these findings, we have turned our attention to the inherently high magnetic anisotropy found in Co(II) for the synthesis of a small organometallic and coordination complexes with the aim of inducing SMM behaviour.

3.2 Magnetic Anisotropy

Having a large (or at least non-zero) spin ground state is essential in the preparation of materials designed to show SMM properties. However, complexes with a smaller spin ground state may exhibit slow magnetic relaxation due to their magnetic anisotropy which allows for

spontaneous magnetization along the magnetic easy axis (Figure 3.4).[62] The magnetic anisotropy is usually defined by the Zero-field splitting parameter (D). If the spin ground state is S ≥ 1, then this state S can be subject to a zero-field splitting (ZFS).

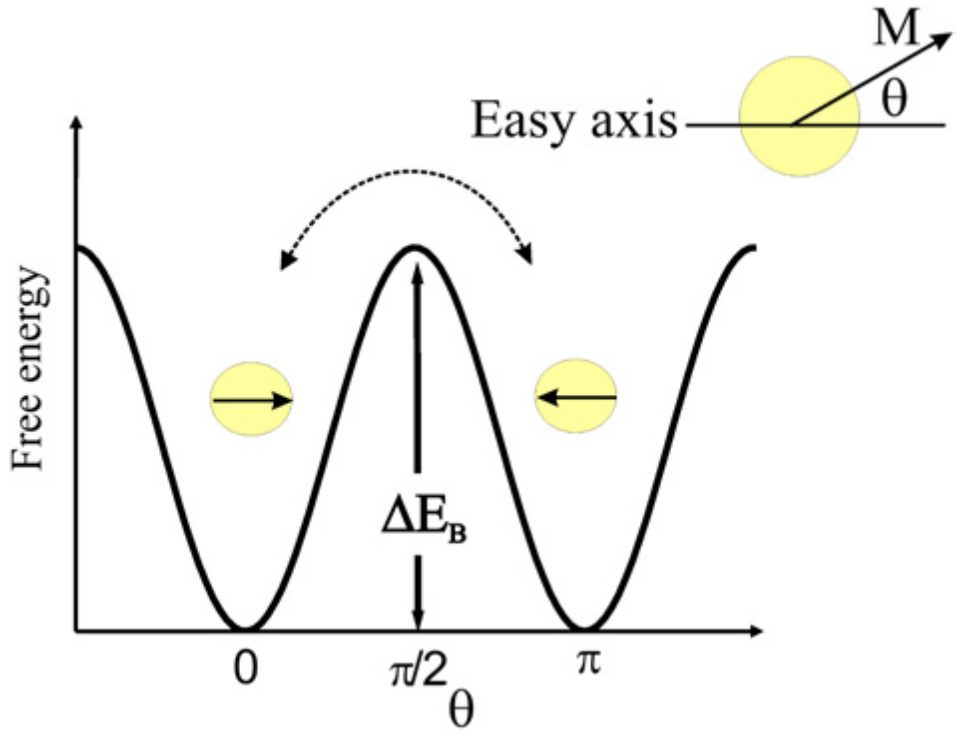

Figure 3.4. Schematic picture of the free energy of a single-domain particle with uniaxial anisotropy as a function of magnetization direction. E_B is the energy barrier hindering the free rotation of the magnetization and θ is the angle between the magnetization *M* and the easy axis.[60]

ZFS is incredibly important for SMMs. Figure 3.5 shows the effect of ZFS on an S = 3/2 state.[63] In the absence of zero-field splitting, the degeneracy of the M_S levels can be removed by an external magnetic field. However, if the crystal field is axial, the degeneracy is partly resolved before the application of the magnetic field and the $M_S = \pm 1/2$ levels are separated

[62] Bedanta, S.; Kleemann, W.; J. Phys. D: Appl. Phys. (2009); 42; 13001.
[63] Carlin, R. L.; Magnetochemistry (1986); Springer; Berlin.

from the $M_S = \pm 3/2$ levels by 2D, where D is the axial ZFS parameter. The term zero-field splitting is used, as the splitting is present in the absence of a magnetic field.[64]

ZFS arises through coupling of the ground state with excited states via spin–orbit coupling. The energetic difference between the easy and hard axes results, in part, from spin–orbit interactions. In general, spin–orbit coupling occurs in conjunction with the effects of a symmetry-lowering structural distortion, e.g. away from O_h symmetry.[1]

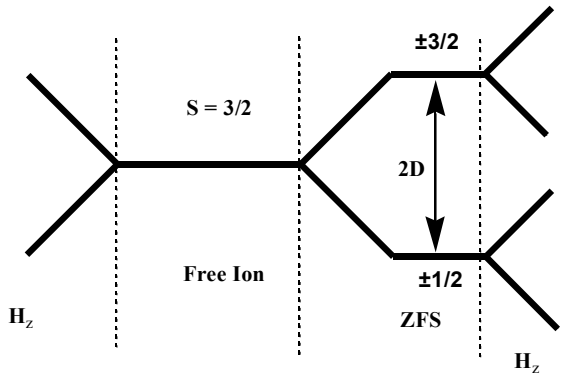

Figure 3.5. Zeeman splitting of an S = 3/2 state in the absence (left) and presence (right) of an axial zero-field splitting. (Figure modified from ref. 63)

The shape of the compound has an effect on the magnetic anisotropy. This specifically refers to the magnetocrystalline properties of the compound. In general, the anisotropy energy is larger in clusters of ions of low symmetry and smaller in lattices of high symmetry. Another important observation is that mononuclear complexes generally tend to possess a higher magnetic anisotropy. For the Mn_{12} acetate complex, the relevant parameters adopt the values S=10 and D=-0.46 cm^{-1}, resulting in a barrier of 72K that has been only recently exceeded by the Mn_6 complex with S= 12 and D=-0.43 cm^{-1} and a corresponding barrier of 86K.[54] Despite the considerable effort devoted to the preparation of high-spin molecules such as the recently

[64] Murrie, M.; Chem. Soc. Rev. (2010); 39; 1986.

reported Mn_{19} complex with S=83/2,[65] the main problem remains the small value of the ZFS parameter. This is clearly seen when comparing the small D values found in polynuclear SMMs with that in, for example, the mononuclear $[Mn(acac)_3]$ complex (D=-4.52 cm^{-1}),[66] with only one metal atom. Thus, the usually compact and symmetric shape of the polynuclear complexes seems to result in a significantly smaller magnetic anisotropy than that found in the isolated building blocks composed of mononuclear metal complexes.[67]

The size of the D parameter will also depend on the transition metal ion in question and its coordination geometry. For example $^4A_2$ octahedral Cr(III), S=3/2 and tetrahedral Co(II), S = 3/2, have different magnetic anisotropies. The former possesses less spin orbit coupling resulting in a lower D parameter, while the latter has a larger spin–orbit coupling constant and hence these complexes can display larger D values. In general, of the first row transition elements, Co(II) has an intrinsically high magnetic anisotropy.[63,68]

By exploiting the inherent magnetic anisotropy in Co(II) ions, it could be possible to infer SMM behaviour into organometallic compounds by fine tuning the coordination environment around the metal.

3.2 The Ligand System

Nitrogen donors have been proven to be versatile ligands in the coordination chemistry of cobalt. Coordination compounds of Co(II), such as those with the Tris(2-pyridylmethyl)amine

[65] Ako, M.; Hewitt, I. J.; Mereacre, V.; Clerac, R.; Wensdorfer, W.; Anson, C. E.; Powell, A. K.; Angew. Chem. Int. Ed. (2006); 45; 4926.
[66] Krzystek, J.; Gregory, J. Y.; Park, J.-H.; Britt, R. D.; Weisel, M. W.; Brunel, L. C.; Telser, J.; Inorg. Chem. (2003); 42; 4610.
[67] Cirera, J.; Ruiz, E.; Alvarez, S.; Neese, F.; Kortus, J.; Chem. Eur. J. (2009); 15; 4078.
[68] Boca, R.; Coord. Chem. Rev. (2004); 248; 757.

(TPA) ligands, are well reviewed in the literature. [69] TPA ligands are known to form mononuclear, five coordinate, trigonal bipyramidal complexes with Co(II). Depending on the steric bulk around the metal centre, there are distortions in the coordination sphere.[70] In these complexes, the Co(II) centres are high spin and a high degree of spin orbit coupling is suggested.[71]

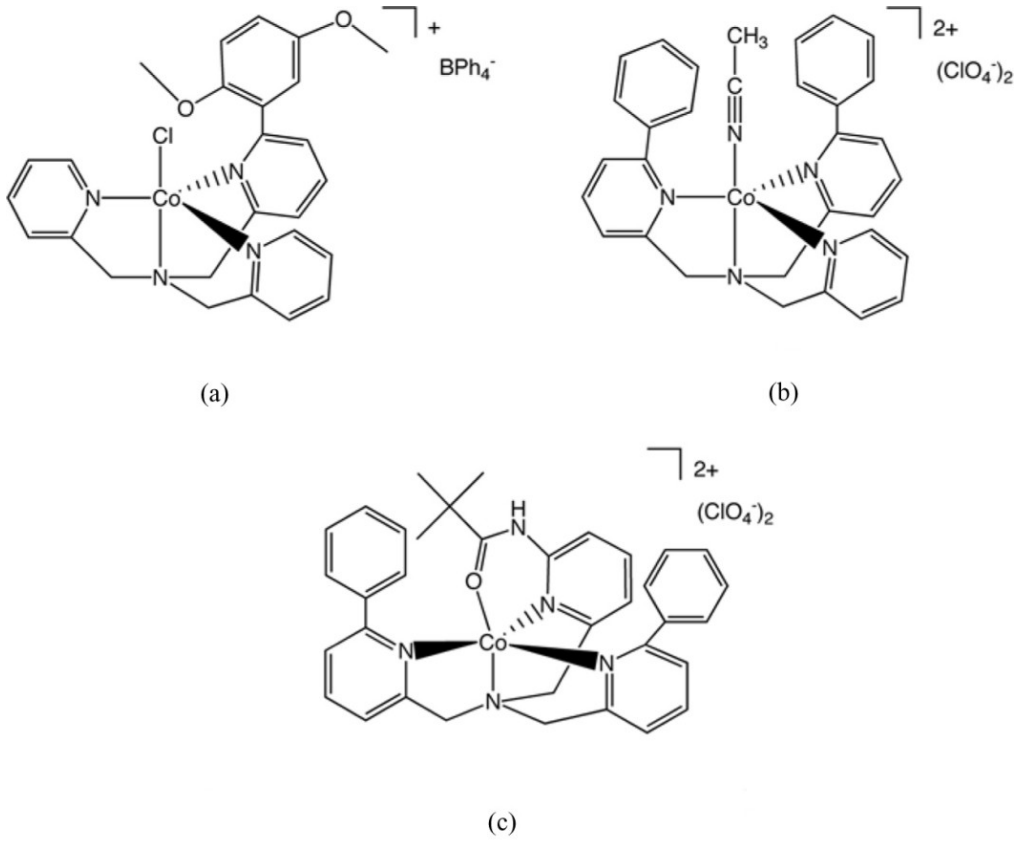

Figure 3.6. Co(II) complexes of TPA ligands: [(6-(2,5-(OMe)$_2$Ph)TPA)CoCl]BPh$_4$ **(a)**, [(6-Ph$_2$TPA)Co(CH$_3$CN)](ClO$_4$)$_2$ **(b)**, and [(bppppa)Co](ClO$_4$)$_2$ (bppppa = (*N*,*N*-bis[(6-phenyl-2-pyridyl)methyl]-*N*-[(6-pivaloylamido-2-pyridyl)methyl]amine)) **(c)**

[69] Berreau, L. M.; Comm. Inorg. Chem. (2007); 28; 123.
[70] Addison, A. W.; Rao, T. N.; Reedijk, J.; van Rijn, J.; Verschoor, G. C.; J. Chem. Soc. Dalton Trans. (1984); 1349.
[71] Jolly, W. L.; The Synthesis and Characterization of Inorganic Compounds (1970); Waveland Press; Prospect Heights, IL.

The use of a rigid chelating N-donor ligand scaffold in the synthesis of Co(II) complexes could yield high spin molecules able to undergo slow magnetic relaxation. Further, a bulky ligand scaffold could be used to induce distortion in the coordination sphere thereby increasing the magnetic anisotropy of the complex and thus the barrier to magnetic relaxation. Our attention was turned to the bis(imino)pyridine ligand family. This family of ligands features a rigid backbone with 3 N-donor ligands. In addition to its rich chemistry[72], substituents at the imine carbons and nitrogens could be varied in order to fine-tune the coordination geometry around the metal centre.

Since their independent publication by Brookhart, Bennett and Gibson,[73] coordination complexes of bis(imino)pyridine ligands with Co(II) and Fe(II) dihalides have been shown, upon activation with MAO, to convert ethylene either to high-density polyethylene or to α-olefins with Schulz–Flory distribution.[73,74] Numerous complexes of various bis(imino)pyridines have been prepared and reported in the literature, with their polymerization activity tuned by modifying the ligand architecture .[75]

---

[72] (a) Vrieze, K.; van Koten, G.; Inorg. Chim. Acta (1985); 100; 79. (b) Knight, P. D.; Clarke, A. J.; Kimberley, B. S.; Jackson, R. A.; Scott, P.; Chem. Commun. (2002); 4; 352. (c) Clentsmith, G. K. B.; Gibson, V. C.; Hitchcock, P. H.; Kimberley, B. S.; Rees, C. W.; Chem. Commun. (2002); 14; 1498. (d) Sugiyama, H.; Gambarotta, S.; Yap, G. P. A.; Wilson, D. R.; Thiele, S. K.-H.; Organometallics (2004); 23; 5054. (e) Bruce, M.; Gibson, V. C.; Redshaw, C.; Solan, G. A.; White, A. J. P.; Williams, D. J.; Chem. Commun. (1998); 2523. (f) Nuckel, S.; Burger, P.; Organometallics (2001); 20; 4345. (g) Reardon, D.; Conan, F.; Gambarotta, S.; Yap, G.; Wang, Q.; J. Am. Chem. Soc. (1999); 121; 9318.

[73] (a) Small, B. L.; Brookhart, M.; J. Am. Chem. Soc. (1998); 120; 7143. (b) Britovsek, G. J. P.; Gibson, V. C.; Kimberley, B. S.; Maddox, S. J.; Solan, G. A.; White, A. J. P.; Williams, D. J.; Chem. Commun. (1998); 849.

[74](a) Small, B. L.; Brookhart, M.; Bennett, A. M. A.; J. Am. Chem. Soc. (1998); 120; 4049. (b) Bennett, A. M. A.; DuPont; WO Patent (1998); 98/27124. (c) Britovsek, G. J. P.; Bruce, M.; Gibson, V. C.; Kimberley, B. S.; Maddox, P. J.; Mastroianni, S.; McTavish, S. J.; Redshaw, C.; Solan, G. A.; Strömberg, S.; White, A. J. P.; Williams, D. J.; J. Am. Chem. Soc. (1999); 121; 8728. (d) Britovsek, G. J. P.; Mastroianni, S.; Solan, G. A.; Baugh, S. P. D.; Redshaw, C.; Gibson, V. C.; White, A. J. P.; Williams, D. J.; Elsegood, M. R. J.; Chem. Eur. J. (2000); 6; 2221.

[75] Bianchini, C.; Giambastiani, G.; Luconi, L.; Meli, A.; Coord. Chem. Rev. (2010); 254; 431.

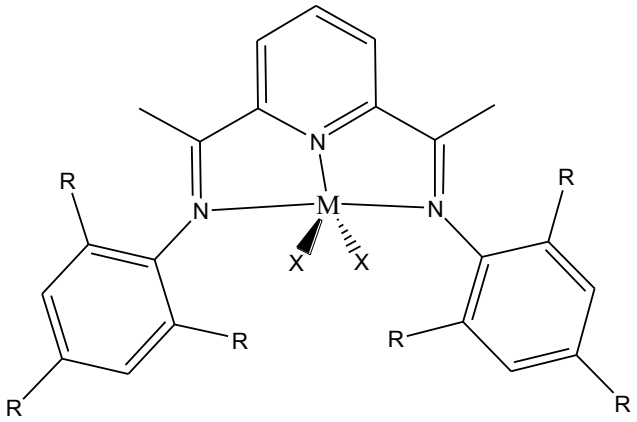

Figure 3.7. General structure of the 2,6-bis(imino)pyridyl Fe(II) or Co(II) dihalide complexes used by Brookhart and Gibson for ethylene polymerization/oligomerization on activation with MAO.

We were also drawn to the recent finding in our lab regarding the unusual bonding interactions shown by an In(I) bis(imino)pyridine complex.[76] In this case, by increasing the steric bulk around the bis(imino)pyridine ligand scaffold, we were successful in the isolation of a low-valent, highly reactive In complex encapsulated in a very weakly coordinating environment was achieved.

Most bis(imino)pyridine complexes of Co(II) are easily accessible through the addition of Co(II) dihalide to the ligand. Reactions yield green crystalline solids. Co(II) centres show room temperature μ_{eff} values ranging from 4.6-5.1 BM, consistent with a high-spin d^7 Co(II) centre.[77] The complexes feature pentacoordinate Co(II) with a coordination geometry varying from

[76] (a) Jurca, T.; Korobkov, I.; Yap, G. P. A.; Gorelsky, S. I.; Richeson, D. S.; Inorg. Chem. (2010); 49; 10635 (b) Jurca, T.; Dawson, K.; Mallov, I.; Burchell, T.; Yap, G. P. A.; Richeson, D. S.; Dalton Trans. (2010); 39; 1266 (c) Jurca, T.; Lummis, J.; Burchell, T.; Gorlesky, S. I.; Richeson, D. S.; J. Am. Chem. Soc. (2009); 131; 4608.

[77] (a) Bianchini, C.; Gatteschi, D.; Giambastiani, G.; Guerrero Rios, I.; Ienco, A.; Laschi, F.; Mealli, C.; Meli, A.; Sorace, L.; Toti, A.; Vizza, F.; Organometallics (2007); 26; 726. (b) Bianchini, C.; Mantovani, G.; Meli, A.; Migliacci, F.; Organometallics (2003); 22; 2545. (c) Sun, W.-H.; Tang, X.; Gao, T.; Wu, B.; Zhang, W.; Ma, H.; Organometallics (2004); 23; 5037. (d) Champouret, Y. D. M.; Fawcett, J.; Nodes, W. J.; Sing, K.; Solan, G. A.; Inorg. Chem. (2006); 45; 9890.(e) Barbaro, P.; Bianchini, C.; Giambastiani, G.; Guerrero Rios, I.; Meli, A.; Oberhauser, W.; Segarra, A. M.; Sorace, L.; Toti, A.; Organometallics (2007); 26; 4639. (f) Bianchini, C.; Giambastiani, G.; Guerrero Rios, I.; Meli, A.; Oberhauser, W.; Sorace, L.; Toti, A.; Organometallics (2007); 26; 5066.

trigonal bipyramidal to square pyramidal depending on the substituents on the N_{Ar} groups. In addition, the presence of a rigid chelating ligand can lead to, in combination with substituent effects, important distortions from ideal geometries.[74]

The bis(imino)pyridine ligand system is a good candidate for the synthesis of complexes that may exhibit slow magnetic relaxation because they are well reviewed, easy to synthesize and tunable. Structures of this ligand framework with Co(II) centres have also been well documented in the literature. This scaffold may be able to provide the necessary coordination environment around a high spin Co(II), maximizing its magnetic anisotropy. This could ultimately lead to complexes displaying slow magnetic relaxation. To this end, we discuss our efforts and findings.

Chapter 4.

Experimental

Unless specified, all reactions were performed in a glovebox under a nitrogen atmosphere, with the exception of ligand synthesis, which was performed using standard Schlenk techniques under a N_2 atmosphere. All solvents were sparged with nitrogen and then dried by passage through a column of activated alumina using an apparatus purchased from Anhydrous Engineering. Cobalt(II) thiocyanate was purchased from Strem Chemicals and used as received. All other chemicals were purchased from Aldrich and used without further purification. NMR spectra were obtained using a Bruker Avance 400 MHz spectrometer. Elemental analyses were performed by Midwest Microlab LLC, Indianapolis IN.

X-Ray Crystallography

Data were collected on a Bruker AXS SMART single crystal diffractometer equipped with a sealed Mo tube source (wavelength 0.71073 Å) APEX II CCD detector. Raw data collection and processing were performed with APEX II software package from BRUKER AXS.[78] Structures were solved by Dr. Ilia Korobkov of the department of chemistry at the University of Ottawa.

Magnetic Measurements

The magnetic susceptibility measurements were obtained using a Quantum Design SQUID magnetometer MPMS-XL7 operating between 1.8 and 300 K for dc-applied fields ranging from −7 to 7 T. Direct current (dc) susceptibility measurements were performed on freshly filtered

[78] APEX Software Suite v.2010; Bruker AXS: Madison, WI, 2005.

crushed polycrystalline sample of **5.3** (19.9 mg) and **5.4** (10.1 mg), wrapped in a polyethylene membrane. Sample preparation was carried out rapidly in order to avoid any solvent loss. Alternating current (ac) susceptibility measurements were carried out under an oscillating ac field of 3 Oe and ac frequencies ranging from 1 to 1500 Hz. In order to eliminate intermolecular interactions in **5.4**, crystals (18.2mg) were fully dissolved in THF in a sealed tube and dc and ac susceptibility measurements were carried out on the resulting frozen solution below 50 K. A diamagnetic correction was applied for the sample holder and Pascal constants were used for the diamagnetic correction of the sample. The magnetization data were collected at 100 K to check for ferromagnetic impurities that were absent in all samples. Magnetic measurements were carried out by Po-Heng Lin of the department of chemistry at the University of Ottawa.

1. Synthesis of dendrimer core and terminal groups

1.1 t-Butyl Azide (^{t}Bu)[79]

A 5.6M H_2SO_4 solution was prepared by addition of 550 g H_2SO_4 to 550 g H_2O over 10 min, with strong stirring in an ice cooled 1-liter flask. The solution was cooled to 0-5^{o}C and sodium azide (72 g, 1.1 mol) was added over 10 minutes while stirring and maintaining the temperature between 0-5°C. When all of the NaN_3 had dissolved, t-butyl alcohol (74 g, 1.0 mol) was added. The resulting solution was stirred for *5* min and allowed to stand at room temperature for 24 h. The solution was stirred for a further *5* min, and allowed to stand for an additional 6 h. The t-butyl azide was isolated using a separatory funnel, washed with 50 ml of 2 M NaOH and dried

[79] Bottaro, J. C.; Penwell, P. E.; Schmitt, R. J.; Synth. Comm. (1997); 27; 1465.

over Na_2SO_4 to give a clear liquid. The product was then decanted into a bottle for long-term storage. Obtained 75.24 g (76%). 1H NMR ($CDCl_3$, 400MHz) δ 1.245 (s, 9H).

1.2 Benzyl azide (Bn)[80]

To a 250 mL round bottom flask equipped with a magnetic stir bar, was added a 0.5 M solution of NaN_3 (1.43 g, 22 mmol) in DMSO (44 mL) at room temp. After stirring for 24 h, benzyl bromide (2.4 mL, 20 mmol) was added, and the mixture was stirred for 2 h. The reaction was quenched with ~100 mL water (slightly exothermic) and then allowed to warm up to room temperature while stirring. The product was then extracted with Et_2O (3 × 50 mL). The combined organic portions were washed with water (4×100 mL) and once with brine (100 mL) and dried over $MgSO_4$, filtered, and the solvent removed *in vacuo* to afford pure benzyl azide as a pale yellow oil (2.2 g, 82% yield). ^{1}H NMR ($CDCl_3$, 400MHz): δ 7.41-7.30 (m, 5H), 4.33 (s, 2H).

1.3 2,4,6-Tris(prop-2-ynyloxy)-1,3,5-triazine (Trz)[81]

Propargyl alcohol (10 ml) was added slowly to a suspension of cyanuric chloride (2.2 g, 12.1 mmol) in 15 ml THF at room temperature. K_2CO_3 (5.2 g, 36.3 mmol) was then added to the reaction mixture. The reaction mixture was refluxed at 60°C overnight. The reaction mixture was filtered and dried *in vacuo*. The residue was then dissolved in 80 ml CH_2Cl_2, and washed with dilute citric acid (10%) and saturated brine. The residue solution was then dried over

[80] Pardin, C.; Roy, I.; Lubell, W. D.; Keillor, J. W.; Chem. Biol. Drug. Des. (2008); 72; 189.
[81] Wu, P.; Feldman, A. K.; Nugent, A. K.; Hawker, C. J.; Scheel, A.; Voit, B.; Pyun, J.; Fréchet, J. M. J.; Sharpless, K. B.; Fokin, V. V.; Angew. Chem. Int. Ed. (2004); 43; 3928.

$MgSO_4$ and evaporated to give the product as white solid (1.91g, 87% yield). 1H NMR (Acetone, 400 MHz): δ 3.13 (t, 3H), 5.10 (d, 6H).

2. Attempted Synthesis of Dendrimers

2.1 Trz-Bn[G1]

To a round bottom flask equipped with a stir bar was added 2,4,6-Tris(prop-2-ynyloxy)-1,3,5-triazine (0.72g, 3.00 mmol) and benzyl azide (1.2g, 9.00 mmol). The mixture was dissolved in 20 ml of 1:1 ^{t}BuOH/H_2O solution. Sodium ascorbate (0.18g, 0.90 mmol, 10 mol%.) was added as a solid, followed by the addition of $CuSO_4.5H_2O$ (0.11g, 0.45 mmol, 5 mol%). The reaction was stirred overnight at room temperature. The white cloudy suspension was diluted with 10 ml H_2O and 1 ml concentrated NH_4OH, stirred for 10 minutes, and then filtered. The resulting filtrate was washed 3 times with 10 ml H_2O and dried to obtain an off white solid. NMR data was inconclusive.

2.2 Trz-^{t}Bu[G1]

To a round bottom flask equipped with a stir bar was added 2,4,6-Tris(prop-2-ynyloxy)-1,3,5-triazine (0.72g, 3.00 mmol) and tert-butyl azide (0.89g, 9.00 mmol). The mixture was dissolved in 20 ml of 1:1 ^{t}BuOH/H_2O solution. Sodium ascorbate (0.18g, 0.90 mmol, 10 mol%) was added as a solid, followed by the addition of $CuSO_4.5H_2O$ (0.11g, 0.45mmol, 5 mol%). The reaction was stirred overnight at room temperature. The white cloudy suspension was diluted with 10 ml H_2O and 1 ml concentrated NH_4OH, stirred for 10 minutes, and then filtered. The resulting

filtrate was washed 3 times with 10 ml H_2O and dried to obtain an off white solid. NMR data indicated an impure product.

2.3 Attempted 1-pot Synthesis of dendrimer [82]

To a round bottom flask equipped with a stir bar benzyl bromide (103 mg, 6.00 mmol) was mixed with 2,4,6-Tris(prop-2-ynyloxy)-1,3,5-triazine (490 mg, 2.00 mmol). To this mixture were added L-proline (140 mg, 1.2 mmol, 20 mol%), Na_2CO_3 (127 mg, 1.2 mmol, 20 mol%), NaN_3 (400 mg, 6.00 mmol), sodium ascorbate (238 mg, 1.2 mmol, 20 mol%), 9:1 DMSO/ H_2O (15 mL), and $CuSO_4.5H_2O$ (150 mg, 0.6 mmol, 10 mol%). The mixture was heated overnight at 65°C. The crude mixture was then poured into dilute NH_4OH (30 mL), and extracted with ethyl acetate (3 x 20 mL). The organic layer was washed with brine (2 x 20 mL), dried over $MgSO_4$, and evaporated to yield a yellow oil. NMR data indicated an impure product.

2.4 Attempted Inorganic Synthesis of Dendrimers [83]

A THF (20ml) solution of 2,4,6-Tris(prop-2-ynyloxy)-1,3,5-triazine (490 mg, 2.00 mmol), benzyl azide (800 mg, 6.00 mmol), N,N-diisopropylethylamine (480 mg, 3.70 mmol), and $Cu(PPh_3)_3Br$ (110 mg, 1,23 mmol) were placed in a microwave reaction vessel. The tube was sealed and was subjected to microwave irradiation at 600W and a temperature of 140°C for 5 minutes. A deep red oil was obtained. NMR data was inconclusive. Attempts to purify product by column chromatography were unsuccessful.

[82] Feldman, A. K.; Colasson, B.; Fokin, V. V.; Org. Lett. (2004); 6; 3897.

[83] Malkoch, M.; Schleicher, K.; Drockenmuller, E.; Hawker, C. J.; Russell, T. P.; Wu, P.; Fokin, V. V.; Macromolecules (2005); 38; 3663.

3. Attempted Synthesis of dendrimer complexes

In a typical attempt, a THF solution of the crude dendrimer product Trz-Bz[G1] (150mg, 0.233mmol, 1eq.) or Trz-^{t}Bu[G1] (150 mg, 0.270 mmol, 1 eq.) was mixed with $CoCl_2.6H_2O$ (164 mg, 0.699 mmol, 3 eq. or 193 mg, 0.811 mmol, 3 eq. respectively). The reaction mixture was stirred overnight to yield a light blue solution. The reaction mixture was then dried *in vacuo* to yield a mixed, blue and white impure solid. All subsequent attempts to synthesize dendrimer complexes yielded no reaction.

4. Synthesis of Ligands

4.1 2,6-Bis(chloromethyl)pyridine[84]

Thionyl chloride (150 ml, 2.06 mol) was slowly added to 2, 6-pyridinemethanol (10 g, 0.07mol) cooled on an ice bath to 0 ^{o}C, with stirring. The mixture was then allowed to warm on the water-bath for 4 hours. The reaction mixture was then cooled, and treated with benzene until a precipitate formed (hydrochloride salt). The precipitated hydrochloride was collected, washed with benzene, dried, dissolved in water, and neutralised with sodium hydrogen carbonate. The crude product was collected and crystallised from light petroleum (b.p. 40-60 ^{o}C) to afford the pure 2,6-bis(chloromethyl)pyridine as white needles (8.0 g, 65% yield). M.P. 72.8-73.7 ^{o}C.

[84] Baker, W.; Buggle, K. M.; McOmie, F. W.; Watkin; D. A. M.; J. Chem. Soc. (1958); 3594.

4.2 2,6-Bis(methylthiomethyl)pyridine[85]

To an ice-cooled solution of 2,6-bis(chloromethyl)pyridine (3.52 g, 20 mmol) in DMF (50 ml) was added sodium methanethiolate (3.1 g, 44 mmol) and the mixture was allowed to warm to room temperature. After 24 h of stirring the solvent was evaporated and the resulting residue partitioned between chloroform (200 ml) and water (100 ml). The organic phase was washed with water, dried over Na_2SO_4 and evaporated to dryness to give an oily product. The pure product was isolated by column chromatography over silica gel eluted with chloroform to yield pure 2,6-bis(methylthiomethyl)pyridine as a pale yellow oil. (3.41 g, 86% yield). ^{1}H NMR ($CDCl_3$, 400MHz): δ 7.64 (t, 1H), 7.23 (d, 2H), 3.78 (s, 4H), 2.05 (s, 6H).

4.3 2,6-Bis[1-(2,6-diisopropylphenylimino)ethyl]pyridine[86]

2,6-Diisopropylaniline (8.7 mL, 46.1 mmol) was added to a solution of 2,6-diacetylpyridine (2.5 g, 15.3 mmol) in absolute methanol (50 mL). After the addition of several drops of formic acid, the reaction mixture was refluxed for 24 h and then allowed to cool down to room temperature. The crude product precipitated as yellow powder. Pure 2,6-Bis[1-(2,6-diisopropylphenylimino)ethyl]pyridine was obtained by recrystallization from methanol (6.35g, 86% yield). 1H NMR (400 MHz, $CDCl_3$): δ 8.47 (d, 2 H), 7.95 (t, 1 H), 7.25-7.15 (m, 6 H), 2.78 (sept, 4 H), 2.30 (s, 6 H), 1.19 (dd, 24 H).

[85] Canovese, L.; Chessa, G.; Marangoni, G.; Pitteri, B.; Uguagliati, P.; Visentin, F.; Inorganica Chimica Acta, (1991); 186; 79.
[86] Fan, R.-Q.; Zhu, D.-S.; Mu, Y.; Li, G.-H.; Yang, Y.-L.; Su, Q.; Feng, S.-H.; Eur. J. Inorg. Chem. (2004); 4891.

4.4 2,6-Bis{[2,6-di(isopropyl)phenyl)imino]benzyl}pyridine[75(b)]

A mixture of 2,6-dibenzoylpyridine (5.0 g, 17.4 mmol), 2,6-diisopropylaniline (7.5 g, 38.3 mmol), and p-toluenesulfonic acid (0.2 mg) in toluene (50 mL) was placed in a round bottom flask equipped with a Dean–Stark trap. Under a nitrogen atmosphere, the reaction mixture was heated to reflux in an oil bath at 140 ^{o}C for 48 h then cooled to room temperature and the solvent was removed under vacuum to give a dark yellow oil. Hexanes were added and a small quantity of a white solid was removed by filtration. The filtrate was evaporated under vacuum yielding a dark yellow oil. Methanol (~400 mL) was added to this oil and the mixture was stirred for several minutes, causing the product to precipitate as a yellow solid which was filtered off and rinsed with methanol. The filtrate was reduced to about half the initial volume under vacuum, and then placed in a refrigerator, causing additional product to precipitate, which was filtered off and rinsed with methanol. The product was obtained as a yellow powder. Yield: 7.2 g (68%). 1H NMR (T = 115^{o}C, d6-dimethyl sulfoxide, 300 MHz): δ 7.82 (br t, 1 H), 7.55–7.20 (br m, 12 H), 6.94 (br s, 6H), 2.90 (m, 4H), 1.00 (d, 24H).

5. Synthesis of complexes

5.1 [Co[2,6-Bis(methylthiomethyl)pyridine]Br_2]

$CoBr_2$ powder (150 mg, 0.69mmol) was added to a clear yellow solution of 2,6-Bis(methylthiomethyl)pyridine (151 mg, 0.76 mmol) in 5 mL of toluene. The reaction mixture was sealed and allowed to stir for 6 h. A color change from translucent yellow to translucent blue was observed after a few hours of stirring. The solution was then held at -20^{o}C for 48 h, to produce a light blue precipitate. The reaction mixture was filtered; the solid was washed with 3

x 5 mL hexanes, and dried under vacuum. The product, a light blue powder, was isolated in 93% yield. Crystals suitable for X-ray analysis were grown by slow vapor diffusion of hexanes into a saturated solution of THF at -20^{o}C for several days. Elemental Analysis for [$C_7H_9Br_2CoNS_2$] Calcd. C 25.86, H 3.13, N 3.35, Found C 25.88, H 2.94, N 3.22

5.2 [Co[2,6-Bis{1-[(2,6-diisopropylphenyl)imino]benzyl}pyridine](Br)$_2$]

$CoBr_2$ powder (150 mg, 0.69 mmol) was added to a clear yellow solution of 2,6-Bis{1-[(2,6-diisopropylphenyl)imino]benzyl}pyridine (460 mg, 0.76 mmol) in 5 mL of toluene. The reaction mixture was sealed and allowed to stir for 6 h. A color change from translucent yellow to translucent brown was observed after a few hours of stirring. The solution was then held at -20^{o}C for 48 h, to produce a light brown precipitate. The reaction mixture was filtered, the solid was washed with 3 x 5 mL hexanes, and dried under vacuum. The product, a light brown powder, was isolated in 95% yield. Crystals suitable for X-ray analysis were grown by slow vapor diffusion of hexanes into a saturated solution of chlorobenzene at -20^{o}C for several days. Elemental Analysis for [$C_{43}H_{47}Br_2CoN_3$] Calcd. C 62.63, H 5.75, N 5.10, Found C 62.61, H 5.78, N 5.03

5.3 [Co[2,6-Bis{1-[(2,6-diisopropylphenyl)imino]ethyl}pyridine](NCS)$_2$]

$Co(SCN)_2$ powder (99 mg, 0.567 mmol) was added to a clear yellow solution of 2,6-Bis[1-(2,6-diisopropylphenylimino)ethyl]pyridine (300 mg, 0.623 mmol) in 5 mL of toluene. The reaction mixture was sealed and allowed to stir for 6 h. A color change from translucent yellow to translucent green was observed after a few hours of stirring. The solution was then held at -

20^{o}C for 48 h, to produce a light green precipitate. The reaction mixture was filtered; the solid was washed with 3 x 5 mL hexanes, and dried under vacuum. The product, a light green powder, was isolated in 97% yield. Crystals suitable for X-ray analysis were grown by slow vapor diffusion of hexanes into a moderately saturated solution of CH_2Cl_2 at -20^{o}C for several days. Elemental analysis performed on crystals grown by layering hexanes into a saturated solution of CH_2Cl_2. Elemental Analysis for $[C_{35}H_{43}CoN_5S_2]_3[CH_2Cl_2]$: Calcd. C 61.94, H 6.42, N 10.22, Found C 62.28 H 6.40, N 10.25.

5.4 [Co[2,6-Bis{1-[(2,6-diisopropylphenyl)imino]benzyl}pyridine](NCS)$_2$]

$Co(NCS)_2$ powder (56 mg, 0.320 mmol) was added to a clear yellow solution of 2,6-Bis{1-[(2,6-diisopropylphenyl)imino]benzyl}pyridine (200 mg, 0.330 mmol) in 5 mL of toluene. The reaction mixture was sealed and allowed to stir for 6 h. A color change from translucent yellow to translucent brown was observed after a few hours of stirring. The solution was then held at -20 ^{o}C for 48 h, to produce a light brown precipitate. The reaction mixture was filtered, the solid was washed with 3 x 5 mL hexanes, and dried under vacuum. The product, a light brown powder, was isolated in 95% yield. Crystals suitable for X-ray analysis were grown by slow vapor diffusion of hexanes into a saturated solution of THF at -20 ^{o}C for several days. Elemental analysis for $[C_{45}H_{47}CoN_5S_2]$: Calcd. C 69.21, H 6.07, N 8.97, Found C 68.95, H 5.99, N 8.88.

Chapter 5.

Results and Discussion

5.1 Synthesis of Dendrimer and Dendrimer Complexes

"Click" reactions were first rediscovered in 2001 by Kolb, Finn and Sharpless as a new strategy for the organic synthesis of functional molecules, developed in particular to meet the growing demands of drug synthesis.[87] This strategy was described by the authors as "the reinvigoration of an old style of organic synthesis".[88]

The discovery was inspired by observation of the natural synthesis of primary metabolites and realising that, in contrast to secondary metabolites (which are substances not directly involved in the organisms growth and development of the organism), the three major families of primary metabolites: polypeptides, polynucleotides and polysaccharides; are constructed from small building blocks utilizing carbon-heteroatom bonds. In a sense, nature is also its own kind of combinatorial chemist, as the strategies used are similar: building larger architectures from small building blocks, and achieves a large diversity of macromolecules from a relatively small number of building blocks.[89]

Click chemistry was developed as described by the authors "In an endeavour to generate substances by joining small units together with heteroatom links (C-X-C). The goal is to develop an expanding set of powerful, selective, and modular "blocks" that work reliably in

[87]Moses, J. E.; Moorhouse, A. D.; Chem. Soc. Rev. (2007); 36; 1249.
[88]Kolb, H. C.; Finn, M. G.; Sharpless, K. B.; Angew. Chem. Int. Ed. (2001); 40; 2004.
[89] (a) Gokel, G.; Lüdke, G.; Ugi, I.; Isonitrile Chemistry (Ed.: I. Ugi); Academic Press, New York, (1971); pp. 145 -199; (b) Ugi, I.; Meyr, R.; Fetzer, U.; Steinbrückner, C.; Angew. Chem. (1959); 71; 386.

both small- and large-scale applications. We have termed the foundation of this approach "click chemistry", and have defined a set of stringent criteria that a process must meet to be useful in this context. The reaction must be modular, wide in scope, give very high yields, generate only inoffensive byproducts that can be removed by nonchromatographic methods, and be stereospecific (but not necessarily enantioselective). The required process characteristics include simple reaction conditions (ideally, the process should be insensitive to oxygen and water), readily available starting materials and reagents, the use of no solvent or a solvent that is benign (such as water) or easily removed, and simple product isolation. Purification, if required, must be by nonchromatographic methods, such as crystallization or distillation, and the product must be stable under physiological conditions."[86]

What is considered as the archetypal example of click chemictry is the Cu(I) catalyzed alkyne-azide cycloadditions (CuAAC) to yield 1,2,3-triazoles.[90] The CuAAC reaction was first reported in 2002 by Sharpless and Meldal independently. In the absence of an appropriate catalyst, this reaction is usually quite slow due to the poor 1,3-dipole acceptor ability of alkynes. However, in the presence of copper(I), which can bind to terminal alkynes, cycloaddition reactions are dramatically accelerated, regioselective, and highly efficient (yields are often above 95%). Moreover, the CuAAC reaction can be performed in various solvents (including water) and in the presence of numerous other functional groups.[91]

[90] (a) Huisgen, R.; Angew. Chem. (1963); 75; 604; Angew. Chem. Int. Ed. Engl. (1963); 2; 565. (b) Huisgen, R.; Angew. Chem. (1963); 75; 742; Angew. Chem. Int. Ed. Engl. (1963); 2; 633.

[91] (a) Rostovtsev, V. V.; Green, L. G.; Fokin, V. V.; Sharpless, K. B.; Angew. Chem. (2002); 114; 2708; Angew. Chem. Int. Ed. (2002); 41; 2596. (b) Tornoe, C. W.; Christensen, C.; Meldal, M.; J. Org. Chem. (2002); 67; 3057.

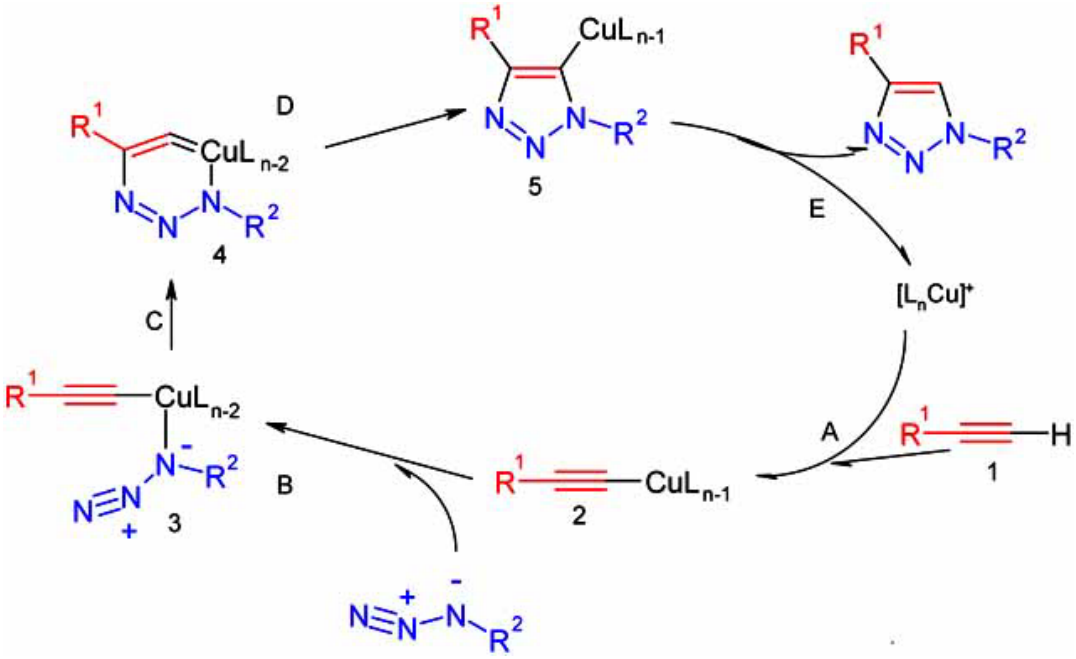

Figure 5.1. Mechanism of the Cu(I)-catalyzed azide/alkyne 1,3-dipolar cycloaddition reaction[92]

The CuAAC reaction has since then developed significantly and now employs various types of Cu(I) catalysts. The most well known catalyst system involves $CuSO_4$/sodium ascorbate. This system has been used and proven effective for synthesis of 1,2,3-triazoles. It is considered the standard catalyst system for this type of reaction. More specialized catalysts and stabilizers for the original Cu(I) catalyst have been developed and are employed[93]. However the $CuSO_4$/sodium ascorbate system still is the most widely used.

Although this methodology was initially developed as a ligation tool for small molecules, it was postulated that this synthetic strategy could have enormous potential in material science. [90,94] This was first illustrated in 2004 by Sharpless, Fokin and Frechet.[95] This was

[92] Binder, W. H.; Kluger, C.; Curr. Org. Chem. (2006); 10; 1791.
[93] (a) Chan, T. R.; Hilgraf, R.; Sharpless, K. B.; Fokin, V. V.; Org. Lett. (2004); 6; 2853. (b) Candelon, N.; Lastécouères, D.; Diallo, A. K.; Aranzaes, J. R.; Astruc, D.; Vincent, J.-M.; Chem. Commun. (2008); 741.
[94] Hawker, C. J.; Wooley, K. L.; Science (2005); 309; 1200.

followed by an increase in the popularity of click chemistry within the materials science community and was, in particular, significantly boosted by the influential works of Hawker, Frechet, and Finn.[96] This synthetic strategy has been used for the design of functional materials such as rotaxanes[97], functionalized linear or three-dimensional polymer chains,[95(a)] and even for the convergent synthesis of dendrimers.[94]

The field of dendrimers has also developed from the basic, low yielding, organic macromolecules to include numerous metallocene containing dendrimers that have shown redox, molecular sensing and catalyst activities (Figure 5.2).[98] We were keen on expanding upon the already rich chemistry of dendrimers, by attempting to design a spin-crossover dendrimer. In addition, click reactions have been already proven as a synthetic methodology for dendrimers, therefore we postulated that click chemistry would provide a straightforward synthetic strategy for the design of our dendritic framework.

---

[95] Wu, P.; Feldman, A. K.; Nugent, A. K.; Hawker, C. J.; Scheel, A.; Voit, B.; Pyun, J.; Fréchet, J. M. J.; Sharpless, K. B.; Fokin, V. V.; Angew. Chem. (2004); 116; 4018; Angew. Chem. Int. Ed. (2004); 43; 3928.

[96] (a) Diaz, D. D.; Punna, S.; Holzer, P.; McPherson, A. K.; Sharpless, K. B.; Fokin, V. V.; Finn, M. G.; J. Polym. Sci. Part A (2004); 42; 4392. (b) Helms, B.; Mynar, J. L.; Hawker, C. J.; Fréchet, J. M. J.; J. Am. Chem. Soc. (2004); 126; 15020. (c) Joralemon, M. J.; O'Reilly, R. K.; Hawker, C. J.; Wooley, K. L.; J. Am. Chem. Soc. (2005); 127; 16892. (d) Joralemon, M. J.; O'Reilly, R. K.; Matson, J. B.; Nugent, A. K.; Hawker, C. J.; Wooley, K. L.; Macromolecules (2005); 38; 5436. (e) Malkoch, M.; Schleicher, K.; Drockenmuller, E.; Hawker, C. J.; Russell, T. P.; Wu, P.; Fokin, V. V.; Macromolecules (2005); 38; 3663.

[97] (a) van Steenis, D. J. V. C.; David, O. R. P.; van Strijdonck, G. P. F.; van Maarseveen, J. H.; Reek, J. N. H.; Chem. Commun. (2005); 4333. (b) Dichtel, W. R.; Miljanic, O. S.; Spruell, J. M.; Heath, J. R.; Stoddart, J. F.; J. Am. Chem. Soc. (2006); 128; 10388. (c) Zhu, Y.; Huang, Y.; Meng, W.-D.; Li, H.; Qing, F.-L.; Polymer (2006); 47; 6272.

[98] (a) Astruc, D.; Ornelas, C; Ruiz, J.; Acc. Chem. Res. (2008); 41; 841. (b) Astruc, D.; Ornelas, C.; Aranzaes, J. R.; J. Inorg. Organomet. Polym. (2008); 18; 4.

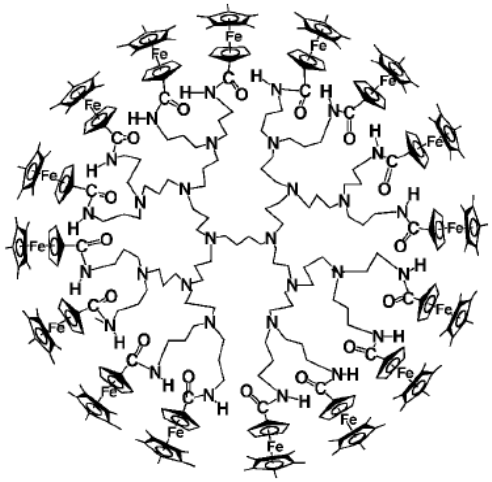

Figure 5.2. Example of a metallocenyl terminated dendrimer showing redox activity.

We had postulated that the presence of TM atoms within certain dendritic frameworks might lead to spin crossover behaviour. This was largely due to the fact that triazoles are known ligands for spin crossover compounds. Lastly, recent reports from Gütlich and coworkers[46] where they were able to successfully show spin crossover behaviour in Fe(II) poly(benzyl)ether dendrons (Figure 5.3) have motivated us to expand upon this effort, incorporating Co(II) ions within dendrimers with the purpose of obtaining spin crossover behaviour.

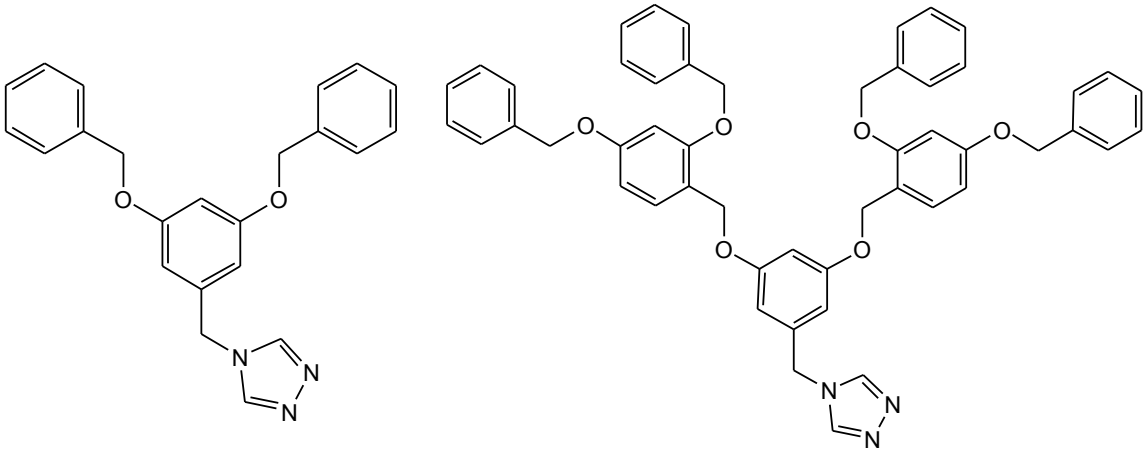

Figure 5.3. First and second generation poly(benzyl)ether dendrons synthesized by Gütlich (modified from ref. 97)

To this end I began efforts in the synthesis of a first generation dendrimer, following the procedure published by Frechet, Sharpless and Fokin.[80] I opted to create a nitrogen rich environment within the dendrimer in order to maximize the possibility of spin crossover behaviour. I chose 2,4,6-Tris(prop-2-ynyloxy)-1,3,5-triazine (Figure 5.4.(a)) as the core due to the presence of nitrogen atoms within its benzene ring. To complete the first generation dendrimer, I chose benzyl azide and t-butyl azide (Figure 5.4.(c)) as terminal groups. The aim in varying the terminal group was to examine the possible effects of steric bulk, the presence or absence of π-interactions on the spin crossover behaviour. Lastly, I chose 2-Chloro-N,N-di-prop-2-ynyl-acetamide (Figure 5.4. (b)) as a focal group for the purpose of expanding the dendritic architecture if needed.

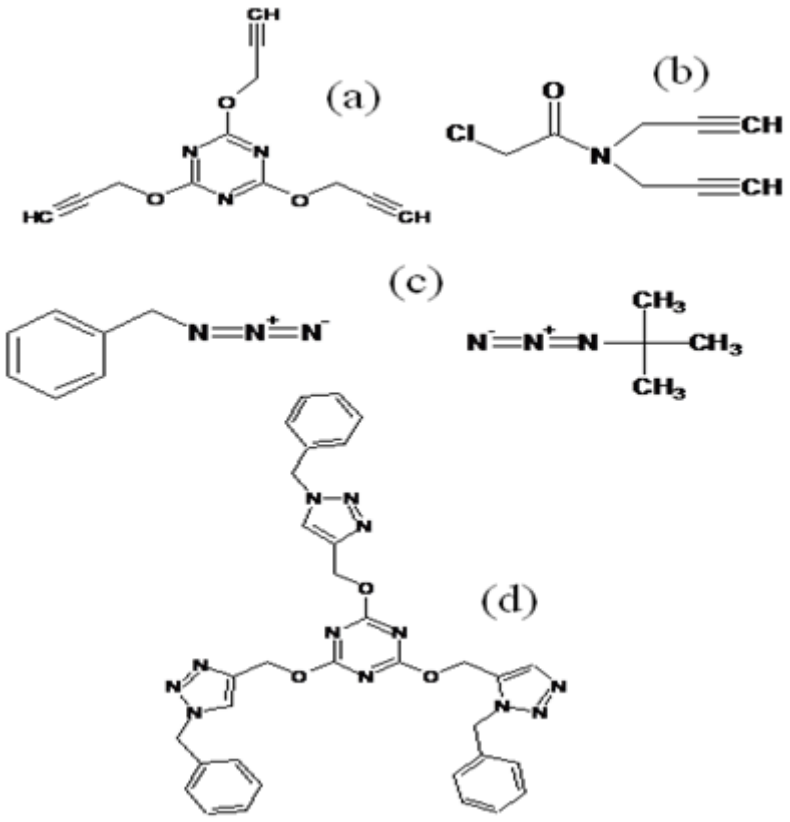

Figure 5.4. Structural formulae of chosen dendrimer core (a), focal point (b), terminal group (c) and a synthesized G-1 dendrimer (d)

The dendrimer core was easily synthesized by the reaction of cyanuric chloride with propargyl alcohol in the presence of K_2CO_3. NMR data indicated a pure product. Similarly, the synthesis of both terminal groups was successfully accomplished with NMR data indicating pure products. The synthetic methodology was scaled up in order to generate a stock solution of both compounds for later use.

The synthesis of the first generation dendrimer was unsuccessful. All attempts at synthesizing the first generation dendrimer in aqueous conditions, utilizing either of the terminal groups, gave impure products and incomplete reactions. The catalyst loading was varied from 5 mol% to 15 mol%. However, the final appearance of the product, as well as spectral data, indicated a similar outcome. Further, we attempted the synthesis in organic media, and utilizing the Cu(I) catalyst $(PPh_3)_3CuBr$ at different catalyst loadings, however these reactions met the same fate as their aqueous counterparts.

A one-pot synthesis of the dendrimer from *in-situ* generated azides was also attempted in a fashion similar to the one described by Fokin. However this methodology did not seem to yield any reaction, possibly due to the nature of the reactants. Our last strategy to synthesize dendrimer complexes were *in-situ* complexation reactions. We had postulated that even though the reaction did not go to completion, it may still be possible to obtain and crystallize a complex of a first generation dendrimer or an incomplete dendrimer, which could serve as a starting point for further investigation. However, numerous attempts using this methodology yielded no reaction.

In light of the numerous unsuccessful attempts, we decided to turn our attention towards a different direction. However, it was later revealed that the dendrimer synthesis is

indeed possible, as demonstrated by a visiting student in our research group, Mahshid Hamzehlooian. She was able to successfully isolate a pure first generation dendrimer and has proved its purity by means of NMR and mass spectrometry. I would like to acknowledge her for her efforts which demonstrated the concept and strategy were indeed valid.

5.2 Synthesis of a Mononuclear Co(II) based SMM

5.2.1 Ligand Synthesis

We turned our attention to the synthesis of SMMs with the aim of obtaining mononuclear complexes whose SMM properties were enhanced by spin-orbit coupling. Recently Chang and Long have reported mononuclear Fe(II) complexes with enhanced spin-orbit coupling resulting from structural distortion within the coordination sphere.[60] To achieve this, we focused our attention to complexes of Co(II) as cobalt has an inherently high orbital angular momentum.

Two ligand scaffolds were attractive to us as good candidates. The bis(imino)pyridine ligand scaffold was chosen as Co(II) complexes containing this ligand are widely known and used as olefin polymerization catalysts. Their Co(II) complexes are known and reported in the literature, however the magnetic properties of complexes of this ligand have not been widely explored. The second ligand scaffold was the bis(methyl)thiomethylpyridine ligand scaffold. Ruthenium and copper complexes of this ligand have been synthesized and reported. Similar to

the bis(imino)pyridine complexes, the magnetic properties of complexes of this ligand system have not been explored.[99]

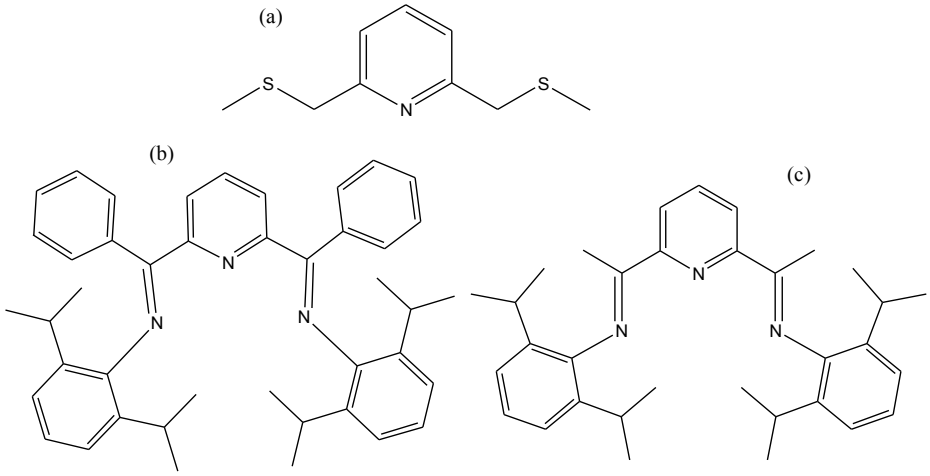

Figure 5.5. Ligands for synthesis of mononuclear Co(II) complexes (a) 2,6-Bis(methylthiomethyl)pyridine (compound 4.2) (b) 2,6-Bis{[2,6-di(isopropyl)phenyl)imino]benzyl}pyridine (compound 4.4) (c) 2,6-Bis[1-(2,6-diisopropylphenylimino)ethyl]pyridine (compound 4.3)

The bis(methyl)thiomethyl pyridine was synthesized in a two step process according to published procedures.[83, 84] The first step involves the reaction of thionyl chloride with 2,6-pyridinemethanol at 0 ^{o}C to yield the bis(chloromethyl)pyridine compound isolated by recrystallization from light petroleum ether. The second step was the reaction of the bis(chloromethyl)pyridine product with sodium methanethiolate in DMF to yield a crude product which is purified by column chromatography. The identities of both compounds were confirmed and were in good agreement with published melting point and spectral data.

With the bis(imino)pyridine ligand scaffold we were able to access two ligand systems both synthesized according to literature procedures. Compound 4.4, possessing phenyl

[99] (a) Klerman, Y.; Ben-Ari, E.; Yael Diskin-Posner, Y.; Leitus, G.; Shimon, L.; Ben-Davida, Y.; Milstein, D.; Dalton Trans. (2008); 3226. (b) Bassetti, M.; Capone, A.; Mastrofrancesco, L.; Salamone, M.; Organometallics (2003); 22; 2535. (c) Constable, E. C.; King, A. C.; Raithby, P. R.; Polyhedron (1998); 17; 4275.

substituents on the imino carbon sites, was synthesized according to a methodology developed by our lab[75(b)] and we were able to prepare the compound with a good yield and its spectral data were in good agreement with the published data. The second compound was the dimethyl bis(imino)pyridine (compound 4.3) and was synthesized according to a procedure published by Feng and coworkers involving the condensation reaction of 2,6-diisopropylaniline with 2,6-diacetylpyridine in methanol with formic acid as a catalyst.[84] The product was also obtained with good yield and spectral data were in good agreement with published data.

5.2.2 Synthesis of Co(II) Complexes

Co (II) complexes of the bis(imino)pyridine ligand scaffold as well as the bis(methyl)thiomethyl pyridine ligand scaffold have been synthesized. All the reactions were carried out under anaerobic conditions.

Complexes were synthesized by the direct reaction of Co(II) salts with the desired ligand in a suitable solvent. We were able to isolate the Co(II) bromide complex of bis(methyl)thiomethylpyridine: [Co[2,6-Bis(methylthiomethyl)pyridine]Br_2] (compound 5.1), the Co(II) bromide complex of the 2,6-Bis{1-[(2,6-diisopropylphenyl)imino]benzyl}pyridine ligand: [Co[2,6-Bis{1-[(2,6-diisopropylphenyl)imino]benzyl}pyridine]$(Br)_2$] (compound 5.2) and the Co(SCN)2 complexes of both bis(imino)pyridine ligands: [Co[2,6-Bis{1-[(2,6-diisopropylphenyl)imino]ethyl}pyridine]$(NCS)_2$] and [Co[2,6-Bis{1-[(2,6-diisopropylphenyl)imino]benzyl}pyridine]$(NCS)_2$] (compounds 5.3 and 5.4 respectively) (Figure 5.6). Structures were determined by single crystal X-ray diffraction. These compounds display five coordinate ligand arrays. There are two classical coordination geometries associated with five ligands: trigonal bipyramidal (tbp) and square pyramidal (sp). These two coordination

geometries can be distinguished by using the "tau" parameter (τ). This parameter is calculated by the following relationship [τ = (β- α)/60]. In this formula, β and α are the two largest angles observed in the coordination sphere of the metal. In the case of a tbp geometry, the largest angle is between the axial groups at 180^{o} = β and the second largest angle would be 120^{o} = α. These values lead to a τ = (180-120)/60 = 1. In contrast, for an sp geometry, the two largest interligand angles are between groups in the basal plane and are 180^{o}. The resulting τ value would be τ = (180-180)/60 = 0. Compounds with intermediate values can be considered distorted tbp or sp depending on whether the τ parameter is less than or greater than 0.5. Compounds 5.1-5.4 have τ parameters of 0.499, 0.135, 0.267 and 0.035 respectively indicating distorted tbp geometries.

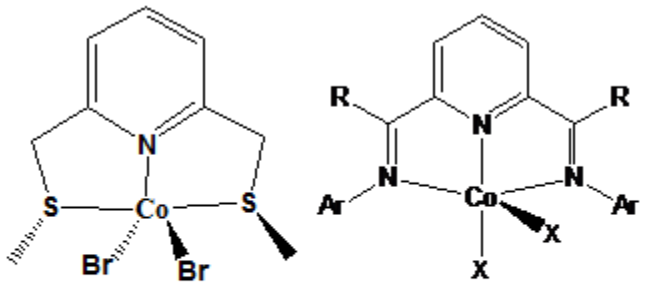

5.1

R = Ph; X = Br (5.2)
R = Ph; X = NCS (5.3)
R = Ph; X = NCS (5.4)

Figure 5.6. Structural formulas of synthesized Co(II) complexes.

Single crystal X-ray diffraction of the bis(methyl)thiomethyl pyridine complex shows a five-coordinate Co(II) centre displaying a distorted square based pyramidal geometry. The pendant methylene groups are rotated outside of the plane of the pyridine group. The packing of molecules within the crystal is such that the pyridine rings align on top of one another and

slightly skewed outwards. The structure shows no short contacts of interest and the metal centers are well separated with a distance of 15.699Å.

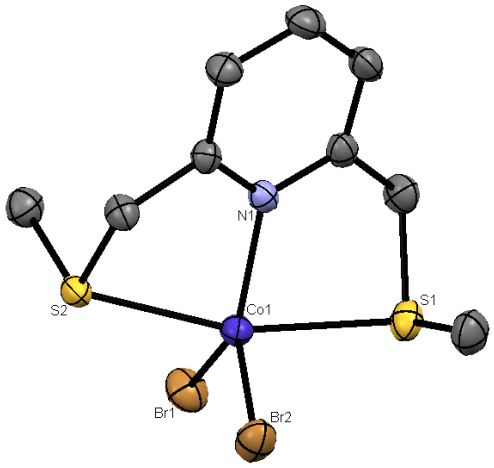

Figure 5.7. Structure and selected atom numbering scheme of compound 5.1. Hydrogen atoms and cocrystallized solvents omitted for clarity.

Table 1. Selected crystal data and structure refinement parameters for compound 5.1

5.1	
Identification code	dr001
formula	C18 H26 Br4 Co2 N2 S4
Formula weight	836.15
Crystal system, space group	Triclinic, P-1
Unit cell dimensions	a = 10.3494(4) A
	alpha = 70.202(2) deg.
	b = 10.8403(4) A
	beta = 77.559(2) deg.

	c = 13.4415(5) A
	gamma = 85.166(2) deg.
Volume	1385.45(9) A^3
Z, Calculated density	2, 2.004 Mg/m^3
Absorption coefficient	7.277 mm^-1
F(000)	812
Crystal size	0.19 x 0.17 x 0.17 mm
Theta range for data collection	2.00 to 28.46 deg.
Limiting indices	-13<=h<=13, -14<=k<=14, -17<=l<=17
Reflections collected / unique	21645 / 6851 [R(int) = 0.0265]
Completeness to theta = 28.46	98.00%
Absorption correction	Semi-empirical from equivalents
Max. and min. transmission	0.3709 and 0.3385
Refinement method	Full-matrix least-squares on F^2
Data / restraints / parameters	6851 / 0 / 271
Goodness-of-fit on F^2	1.015
Final R indices [I>2sigma(I)]	R1 = 0.0266, wR2 = 0.0621
R indices (all data)	R1 = 0.0357, wR2 = 0.0653

Table 2. Selected bond distances (Å) and angles (°) for compound 5.1

Co(1)-N(1)	2.065(2)
Co(1)-Br(1)	2.3987(4)
Co(1)-Br(2)	2.4100(4)
Co(1)-S(2)	2.4945(6)
Co(1)-S(1)	2.5028(6)
N(1)-Co(1)-Br(1)	133.28(5)
N(1)-Co(1)-Br(2)	108.89(5)
Br(1)-Co(1)-Br(2)	117.759(17)
N(1)-Co(1)-S(2)	81.56(5)
Br(1)-Co(1)-S(2)	95.448(18)
Br(2)-Co(1)-S(2)	90.114(18)
N(1)-Co(1)-S(1)	81.73(5)
Br(1)-Co(1)-S(1)	95.027(19)
Br(2)-Co(1)-S(1)	96.521(19)
S(2)-Co(1)-S(1)	163.25(3)

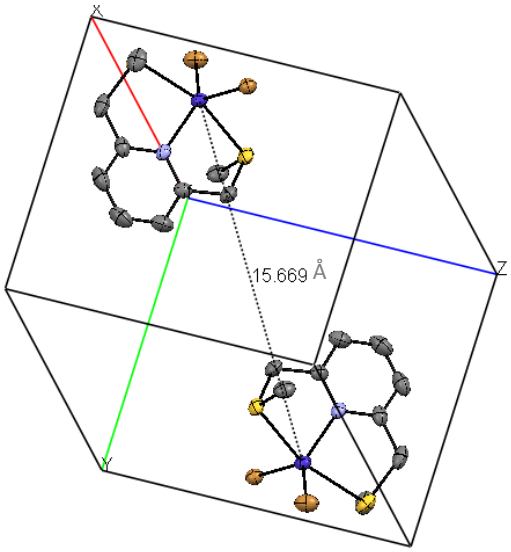

Figure 5.8. Packing arrangement and intermolecular Co-Co distance for compound 5.1.

Magnetic measurements were conducted on crystalline samples. The first plot is the Magnetization vs. Field (M vs. H) plot at 100K. This is used as a test for ferromagnetic impurities that might be present in the sample. For pure paramagnetic or diamagnetic systems, a straight line through the origin is expected. This is indicative of a pure sample and it is therefore feasible to carry out more SQUID measurements.

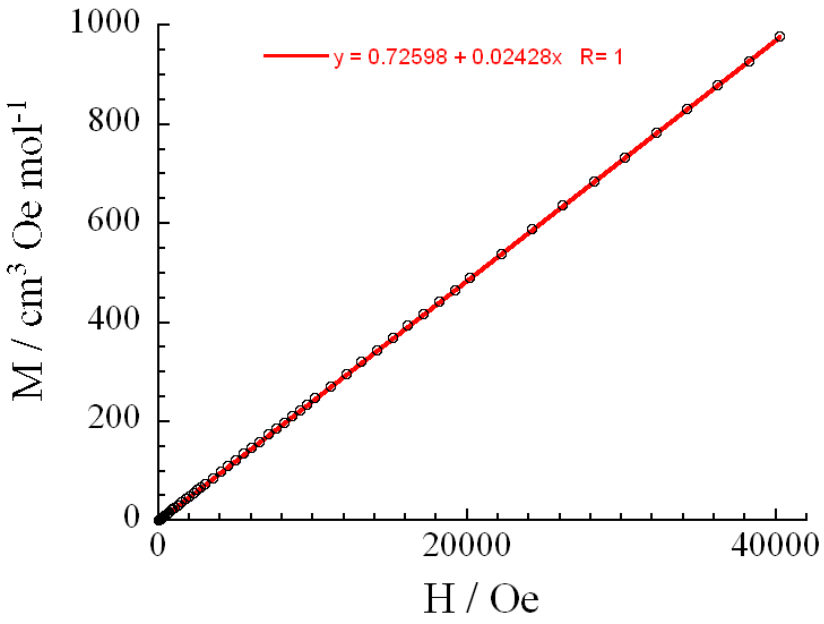

Figure 5.9. M vs. H plot of [Co[2,6-Bis(methylthiomethyl)pyridine]Br_2] (compound 5.1).

The next magnetic measurement was to obtain a χT vs. T plot. Measurements were carried out at 1,000 Oe and 10,000 Oe and two curves were generated (Figure 5.10). Room temperature χT product was 2.63cm^3K/mol, which decreased to a minimum value of 0.74 cm^3K/mol at 1.8 K and under an applied field of 1,000Oe. Interestingly, the χT value is high compared to the predicted spin-only value (1.88 cm^3K/mol) value for an S = 3/2 metal centre (g = 2). While the value is higher than expected, it lies within the range of 2.1-3.4 cm^3 K/mol for experimentally observed highly anisotropic Co(II) ions, which is indicative of a high degree of spin-orbit coupling.[100]

[100] Mabbs, F. E.; Machin, D. J.; Magnetism and Transition Metal Complexes (2008); Dover Publications.

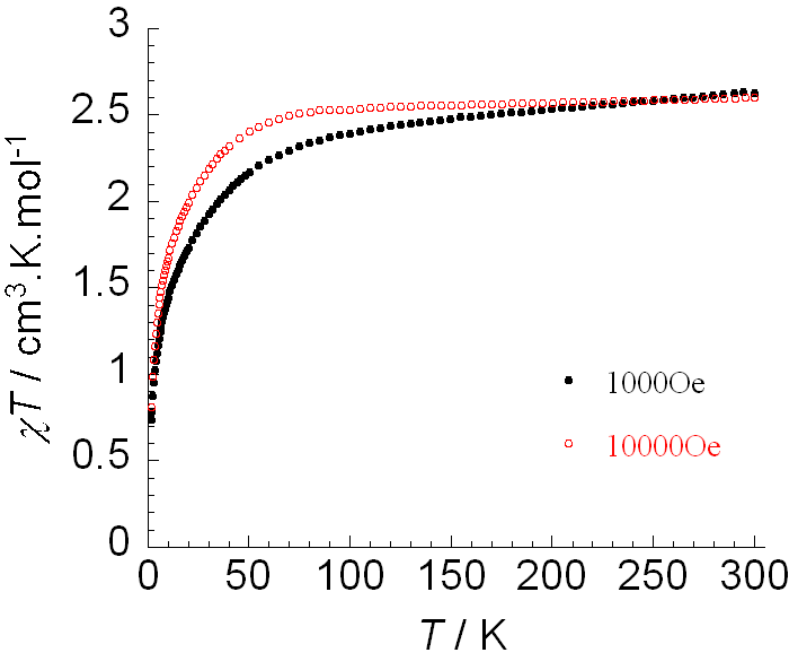

Figure 5.10. χT vs. T plot at 1,000 and 10,000 Oe for compound 5.1

Measurements to determine the field dependence of magnetization between 1.8 K and 8 K are shown in Figure 5.11. In these plots, we find that magnetization increases with field between 1.8 and 8 K. The saturation of magnetization at 7 T (1 T = 10^4 Oe) decreases with increasing temperatures with values of 2.23 and 1.83 μ_B at 1.8 K and 8 K respectively.

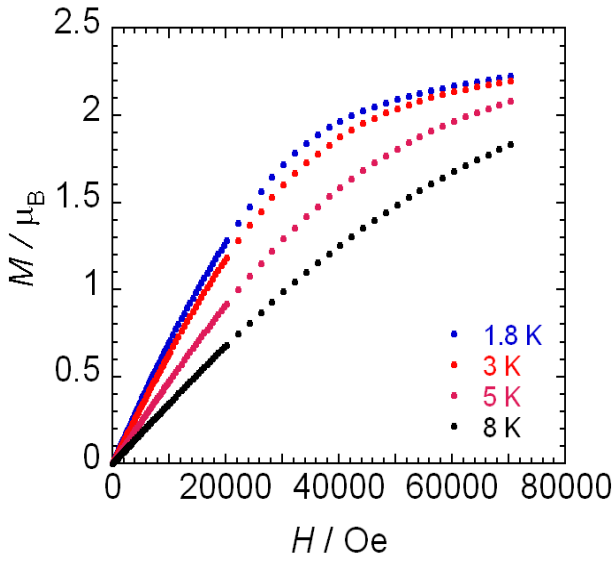

Figure 5.11. Plot of field dependence of magnetization below 8 K for compound 5.1.

Alternating current (ac) susceptibility measurements were carried out in order to determine whether or not the compound could behave as a single molecule magnet. However we were unable to obtain this data and decided to focus our attention on the other compounds that were synthesized.

The compound [Co[2,6-bis{1-[(2,6-diisopropylphenyl)imino]benzyl}pyridine]$(Br)_2$] (compound 5.2) was synthesized by the direct reaction of anhydrous $CoBr_2$ with the bis(imino)pyridine ligand under a nitrogen environment. Analogous compounds were reported by Brookhart and Gibson using less sterically bulky bis(imino)pyridine ligands. We attempted to synthesize this compound using our more bulky bis(imino)pyridine as a proof of concept, in order to determine whether our more sterically bulky ligand would react well with Co(II) salts to produce the desired products in a high yield. Indeed the reaction methodology works well as is evident from the good yield in which the product was obtained.

Single crystal X-ray diffraction of compound 5.2 reveals a mononuclear, five-coordinate Co(II) complex. The coordination geometry is a distorted square based pyramidal, and computational analysis suggests a high-spin ground state of 3/2 for the Co(II) center.

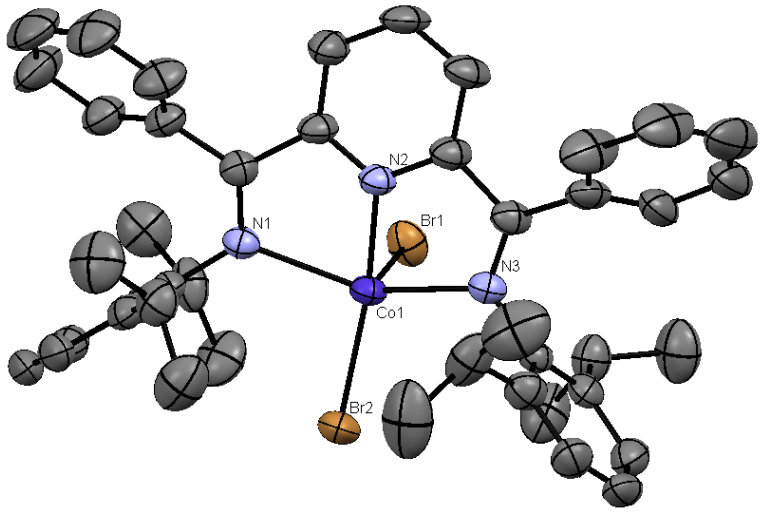

Figure 5.12 Structure and selected atom numbering scheme of compound 5.2. Hydrogen atoms and cocrystallized solvents omitted for clarity.

Table 3. Selected crystal data and structure refinement parameters for compound 5.2

5.2	
Identification code	dr003
Empirical formula	C52 H54.50 Br2 Cl1.50 Co N3
Formula weight	993.41
Crystal system, space group	Monoclinic, C2/c
Unit cell dimensions	a = 55.973(3) A
	alpha = 90 deg.

	b = 10.5504(5) A
	beta = 109.029(2) deg.
	c = 19.2842(10) A
	gamma = 90 deg.
Volume	10765.6(9) A^3
Z, Calculated density	8, 1.226 Mg/m^3
Absorption coefficient	1.911 mm^-1
F(000)	4080
Crystal size	0.26 x 0.17 x 0.15 mm
Theta range for data collection	1.54 to 24.14 deg.
Limiting indices	-64<=h<=63, -12<=k<=11, -22<=l<=22
Reflections collected / unique	37930 / 8465 [R(int) = 0.0435]
Completeness to theta = 24.14	98.50%
Absorption correction	Semi-empirical from equivalents
Max. and min. Transmission	0.7625 and 0.6364
Refinement method	Full-matrix least-squares on F^2
Data / restraints / parameters	8465 / 0 / 505
Goodness-of-fit on F^2	1.031
Final R indices [I>2sigma(I)]	R1 = 0.0745, wR2 = 0.2039
R indices (all data)	R1 = 0.1070, wR2 = 0.2303

Table 4. Selected bond distances (Å) and angles (°) for compound 5.2

Co(1)-N(2)	2.032(5)
Co(1)-N(3)	2.222(5)
Co(1)-N(1)	2.281(5)
Co(1)-Br(2)	2.3576(10)
Co(1)-Br(1)	2.4354(11)
N(2)-Co(1)-N(3)	74.92(19)
N(2)-Co(1)-N(1)	73.93(19)
N(3)-Co(1)-N(1)	143.72(18)
N(2)-Co(1)-Br(2)	151.83(15)
N(3)-Co(1)-Br(2)	100.32(13)
N(1)-Co(1)-Br(2)	98.39(13)
N(2)-Co(1)-Br(1)	92.72(15)
N(3)-Co(1)-Br(1)	98.13(13)
N(1)-Co(1)-Br(1)	101.45(13)
Br(2)-Co(1)-Br(1)	115.45(4)

As with the previous compound, we start by checking for ferromagnetic impurities that may exist in any compound by measuring the magnetization as a function of field at 100 K. The magnetization vs. field plot for the complex shows no presence of ferromagnetic impurities.

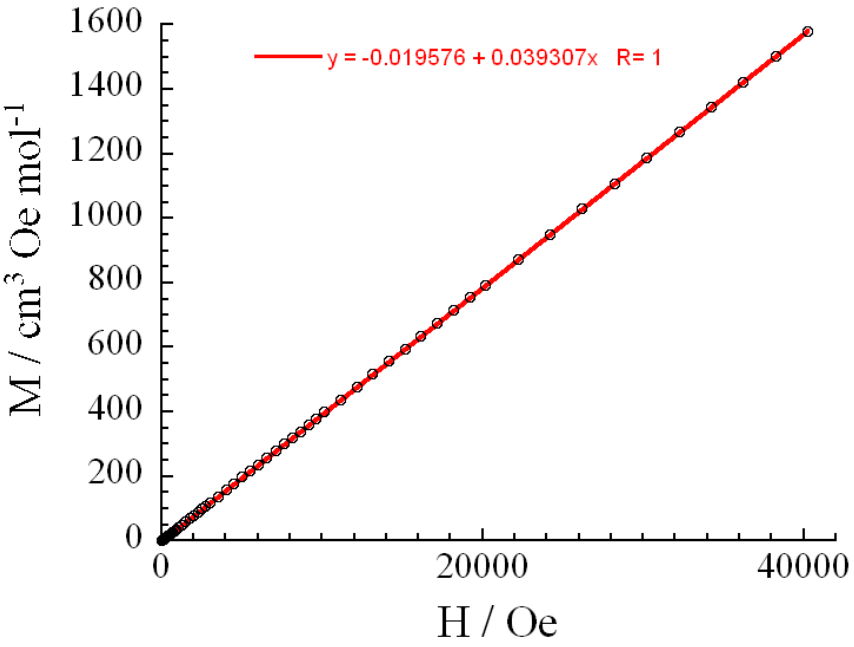

Figure 5.13. M vs. H plot of compound 5.2.

From the plot, we can calculate the magnetic susceptibility of the material as 0.039 cm^3/mol. This is in good agreement with the susceptibility measured at 1,000 Oe and 1 T. At room temperature the χT product was 3.98 cm^3K/mol, and decreases to a minimum value of 2.6 cm^3K/mol at 1.8 K and 10,000 Oe.

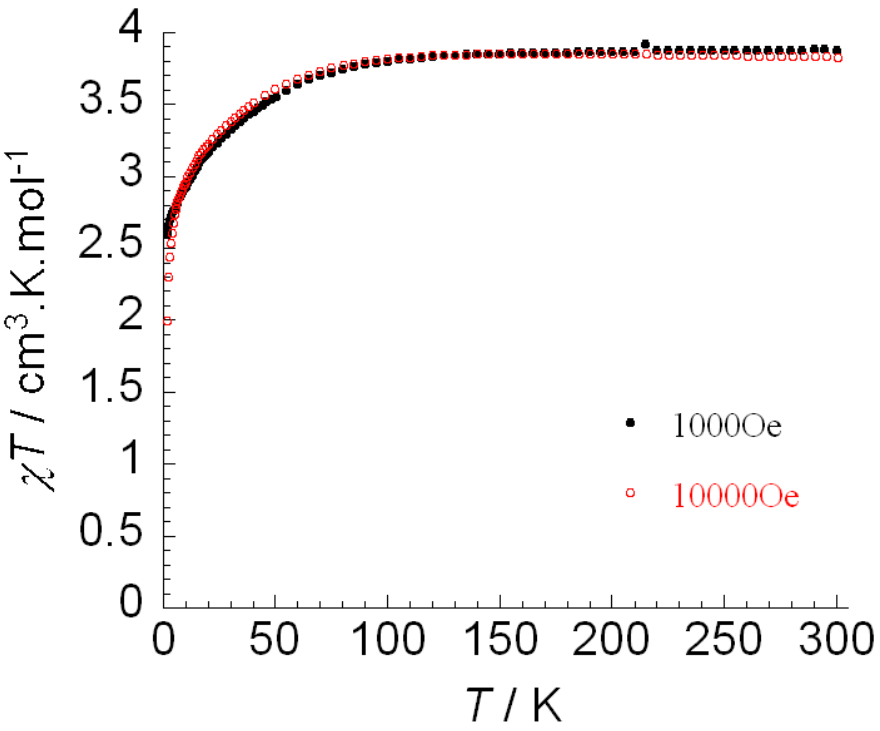

Figure 5.14. χT vs. T plot at 1,000 and 10,000 Oe for compound 5.2.

The plot shows that there is an antiferromagnetic interaction, which is evident from the decrease in the χT product and is indicative of a Curie-Wiess behaviour. What is interesting is the fact that such an interaction is present since the complex is a mononuclear one, and this means that there should be some sort of long range interaction between spin carriers on different molecules. It was postulated that this could be as a result of π-stacking between ligands, however, observing the packing between molecules in the crystal structure does not show any likely interaction in terms of π-stacking. Another interesting point is the fact that the measured χT is quite high compared to the χT value calculated from the spin only formula 1.88 cm^3K/mol for a S=3/2 Co(II) centre, which could be due to an intrinsically higher spin-orbit coupling, as is seen with the previous compound.

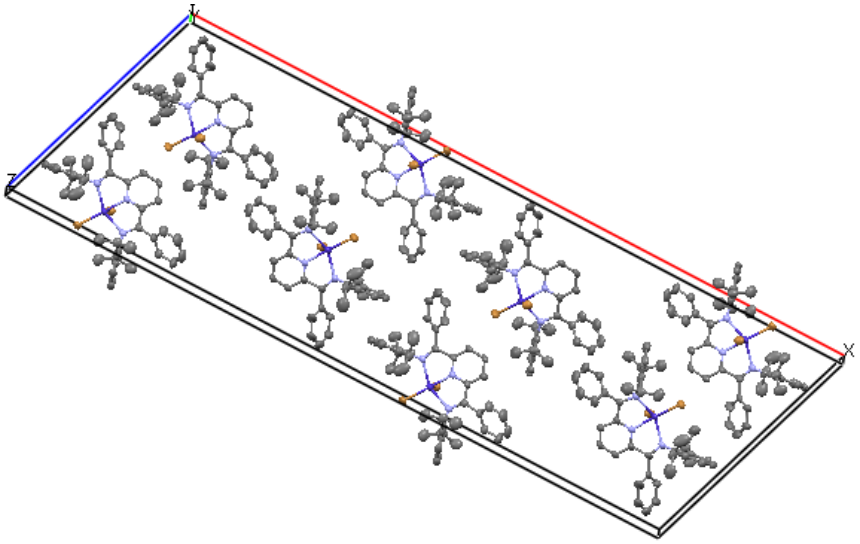

Figure 5.15. Crystal packing for compound 5.2.

The field dependence of the magnetization below 8 K reveals an increase with magnetization reaching a saturation value at 70,000 Oe. The magnetization at 1.8 K and 7 T reaches saturation at 2.9 μ_B, with the value of saturation magnetization decreasing with increasing temperature.

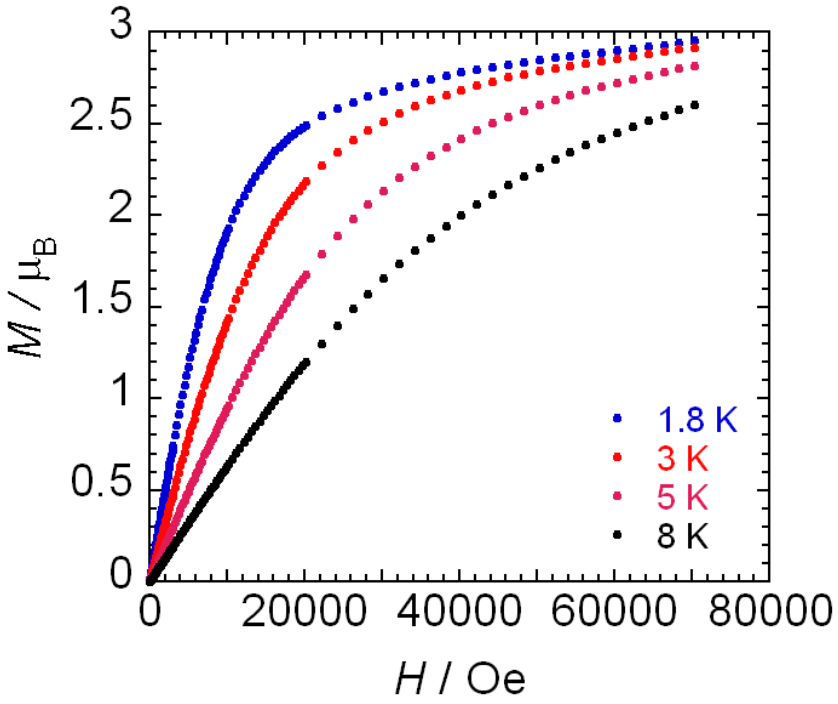

Figure 5.16. Plot of field dependence of magnetization below 8 K for compound 5.2.

Compounds 5.3 and 5.4 will be discussed together to compare the effects of modifying the ligand's pendant group from a methyl to phenyl on the magnetic properties of the complexes. Both of these compounds were synthesized by direct reaction of anhydrous $Co(SCN)_2$ with the respective ligands to yield the compounds 5.3 and 5.4 as green and light brown powders respectively in good yield.

UV-Vis spectra of these two compounds revealed very similar profiles with 5.4 displaying a slightly blue-shifted (≤8 nm) spectrum (Figure 5.17.). The room temperature magnetic susceptibilities of 5.3 and 5.4 (1,000 Oe) afforded χT values of 3.01 and 3.05 cm^3 K/mol, respectively. These values, again, while larger than the anticipated spin-only value for S = 3/2 of 1.88 cm^3 K/mol, fall within the range of 2.1-3.4 cm^3 K/mol, which is experimentally

observed for highly anisotropic Co(II) ions. These observations can be attributed to significant spin-orbit coupling usually seen in these d^7 complexes.

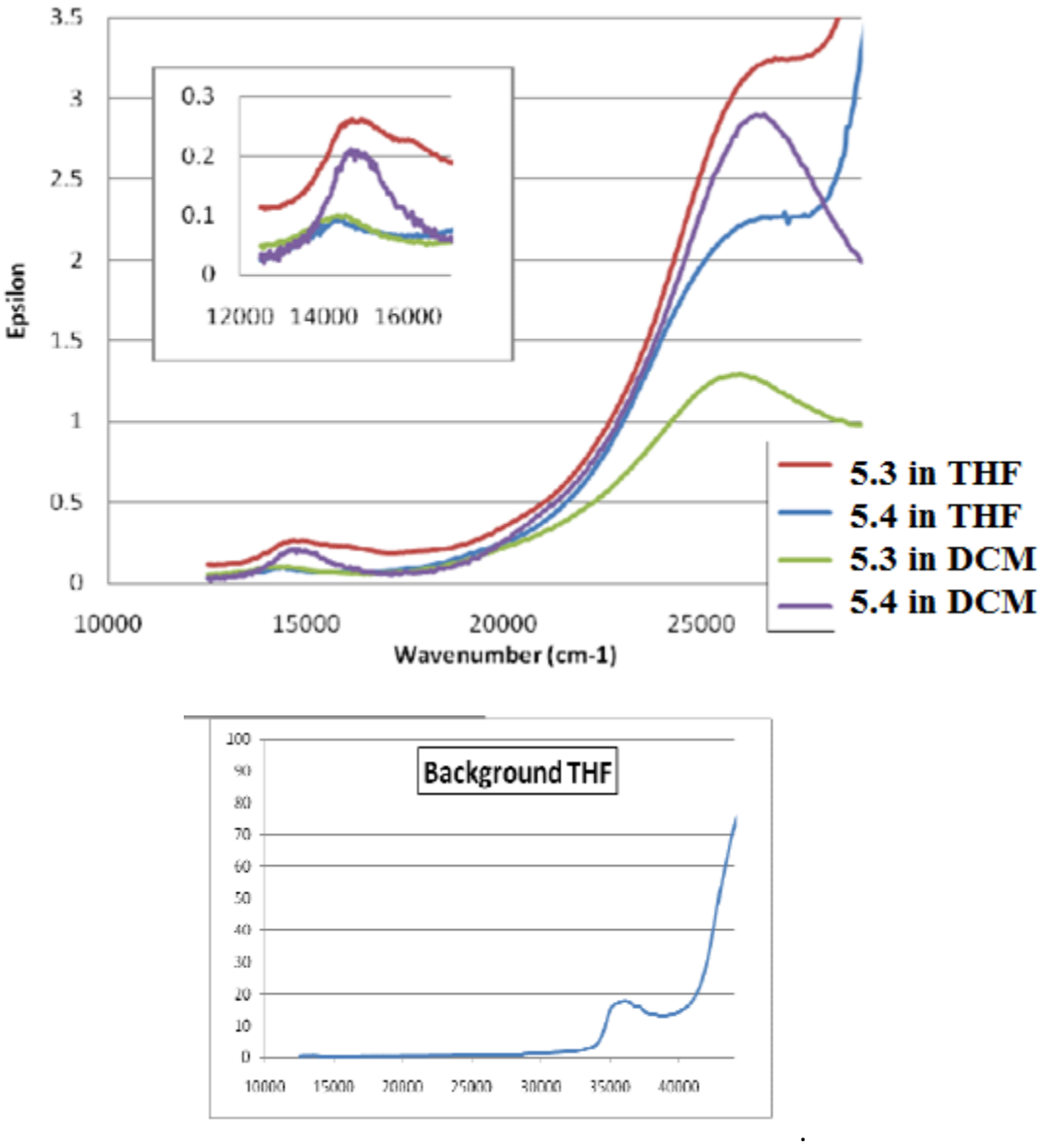

Figure 5.17. UV-Vis spectrum of compounds 5.3 and 5.4 obtained in DCM and THF. The THF recorded spectra of compound 5.3 is shown in red and compound 5.4 in blue. The DCM recorded spectrum of 5.3 is shown in green and compound 5.4 in purple. The maximum wavenumber value was determined by background THF absorbance (shown below). The inset provides a magnification of the low energy bands.

Table 5. UV-Vis data for compounds 5.3 and 5.4

νmax, λmax (cm^{-1}) (εmolar)			
5.3 in THF	5.4 in THF	5.3 in DCM	5.4 in DCM
26800, 373, 3250	27100, 369, 2300	25900, 386, 2600	26600, 376, 2900
14700, 680, 260	14400, 694, 100	14500, 690, 200	14600, 685, 210

The results of structural analyses for 5.3 and 5.4 are presented in Figures 5.18 and 5.19. As anticipated, the pentacoordinate Co(II) centers reside in distorted square pyramidal geometries in which the coordinated nitrogen atoms from the chelate ligand and from one isothiocyanate form the base. The second isothiocyanate ligand lies in the apical position. The diisopropylaryl substituents on the coordinated imine nitrogen centers lie orthogonal to the basal plane of the complex. In the case of compound 5.4, the phenyl substituents of the iminocarbon atoms are clearly rotated out of the plane of the Schiff base functional groups, to avoid steric interaction with the bulky aryl substituents and contact with the central pyridyl group. As anticipated, the ligand R groups do play a role on the distortion of the metal geometry as revealed by these structures. In 5.3, the cobalt sits above the basal N4 mean plane by 0.39 Å. Changing the substituent to R = Ph (5.4) leads to a more pronounced distortion with the metal center lying out of the basal N4 plane by 0.52 Å (Figure 5.21).

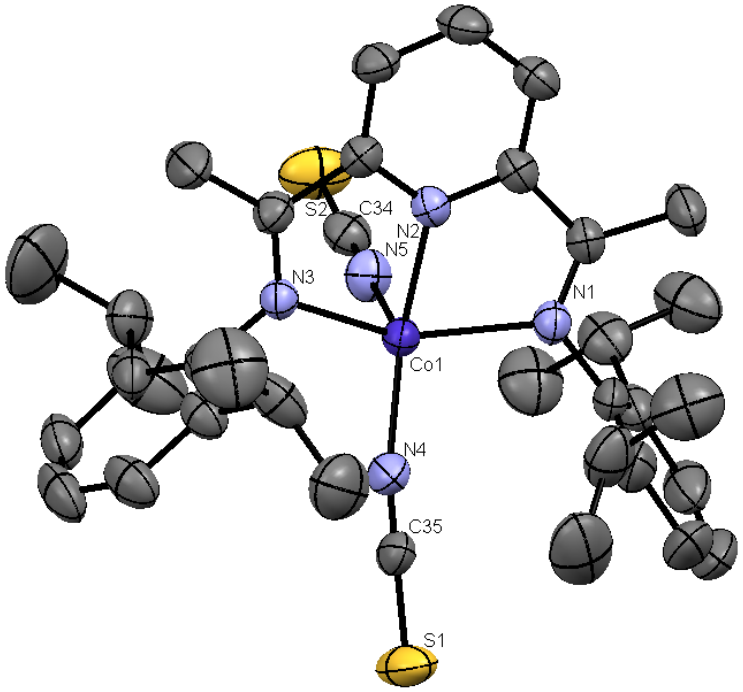

Figure 5.18. Structure and selected atom numbering scheme of compounds 5.3 Hydrogen atoms and cocrystallized solvents omitted for clarity.

Table 6. Selected crystal data and structure refinement parameters for compound 5.3

5.3	
Identification code	dr027a
formula	C36 H45 Cl2 Co N5 S2
Formula weight	741.72
Crystal system, space group	Monoclinic, P2(1)/c
Unit cell dimensions	a = 21.258(5) A
	alpha = 90 deg.
	b = 9.278(2) A
	beta = 92.684(9) deg.

	c = 19.752(5) A
	gamma = 90 deg.
Volume	3891.5(16) A^3
Z, Calculated density	4, 1.266 Mg/m^3
Absorption coefficient	0.716 mm^-1
F(000)	1556
Crystal size	0.23 x 0.19 x 0.06 mm
Theta range for data collection	2.06 to 28.42 deg.
Limiting indices	-28<=h<=22, -12<=k<=12, -26<=l<=24
Reflections collected / unique	45073 / 8331 [R(int) = 0.0453]
Completeness to theta = 28.42	85.00%
Absorption correction	Semi-empirical from equivalents
Max. and min. transmission	0.9583 and 0.8526
Refinement method	Full-matrix least-squares on F^2
Data / restraints / parameters	8331 / 2 / 424
Goodness-of-fit on F^2	1.033
Final R indices [I>2sigma(I)]	R1 = 0.0723, wR2 = 0.1714
R indices (all data)	R1 = 0.0982, wR2 = 0.1879

Table 7. Selected bond distances (Å) and angles (°) for compound 5.3

Co(1)-N(4)	1.948(4)
Co(1)-N(5)	1.993(4)
Co(1)-N(2)	2.054(3)
Co(1)-N(1)	2.153(3)
Co(1)-N(3)	2.159(3)
N(4)-Co(1)-N(5)	111.23(16)
N(4)-Co(1)-N(2)	159.72(15)
N(5)-Co(1)-N(2)	89.01(14)
N(4)-Co(1)-N(1)	100.53(14)
N(5)-Co(1)-N(1)	97.79(14)
N(2)-Co(1)-N(1)	74.54(12)
N(4)-Co(1)-N(3)	101.92(13)
N(5)-Co(1)-N(3)	100.15(14)
N(2)-Co(1)-N(3)	74.50(12)
N(1)-Co(1)-N(3)	143.71(12)

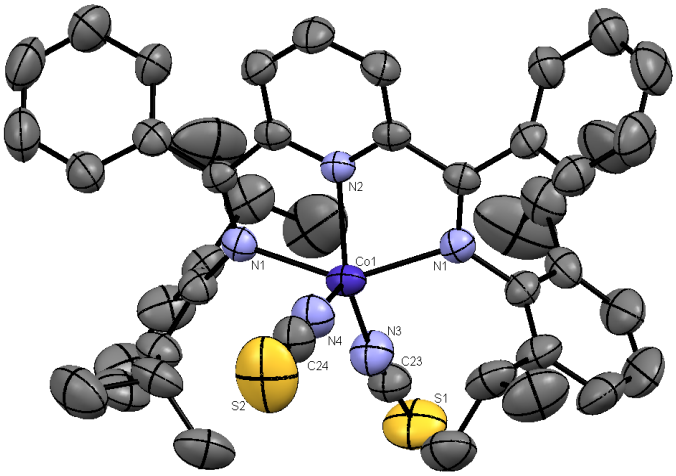

Figure 5.19. Structure and selected atom numbering scheme of compounds 5.4 Hydrogen atoms and cocrystallized solvents omitted for clarity.

Table 8. Selected crystal data and structure refinement parameters for compound 5.4

5.4	
Identification code	dr011
formula	C47 H51 Co N5 O0.50 S2
Formula weight	816.98
Crystal system, space group	Orthorhombic, Cmc2(1)
Unit cell dimensions	a = 16.2916(5) A
	alpha = 90 deg.
	b = 18.6440(6) A
	beta = 90 deg.
	c = 15.7275(5) A
	gamma = 90
Volume	4777.1(3) A^3

Z, Calculated density	4, 1.136 Mg/m^3
Absorption coefficient	0.482 mm^-1
F(000)	1724
Crystal size	0.17 x 0.05 x 0.03 mm
Theta range for data collection	2.11 to 28.30 deg.
Limiting indices	-19<=h<=21, -24<=k<=24, -20<=l<=20
Reflections collected / unique	66076 / 6018 [R(int) = 0.1278]
Completeness to theta = 28.30	99.10%
Absorption correction	Semi-empirical from equivalents
Max. and min. transmission	0.9857 and 0.9225
Refinement method	Full-matrix least-squares on F^2
Data / restraints / parameters	6018 / 1 / 283
Goodness-of-fit on F^2	1.002
Final R indices [I>2sigma(I)]	R1 = 0.0693, wR2 = 0.1064
R indices (all data)	R1 = 0.1705, wR2 = 0.1323

Table 9. Selected bond distances (Å) and angles (^{o}) for compound 5.4

Co(1)-N(3)	1.949(5)
Co(1)-N(4)	1.968(5)
Co(1)-N(2)	2.044(3)
Co(1)-N(1)	2.222(3)

N(3)-Co(1)-N(4)	120.6(2)
N(3)-Co(1)-N(2)	144.6(2)
N(4)-Co(1)-N(2)	94.8(2)
N(3)-Co(1)-N(1)	98.05(8)
N(4)-Co(1)-N(1)	98.28(8)
N(2)-Co(1)-N(1)	74.99(8)
N(1)-Co(1)-N(1)#1	146.69(15)

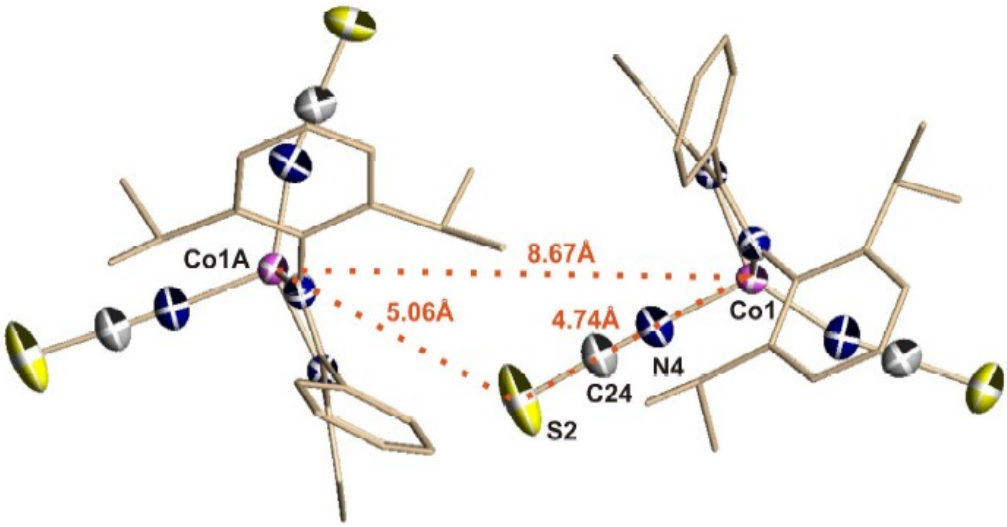

Figure 5.20. Intermolecular interactions displayed by compound 5.4

The structures of both species show no short intermolecular contacts. However, compound 5.4 does display an interesting packing arrangement. The S2 center of the apical isothiocyanate is oriented toward the open face of an adjacent Co center along the c-axis (d = 5.06 Å). However, the Co centers are well separated by 8.67Å (Figure 5.20.). The methyl

analogue, 5.3, does not display any such long distance interaction, and the shortest Co-Co distance in the structure of 5.3 is 9.90 Å.

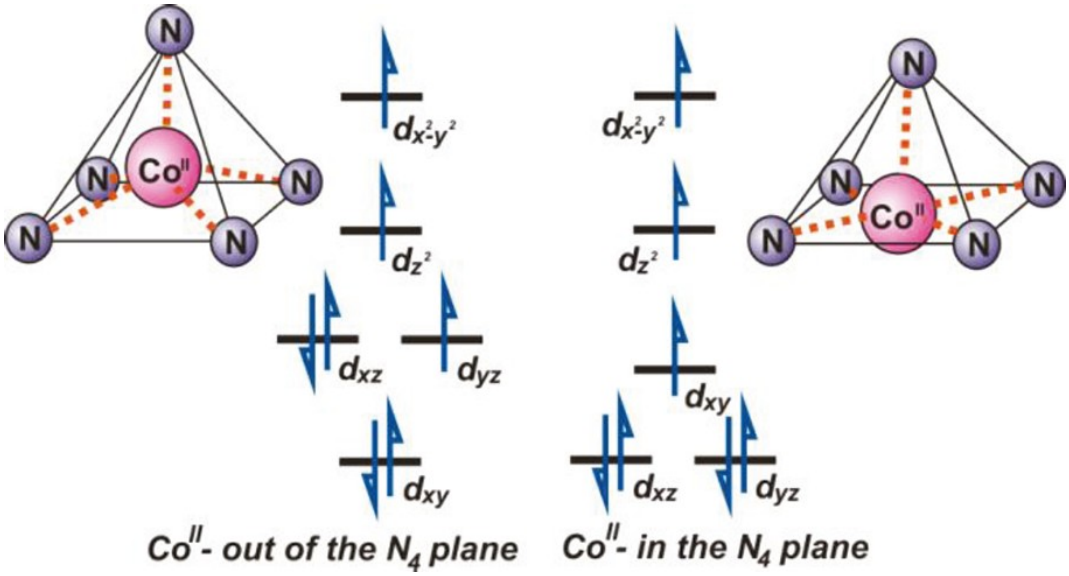

Figure 5.21. Simplified Model of d-Orbital Energy Diagram for a Square-Based Pyramid with the Metal out of the Basal Plane (Left) and in the Basal Plane (Right)

The elevation of the Co centers out of the square pyramidal basal plane, as is observed for compounds 5.3 and 5.4, has a profound effect on spin-orbit coupling for these species. A simplified model for the orbital configuration that is associated with this distortion is shown in Figure 5.21 and reveals the significant spin-orbital coupling arising from the 90° rotational transformation along the z-axis between the partially filled degenerate d_{xy}, d_{yz} orbitals. In contrast, an ideal square pyramidal coordination geometry with the metal center lying in the basal plane displays lower lying, degenerate d_{xy}, d_{yz} orbitals that are fully occupied. To confirm the effect of metal elevation on the relative orbital energies, we turned to computational methods. The distortion of the ligand environment around the Co center was modeled using

DFT computations that were carried out using the Gaussian 09 program suite and employing the B3LYP functional and DGDZVP basis set. The model compound $Co(NH_3)_5^{2+}$ was examined using two different geometric ligand arrays; a square pyramidal ligand geometry with the Co center in the basal plane ("ideal") and a geometry with the Co center raised by 0.5 Å out of the basal plane ("elevated"). The metal ligand bond lengths (Co-NH_3 = 1.86 Å) were kept constant for both "ideal" and "elevated" geometries.

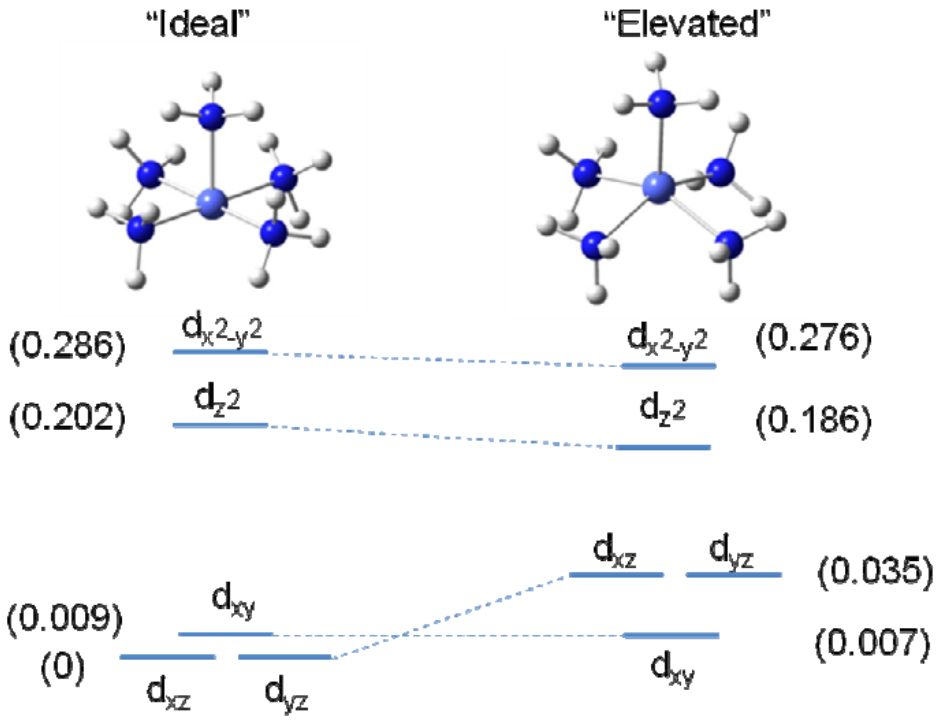

Figure 5.22. Results of DFT study on the simplified Co compound $Co(NH_3)_5^{2+}$ showing the effects of elevation of the Co(II) center on the relative orbital energies. The orbital energies are in atomic units and have been listed relative to the lowest energy orbital having a zero value

Geometrical distortion as well as an intrinsically high spin-orbit coupling in both complexes indicated the possibility of SMM behaviour. To this end, we undertook a detailed study of the magnetic properties of both complexes.

We began with identifying any bulk ferromagnetic impurities in both complexes using the M vs. H plot. The straight line obtained for both complexes indicated that both samples did not contain any ferromagnetic impurities and therefore we could proceed with our investigation of the complexes' magnetic properties.

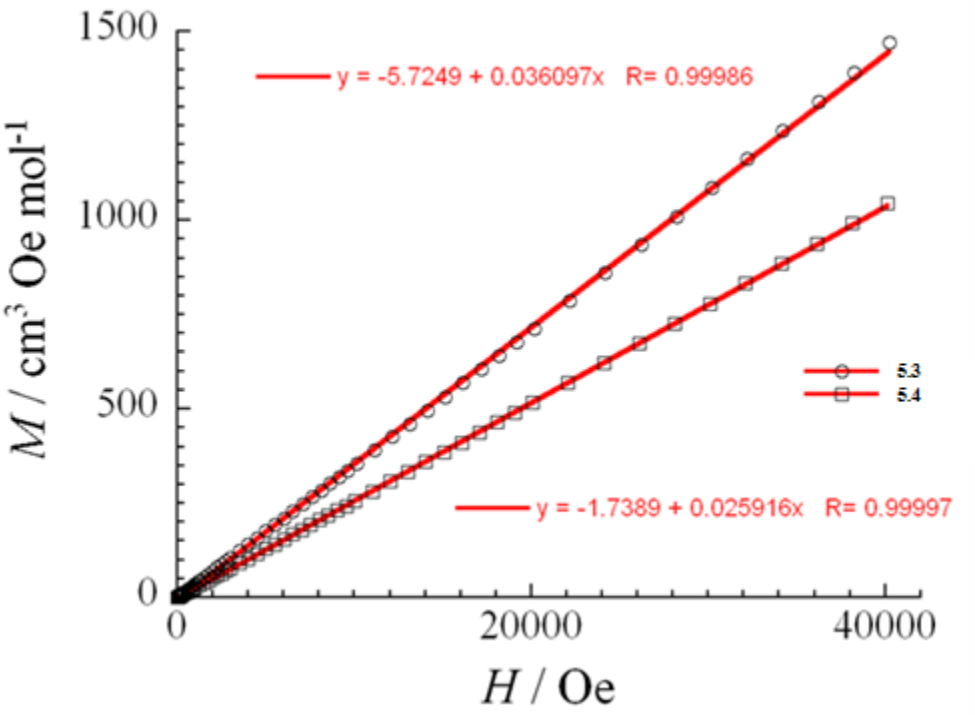

Figure 5.23. The field-dependent magnetization measured at 100 K for 5.3 and 5.4 in order to detect the presence of any bulk ferromagnetic impurities.

Variable temperature dc susceptibility measurements were collected on powdered crystalline samples of 5.3 and 5.4 at a field of 1,000 Oe over the 2-300 K temperature range

(Figure 5.24.). For both compounds, the χT value remains roughly constant from room temperature to 100 K, before decreasing slightly. This temperature profile is consistent with Curie-type behavior for non-interacting mononuclear Co(II) centers, whereas the observed decrease seen below 100 K is most likely due to intrinsic magnetic anisotropy of the Co(II) ions rather than antiferromagnetic interactions between the spin carriers. For compound 5.3, below 100 K, the χTproduct decreases with decreasing temperature to reach a value of 2.07 cm^3K/mol at 2.5 K. In the case of complex 5.4, the χT value decreases to 2.48 cm^3K/mol at 12 K and then increases rapidly to reach a maximum of 3.21 at 3 K followed by a rapid drop to 3.03 cm^3K/mol at 2.5 K. The sharp increase observed in the latter case is most likely due to intermolecular ferromagnetic interactions, which is a remarkable feature for a mononuclear system with metal centers relatively well separated (8.67 Å). This long-range pathway is likely provided by the apical isothiocyanate oriented toward the open face of an adjacent Co center along the c-axis (Figure 5.20.).

Such intermolecular interactions can be removed by separating the magnetic centers through solution susceptibility measurements. Therefore, crystals of 5.4 were fully dissolved in THF in a sealed tube and dc susceptibility measurements were carried out on the resulting frozen solution below 50 K (Figure 5.24., red dots). As expected, these data parallel the solid-state data showing a clear decrease in χT with decreasing temperature to reach a value of 2.1 cm^3K/mol at 2.5 K. The absence of an increase in χT for this solution sample clearly demonstrates the presence of long-range interactions between the highly anisotropic spin carriers in the solid state of 5.4. The observation of χT values of 3.01 (for 5.3) and 3.05

cm^3K/mol (for 5.4) at room temperature is consistent with the possible value of 3.38 cm^3K/mol ($\mu_{eff} = [g^2S(S + 1) + L(L + 1)]^{1/2}$), which includes the orbital contribution.[99]

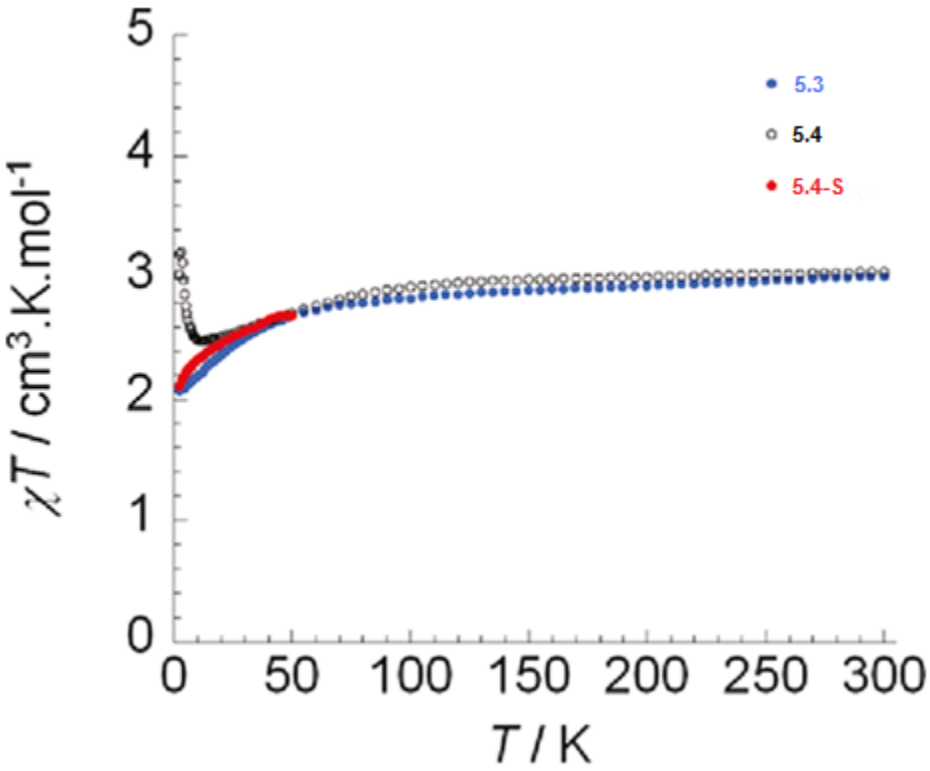

Figure 5.24. Temperature dependence of the χT product at 1,000 Oe for complexes 5.3 and 5.4 (with χ being the molar susceptibility per mononuclear complex defined as M/H). Blue and black data points are for solid samples of 5.3 and 5.4, respectively. Red data points (labeled 5.4-S) are for a THF solution sample of 5.4.

The field dependence of the magnetization of 5.3, 5.4, and 5.4-S were performed at fields ranging from 0 to 7 T between 2.2 and 8 K (Figure 5.25. a-c and Figure 5.26. a-c). The M vs H data below 8 K revealed a rapid increase of the magnetization at low magnetic fields. At higher fields, M increases linearly without clear saturation to ultimately reach 3.04 μ_B (H = 7 T, at 2.5 K) for 5.3, 3.2 μ_B (H = 7 T, at 2.2 K) for 5.4, and 2.5 μ_B (H= 7 T, at 2.5 K) for 5.4-S. The lack of saturation and non-superposition on a single master curve of M vs H/T data for both

complexes also suggests the presence of magnetic anisotropy (Figure 5.26. a-c). Several attempts to fit the reduced magnetization data using the Magnet[101] program were unsuccessful. The latter program employs matrix diagonalization to a model that assumes only the ground state is populated, includes axial zero-field splitting (DS^2 z) and Zeeman interactions, and incorporates a full powder average. However no rhombic (E) term can be introduced, thus more sophisticated software needs to be employed to achieve reasonable fits. Furthermore, the susceptibility data can be fitted (Figure 5.27.) assuming a simple zero-field splitting effect[102] which leads to D values of -40.5 K for 5.3 and -40.6 K for 5.4, imply a significant uniaxial anisotropy.

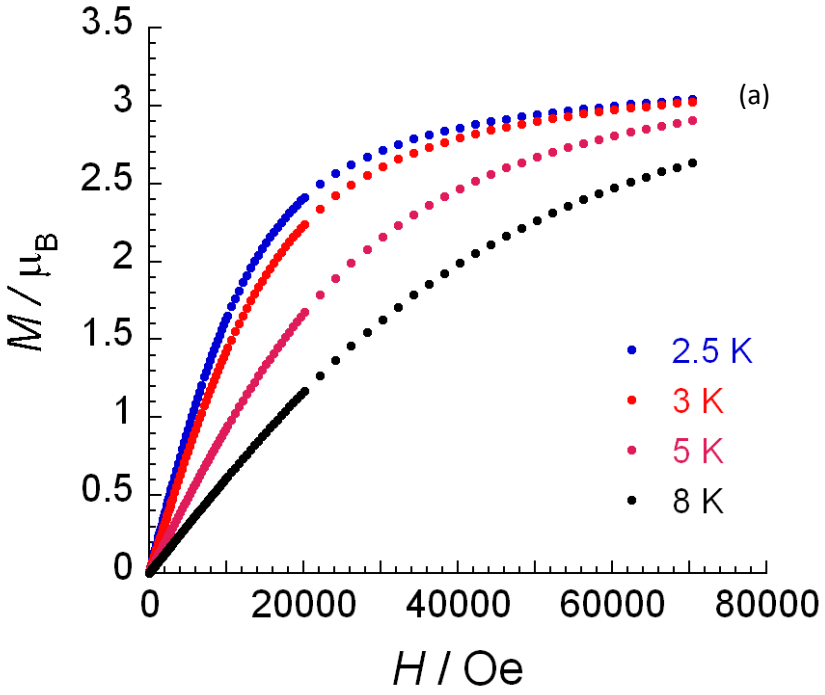

[101] Davidson, E. R. MAGNET (1999); Indiana University: Bloomington, IN.
[102] (a) Chirico, R. D.; Carlin, R. L.; Inorg. Chem. (1980); 19; 3031. (b) Hung, S.-W.; Yang, F.-A.; Chen, J.-H.; Wang, S.-S.; Tung, J.-Y.; Inorg. Chem. (2008); 47; 7202.

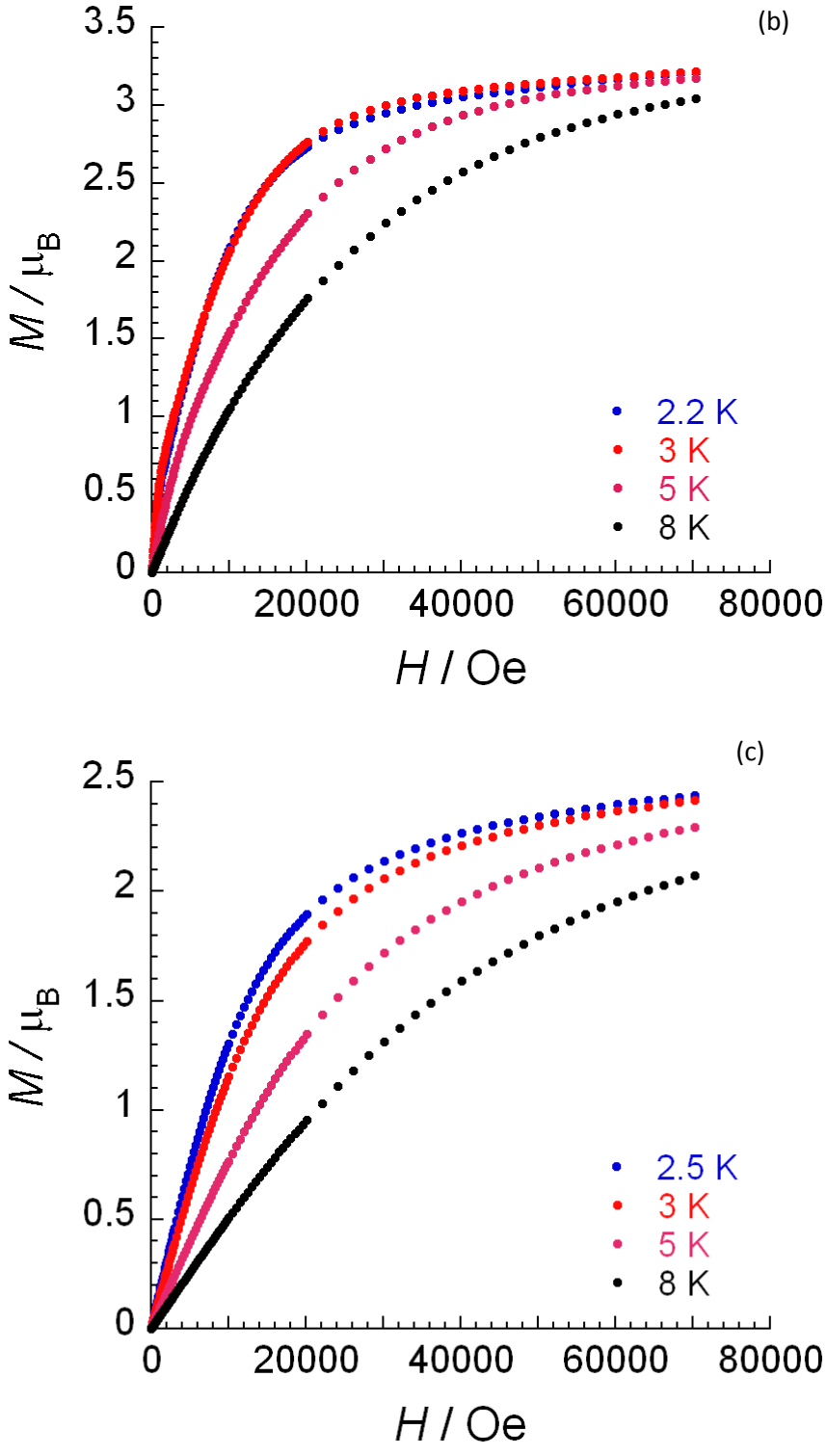

Figure 5.25 (a) Field dependence of the magnetization, *M*, at 2.5, 3, 5 and 8 K for 5.3 (b) Field dependence of the magnetization, *M*, at 2.2, 3, 5 and 8 K for 5.4 (c) Field dependence of the magnetization, *M*, at 2.5, 3, 5 and 8 K for 5.4-S

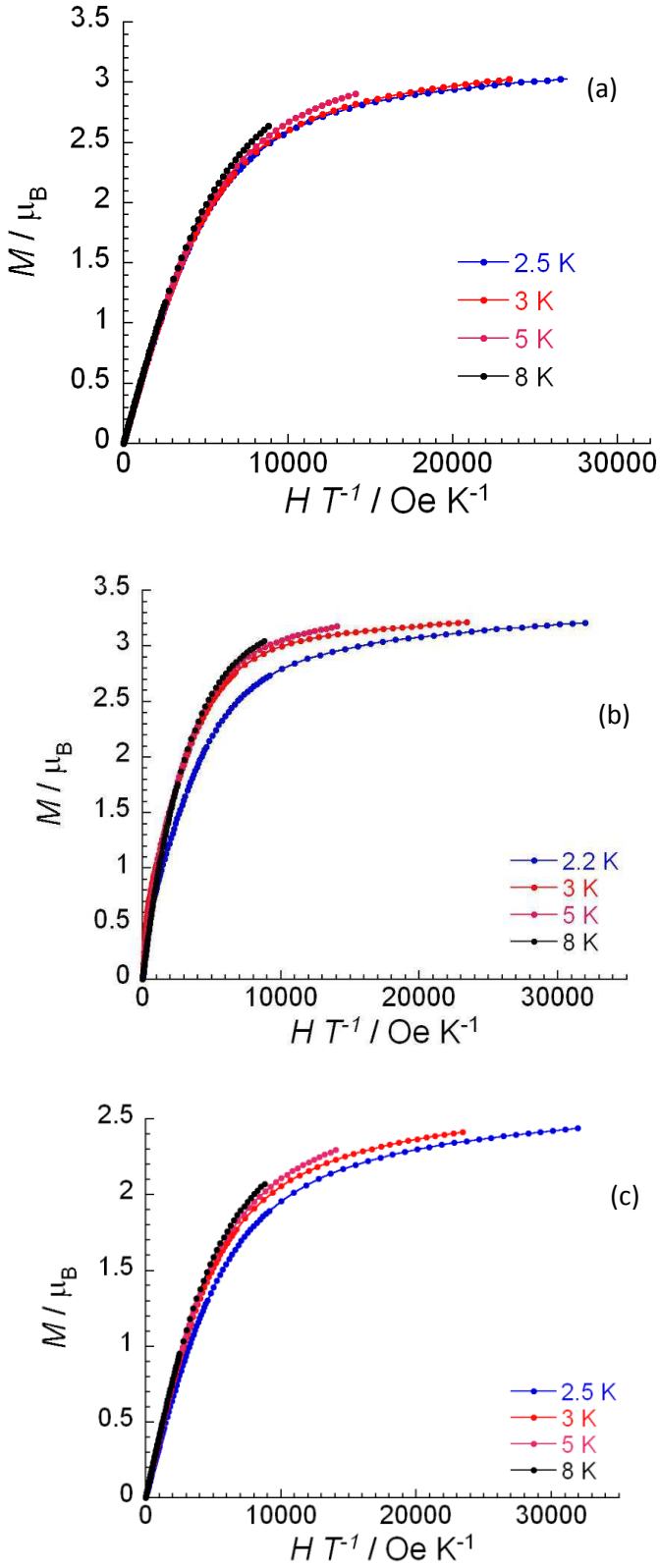

Figure 5.26. (a) *M vs. H/T* plots at 2.5, 3, 5 and 8 K for 5.3. (b) *M vs. H/T* plots at 2.2, 3, 5 and 8 K for 5.4. (c) *M vs. H/T* plots at 2.5, 3, 5 and 8 K for 5.4-S.

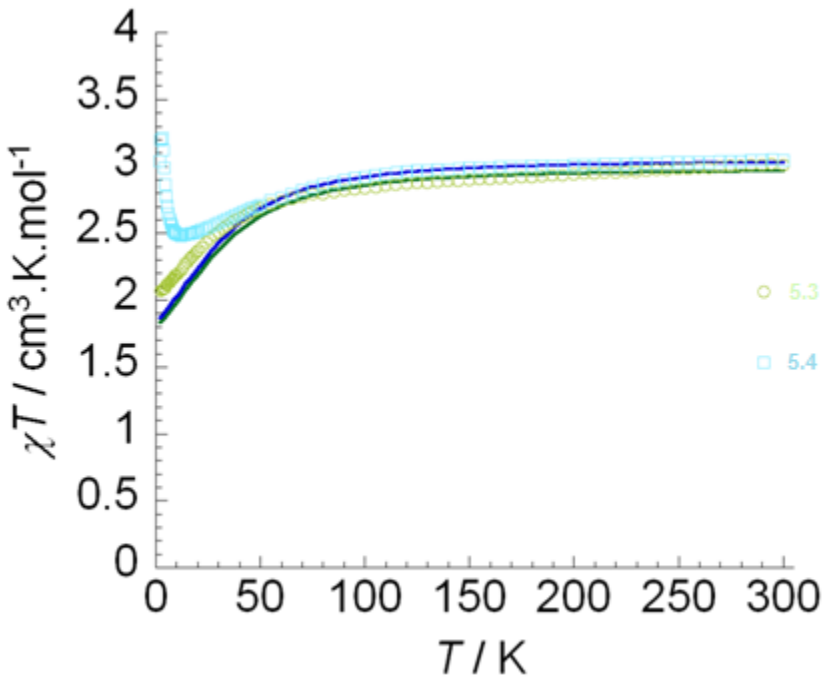

Figure 5.27. Temperature dependence of the χ*T* product at 1,000 Oe for complexes 5.3 and 5.4 (with χ being the molar susceptibility per mononuclear complex defined as *M*/*H*). Pale green and blue data points are for solid samples of 5.3 and 5.4, respectively. Solid lines represent the obtained fits using the following equation, which includes axial zero-field splitting parameter.

$$\chi T = \frac{Ng^2}{k}\frac{1+9e^{-2x}}{4(1+e^{-2x})} + \frac{2Ng^2\beta^2}{k}\frac{4+\frac{3}{x}(1-e^{-2x})}{4(1+e^{-2x})}$$

Where x=D/kT

To probe the SMM behaviour in complexes 5.3 and 5.4, temperature and frequency dependence of the ac susceptibility measurements were measured in the temperature range 2-10 K. These measurements were carried out on a solid state sample for 5.3 and both solid state

and solution phase samples of 5.4. Under a zero dc field and a 3 Oe ac field oscillating at frequencies between 1 and 1,500 Hz, no ac signal was observed. However, when a static dc field was applied, both compounds displayed a frequency dependent signal (Figures 5.28. and 5.29.). Such behaviour generally indicates that slow relaxation of the magnetization is subjected to quantum tunneling of the magnetization (QTM) through the spin reversal barrier via degenerate $\pm M_s$ energy levels.[59]

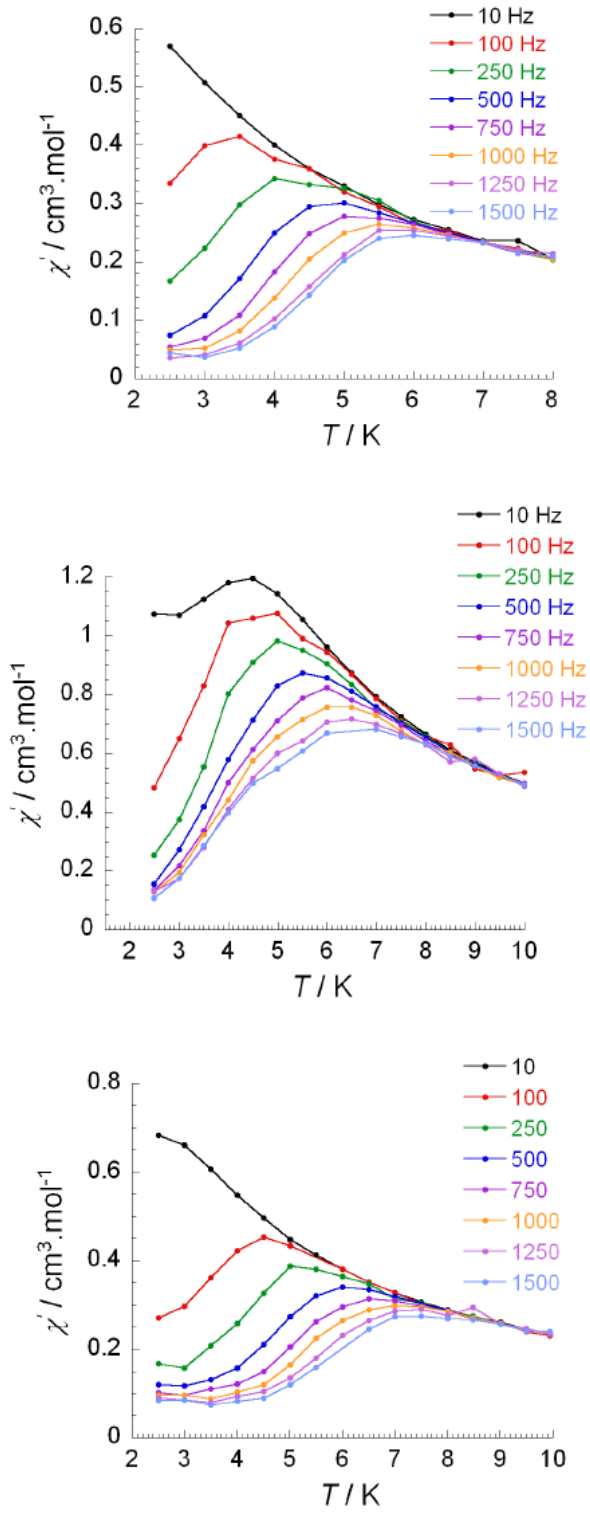

Figure 5.28. Temperature dependence of the in-phase χ' ac susceptibility signals 5.3 (top) and 5.4 (middle: solid state, bottom: solution), collected over the temperature range 2.5-10 K at under an applied dc field of 2,000 Oe.

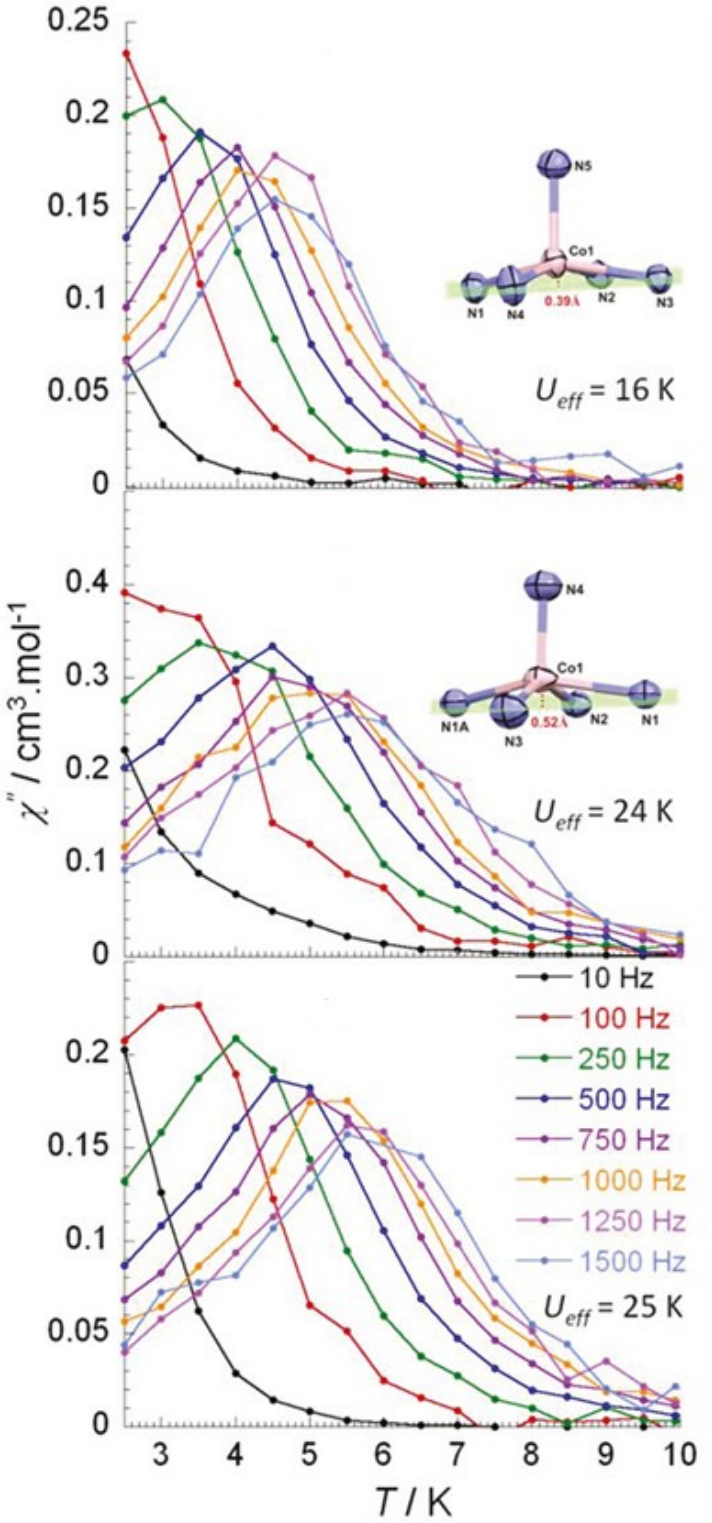

Figure 5.29. Variable-frequency out-of-phase ac susceptibility data for 5.3 (top) and 5.4 (middle: solid state, bottom: solution), collected over the temperature range 2-10 K under an applied dc field of 2,000 Oe. Inset diagrams of the CoN_5 core emphasize the displacement of the metal out of the basal plane at the indicated distances.

For an Ising-like anisotropic system, assuming only the lowest energy levels are populated, spins then reverse by QTM via the ground state doublet ±S.[103] It is noteworthy that for a half integer spin system such as 5.3, or 5.4, QTM should be suppressed at zero field due to spin parity effects.[104] Therefore, the observed QTM is most likely due to effects such as environmental degrees of freedom as well as hyperfine and dipolar coupling via a transverse field component. Hence, ac measurements under various dc fields were performed in order to determine the optimum field for which the QTM effect would be reduced. This search indicated minima with optimum fields of 700 and 2,000 Oe for 5.3 and 5.4, respectively (Figure 5.30.). Ac measurements under these optimal applied dc fields reveal a frequency dependent signal with a clear out-of-phase (χ'') peak for both complexes.

[103] Luis, F.; Mettes, F.; Evangelisti, M.; Morello, A.; de Jongh, L. J.; J. Phys. Chem. Solids (2004); 65; 763.
[104] (a) Wernsdorfer, W.; Bhaduri, S.; Boskovic, C.; Christou, G.; Hendrickson, D. N.; Phys. Rev. B (2002); 65; 180403. (b) Wernsdorfer, W.; Chakov, N. E.; Christou, G.; Phys. Rev. Lett. (2005); 95; 037203.

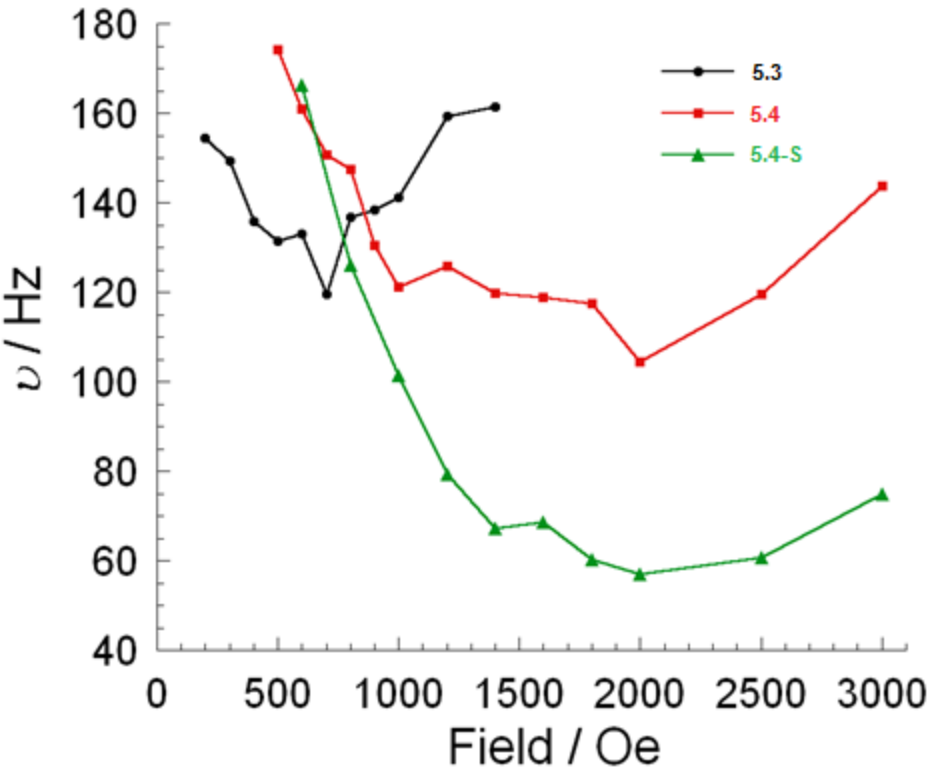

Figure 5.30. Field dependence of the characteristic frequency (maximum of χ″) as a function of the applied dc field for 5.3 (black circle), 5.4 (red square) and 5.4-S (green triangles) at 3 K. Line is guide for the eyes.

In order to compare the energy barriers for both complexes ac measurements were carried out under 2,000 Oe for solid (5.3, 5.4) and solution (5.4) samples and are shown in Figure 5.29. (see also Figure 5.28.). The observed single relaxation process behaviour is indicative of super paramagnet-like slow magnetization relaxation of an SMM.

The anisotropic energy barrier, U_{eff}, can be obtained from the high temperature regime of the relaxation where it is thermally induced (Arrhenius law, $\tau = \tau_0 \exp(\mu_{eff}/kT)$). In fact, at a high temperature limit (above 4 K) the data exhibit a linear correlation indicating that it follows the Arrhenius Law. Relaxation times, τ, are extracted from these data allowing the calculation of a thermally induced anisotropic energy barrier, μ_{eff}, between the magnetic ground states.

The effective energy barriers obtained from the fitting procedure (Figures 5.31 and 5.32) are U_{eff} = 16 K (τ_0 = 3.6 x 10^{-6} s) for 5.3 and 24 K (τ_0 = 5.1 x 10^{-7} s) for 5.4. The latter U_{eff} of 5.4 obtained from solid-state measurement was also confirmed through ac measurement on a frozen solution with an effective barrier of 25 K (τ_0=1.6 x 10^{-6} s) (Figure 5.29. bottom). This clearly confirms that the slow relaxation of the magnetization is molecular in origin. The observed relaxation mechanism follows thermally activated behavior at high temperature which indicates the Orbach process is the predominant relaxation pathway.[105] Relaxation associated with the thermally activated regime takes place by excitation to higher M_s =±1/2 level with the absorption of phonons from the lattice, followed by a de-excitation to the final state in which the phonons are emitted.[101]

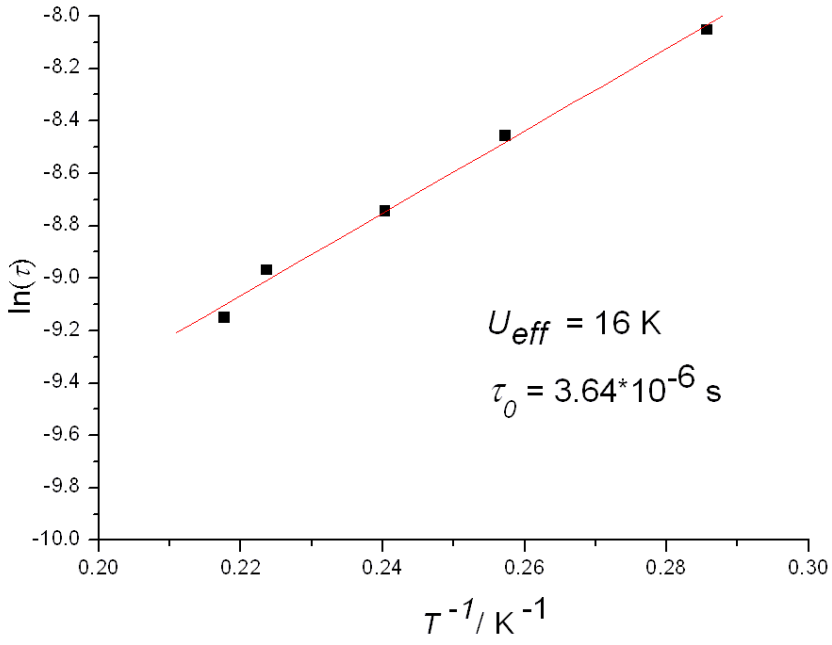

Figure 5.31. Relaxation time of the magnetization ln(τ) *vs.* T^{-1} (Arrhenius Plot using ac data) of 5.3. The solid line corresponds to the fit.

[105] (a) Orbach, R.; Proc. R. Soc. London, Ser. A (1961); 264; 458. (b) Orbach, R.; Proc. R. Soc. London, Ser. A (1961); 264; 485.

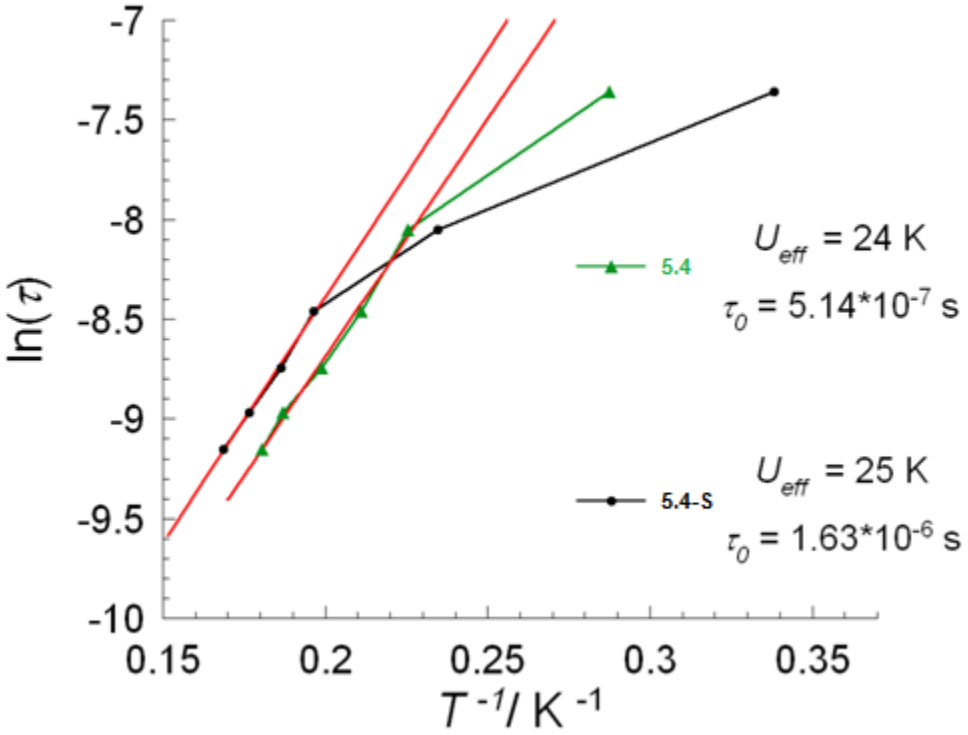

Figure 5.32. Relaxation time of the magnetization ln(τ) *vs.* T^{-1} (Arrhenius Plot using ac data) of 5.4 (triangle) and 5.4-S (circle). The solid red line corresponds to the fit.

The U_{eff} values are comparable in magnitude for 5.3 and 5.4; the difference between them primarily arises from the zero-field fitting parameter since the spin values are equivalent for these compounds. In fact, it appears that the structural distortion around the metal center plays a key role in the overall magnetic anisotropy. Elevating the Co(II) center above theN4 mean plane from 0.39Å in complex 5.3 to 0.52Å in 5.4 (Figure 5.29. insets) is a structural anisotropy that may lead to the difference in the magnetic anisotropy observed for these two compounds. Although the axial zero-field splitting parameter (D) was not obtained using reduced magnetization data, it is reasonable to estimate a negative D value from the acquired

barriers ($U = (S^2 - 1/4)|D|$). As such, D values of -8 K and -12 K can be obtained for 5.3 and 5.4, respectively. These estimated values are lower than the values determined through the dc susceptibility fit (vide supra), and this may be due to the nonnegligible QTM present in these molecules.

Chapter 6

Conclusions

The field of molecular magnetism has gained a great deal of attention from researchers in a variety of scientific fields including chemists. Spin crossover systems (SCO) and single molecule magnets (SMMs) present two very important classes of magnetic materials. Since their inception, they have been proposed for use in microelectronics as well as other applications. SCO compounds, because of the many factors that affect spin state combined with the observed physical changes accompanying spin transition, have been suggested for use in applications such as contrast agents for magnetic resonance imaging, molecular switches, and molecular sensors (for example pressure sensors in systems where the spin transition is activated by changes in pressure).[7, 106] Single molecule magnets, which present the smallest possible magnetic devices, have also been proposed for use in numerous technological applications such as data storage devices , quantum computing and magnetic refrigeration.[107]

The main aim of this research project was the synthesis of novel Co(II) based magnetic systems and was divided into two parts. First, we were interested in the synthesis of spin crossover materials within dendritic frameworks. This work was partially inspired by that recently published by Fujiyaga[45] and Gutlich[46], where they were able to successfully synthesize an Fe(II) based spin crossover system within a reduced dendritic framework. This research used a triazole, albeit a different structural isomer, -based dendritic wedge to synthesize materials

[106] Real, J.A.; Gaspara, A.B.; Munoz, M.C.; Dalton Trans. (2005); 2062
[107] Milios, C.J.; Piligkos, S.; Brechin, E.K.; Dalton Trans. (2008); 1809

that have shown spin transition behaviour and has then extended his work in order to draw conclusions on the effects of coordinated water molecules on the spin transition behaviour.

We faced numerous challenges in the synthesis of our dendrimer of choice. Our attempts to synthesize the product using published methods as well as modifications of such methods either yielded impure products or did not react. However, we were recently able to synthesize a pure dendrimer and characterize it thanks to the efforts of our coworker Mahshid Hamzehlooain.

Since we now have a pure dendritic product, the next logical step is to examine the coordination ability of Co(II) metal centres within this framework, and in turn examine the spin crossover profiles it may produce. If we have on hand a spin crossover capable material, the next step is to examine the effects of generation numbers on the spin crossover behaviour, as was shown by Fujiyaga and coworkers for their Fe(II) system.

The second part of the project involved the synthesis of mononuclear Co(II) systems that make use of the high intrinsic anisotropy of cobalt, as well as geometric distortions within the coordination sphere in order to impart SMM behaviour on these complexes. SMMs based on transition metals have been, for the most part, designed with an approach that utilizes a high spin ground state through the use of intermolecular interactions within the ligand framework that could in turn result in large cluster with a large total spin ground state. The use of high anisotropy for the synthesis of SMMs has been mainly reserved for the lanthanide series.

Recently, reports from the labs of Chang and Long have shown that mononuclear SMMs are possible, and that structural distortions within the coordination geometry do play a role in the enhancement of spin-orbit coupling, resulting in slow magnetic relaxation. They have

shown this using Fe(II).[59] We have extended this idea towards Co(II) mainly due to the fact that it possesses a high magnetic anisotropy among the first row transition metals.

To this end, we were successful in synthesizing a family of five-coordinate Co(II) compounds, and have carried out extensive magnetic studies on the two most promising compounds from that family (5.3 and 5.4). We were able to show through single crystal X-ray diffraction that one of these two compounds (5.4) exhibits a long range interaction through its crystal packing. We have shown the importance of structural distortions in the augmentation of spin-orbit coupling, and have also shown that SMM behaviour is possible in such compounds. The energy barriers to relaxation as well as the relaxation times were calculated for both complexes. Further, we were able to show that the magnetic relaxation is molecular in nature, by performing magnetic measurements on a solution sample of compound 5.4. (labelled 5.4-S), which would separate the magnetic centers, removing these long range intermolecular interactions. Lastly, from the obtained μ_{eff} values obtained for these compounds, we were able to estimate ZFS parameters for both compounds. These values were lower than those obtained through dc susceptibility fits, and we believe this can be attributed to QTM effect that is significant in the relaxation of magnetization for these compounds. We will continue our efforts to study these compounds, and current plans include high-field (HF) EPR studies in order to quantify the ZFS parameters for both compounds. Further, we have begun investigating the possibility of extending our findings to Fe(II) and examining whether our ligand systems could also lead to SMM behaviour. This work has been undertaken by a new graduate student in our group, Nastaran, who was successful in isolating a Fe(II) compound using the 2,6-bis{[2,6-di(isopropyl)phenyl)imino]benzyl}pyridine. The X-ray structure of this compound is shown in

Figure 6.1. This is a very exciting first step towards expanding our research on these systems and will aid in solidifying our understanding of the magnetic properties shown by our systems.

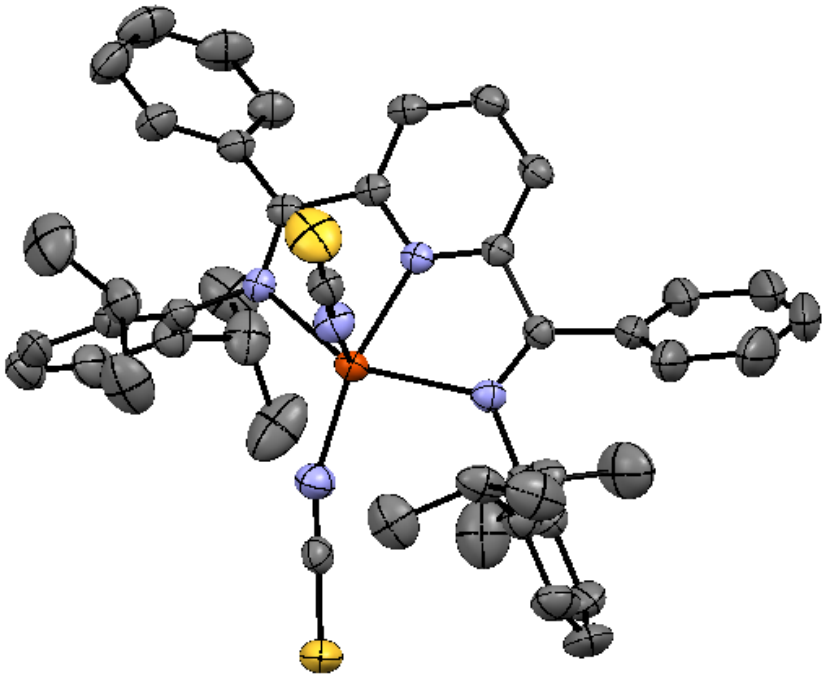

Figure 6.1. Structure and selected atom numbering scheme of [Fe[2,6-Bis{1-[(2,6-diisopropylphenyl)imino]benzyl}pyridine]$(NCS)_2$]. Hydrogen atoms and cocrystallized solvents omitted for clarity.

The field of molecular magnetism is still young and blossoming and continues to present scientists with numerous challenges. Although we now have a much clearer understanding of the fundamental concepts and mechanisms governing these magnetic behaviours, there is still much to be learned. This area of research will continue to challenge and fascinate us for many more decades to come.

For the purposes of this research project, I was involved in the literature review, synthesis and structural analysis of all ligands and compounds as well as writing up all

experimental procedures. The following non-refereed contributions presented and discussed this research project:

- Poster presentation entitled “Inducing a Solution-Phase, Single-Molecule Magnet with a Single Metal Center through Peripheral Ligand Modifications”. - Canadian Society for Chemistry 94th Canadian Chemistry Conference and Exhibition, Montreal, QC; 2011.

- Oral Presentation entitled “Inducing a Solution-Phase, Single-Molecule Magnet with a Single Metal Center through Peripheral Ligand Modifications”. - Ottawa-Carleton Chemical Institute Day, Ottawa, ON; 2011.

- Poster Presentation entitled “Synthesis and Magnetic Properties of Five-coordinate Cobalt Complexes of Bis(imino)pyridine and Bis(methyl)thiomethylpyridine Pincer Ligands.”. – 43rd Inorganic Discussion Weekend, Windsor, ON; 2010.

- Poster presentation entitled “Spin-Crossover Systems in a Dendritic Framework”. - Canadian Society for Chemistry 92nd Canadian Chemistry Conference and Exhibition, Hamilton, ON; 2009.

The following publication resulted from our research involving bis(imino)pyridine ligands in the synthesis of Co(II) SMMs:

- Titel Jurca, Ahmed Farghal, Po-Heng Lin, Ilia Korobkov, Muralee Murugesu*, and Darrin S. Richeson* ; “Single-Molecule Magnet Behavior with a Single Metal Center Enhanced through Peripheral Ligand Modifications”; J. Am. Chem. Soc., Article ASAP; Publication Date (Web): September 7, 2011; DOI: 10.1021/ja204562m

List of references

1. Kahn, O.; Molecular Magnetism (1993); VCH Publishers Inc.

2. (a) Gatteschi, D.; Sessoli, R.; Villain, J.; Molecular Magnets; Oxford University Press, Inc.; N.Y. (2006) (b) Murugesu, M.; Special Topics in Inorganic Chemistry: Molecular Magnetism (2009); Department of Chemistry; University of Ottawa

3. Morgenstern-Badarau, I.; Cocco, D.; Desideri, A.; Rotilio, G.; Jordanov, J.; Dupré, N.; J. Am. Chem. Soc (1998); 108; 300

4. (a) Bain, G. A.; Berry, J. F.; J. Chem. Ed. (2008); 85; 532. (b) Carlin, R. L.; Magnetochemistry (1986); Springer-Verlag: Berlin. (c) Drago, R. S. Physical Methods in Chemistry (1992); W. B. Saunders Company: Philadelphia.

5. Image retrieved from http://gravmag.ou.edu/mag_rock/mag_rock.html

6. *Curie–Weiss law: graphic representation*. Art. *Encyclopædia Britannica Online*. Web. 27 Jun. 2011. <http://www.britannica.com/EBchecked/media/1364/Plot-of-1chi>.

7. Gütlich, P; Goodwin, H. A.; Top. Curr. Chem. (2004); Vol. 233 Spin Crossover in Transition Metal Compounds I; Springer-Verlag; Berlin Heidelberg.

8. (a) Pauling, L.; J. Am. Chem. Soc. (1932); 54; 988. (b) Pauling, L; The Nature of the Chemical Bond, 2nd ed. (1940); Oxford University Press.

9. Cambi, L.; Szego, L.; Ber. Deutsch. Chem. Ges. (1931); 64; 167.

10. Pauling, L.; J. Am. Chem. Soc. (1937); 59; 633.

11. (a) Figgins, D. E.; Busch, D. H.; J. Am. Chem. Soc. (1960); 82; 820. (b) Robinson, M. A.; Curry, J. D.; Busch, D. H.; Inorg. Chem. (1963); 2; 1178.

12. Madeja, K.; Konig, E.; J. Inorg. Nucl. Chem. (1963); 25; 377.

13. Ewald, A. H.; Martin, R. L.; Ross, I. G.; White, A. H.; Proc. R. Soc. A. (1964); 280; 235.

14. Kahn, O.; Launay, J. P.; Chemtronics (1988); 3; 140.

15. Muller, R. N.; Elst, L. V.; Larent, S.; J. Am. Chem. Soc. (2003); 125; 8405.

16. Gütlich, P.; Garcia, Y.; Goodwin, H. A.; Chem. Soc. Rev. (2000); 29; 419.

17. (a) Lindoy, L. F.; Livingstone, S. E.; Coord. Chem. Rev. (1967); 2; 173. (b) Barefield, E. K.; Busch, D. H.; Nelson, Q.; Rev. Chem. Soc. (1968); 22; 457 (c) Martin, R. L.; White, A. H.; Transition Met. Chem. (1968); 4; 113.

18. Konig, E.; Kremers, S.; Theor. Chim. Acta (1971); 23; 12.

19. Reinen, D.; Friebel, C.; Propach, V.; Z. Anorg. Allg. Chem. (1974); 408; 187.

20. Chang, H-R; McCusker, J. K.; Toftlund, H.; Wilson, S. R.; Trautwein, A. X.; Winkler, H.; Hendrickson, D. N.; J. Am. Chem. Soc. (1990); 112; 6814.

21. Nihei, M.; Shiga, T.; Maeda, Y.; Oshio, H.; Coord. Chem. Rev. (2007); 251; 2606.

22. (a) Timken, M. D.; Abdel-Mawgoud, A. M.; Hendrickson, D. N.; Inorg. Chem. (1986); 25; 160. (b) Nishida, Y.; Oshio, S.; Kida, S.; Bull. Chem. Soc. Jpn. (1977); 50; 199. (c) Kennedy, B. J.; McGrath, A. C.; Murray, K. S.; Skelton, B. W.; White, A. H.; Inorg. Chem. (1987); 26; 483. (d) Oshio, H.; Maeda, Y.; Takashima, Y.; Inorg. Chem. (1983); 22; 2684. (e) Oshio, H.; Kitazaki, K.; Mishiro, K. J; Kato, N.; Maeda, Y.; Takashima, Y.; J. Chem. Soc. Dalton Trans. (1987); 1341. (f) Maeda, Y.; Tsutsumi, N.; Takashima, Y.; Inorg. Chem. (1984); 23; 2440.

23. Merrithew, P. B.; Rasmussen, P. G; Inorg. Chem. (1972); 11; 325.

24. Kunze, K. R.; Perry, D. L.; Wilson, L. J.; Inorg. Chem. (1977); 16; 594.

25. (a) Spiering, H.; Top. Curr. Chem. (2004); 235; 171; (b) Spiering, H.; Boukheddaden, K.; Linares, J.; Varret, F.; Phys. Rev. B (2004); 70; 184 (c) Spiering, H.; Meissner, E.; Koppen, H.; Muller, E. W.; Gütlich, P.; Chem. Phys. (1982); 68; 65.

26. Kahn, O.; Martinez, C. J.; Science (1998); 279;44.

27. Kahn, O.; Codjovi, E.; Garcia, Y.; van Koningsbruggen, P. J.; Lapuoyadi, R.; Sommier, L.; Molecule Based Magneic Materials; ACS Symposium Series (1996); 644; 44.

28. Juhász, G.; Hayami, S.; Sato, O.; Maeda, Y.; Chem. Phys. Lett. (2002); 364; 164.

29. Ryabova, N. A.; Ponomarev, V. I; Zelentsov, V. V.; Shipilov, V. I.; Atovmyan, L. O.; J. Struc. Chem. (1981); 22; 234.

30. Ritter, G.; Konig, E.; Irler, W.; Goodwin, H. A.; Inorg. Chem. (1978); 17; 224.

31. (a)Buchen, T.; Gütlich, P.; Inorg. Chem. (1994); 33; 4573 (b) Buchen, T.; Gütlich, P.; Sugiyarto, K. H.; Goodwin, H. A.; Chem. Eur. J. (1996); 2; 1134.

32. Hayami, S.; Maeda, Y.; Inorg. Chim. Acta (1997); 255; 181.

33. Moliner, N.; Gaspar, A. B.; Munoz, M.C.; Niel, V.; Cano, J.; Real, J. A.; Inorg. Chem. (2001); 40; 3986.

34. (a) Fréchet, J. M. J.; Tomalia, D. A.; Dendrimers and Other Dendritic Polymers (2000); VCH-Wiley: New York. (b) Narayanan, V. N.; Newkome, G. R.; Top. Curr. Chem. (1998); 197; 19. (c) Bosman, A. W.; Janssen, H. M.; Meijer, E. W.; Chem. Rev. (1999); 99; 1665. (d) Tomalia, D. A.; Aldrichimica Acta (2004); 37; 39.

35. (a) Serrette, A. G.; Swager, T. M.; J. Am. Chem. Soc. (1993); 115; 8879. (b) Lehmann, M.; Sierra, T.; Barber, J.; Serrano, J. L.; Parker, R.; J. Mater. Chem. (2002); 12; 1342. (c) Percec, V.; Johansson, G.; Heck, J.; Ungar, G.; Batty, S. V.; J. Chem. Soc., Perkin Trans. 1 (1993); 1411. (d) Percec, V.; Johansson, G.; Ungar, G.; Zhou, J.; J. Am. Chem. Soc. (1996); 118; 9855. (e) Percec, V.; Cho, W.-D.; Ungar, G.; Yeardley, D. J. P.; Chem. Eur. J. (2002); 8; 2011. (f) Percec, V.; Holerca, M. N.; Uchida, S.; Cho, W. D.; Ungar, G.; Lee, Y.; Yeardley, D. J. P.; Chem. Eur. J. (2002); 8; 1106.

36. (a) Percec, V.; Glodde, M.; Bera, T. K.; Miura, Y.; Shiyanovskaya, I.; Singer, K. D.; Balagurusamy, V. S. K.; Heiney, P. A.; Schnell, I.; Rapp, A.; Spiess, H.-W.; Hudson, S. D.; Duan, H.; Nature (2002); 417; 384. (b) Yamaguchi, T.; Ishii, N.; Tashiro, K.; Aida, T.; J. Am. Chem. Soc. (2003); 125; 13934.

37. (a)Schultz, L. G.; Zhao, Y.; Zimmerman, S. C.; Angew. Chem., Int. Ed. (2001); 40; 1962. (b) Kim, Y.; Mayer, M. F.; Zimmerman, S. C.; Angew. Chem., Int. Ed. (2003); 42; 1121.

38. Percec, V.; Dulcey, A. E.; Balagurusamy, V. S. K.; Miura, Y.; Smidrkal, J.; Peterca, M.; Nummelin, S.; Edlund, U.; Hudson, S. D.; Heiney, P. A.; Duan, H.; Magonov, S. N.; Vinogradov, S. A.; Nature (2004); 430; 764.

39. Landskron, K.; Ozin, G. A.; Science (2004); 306; 1529.

40. Newkome, G. R.; He, E.; Moorefield, C. N.; Chem. Rev. (1999); 99; 1689.

41. Hwang, S. H.; Shreiner, C. D.; Moorefield, C. N.; Newkome, G. R.; New J. Chem. (2007); 31; 1192.

42. Astruc, D.; Ornelas, C.; Ruiz, J.; Acc. Chem. Res. (2008); 41; 841.

43. (a)Balzani, V.; Ceroni, P.; Juris, A.; Venturi, M.; Campagna, S.; Puntoriero, F.; Serroni, S.; Coord. Chem. Rev. (2001); 219; 545. (b) Gorman, C. B.; Smith, J. C.; Acc. Chem. Res. (2001); 34; 60. (c) Casado, C. M.; Cuadrado, I.; Moran, M.; Alonso, B.; Garcia, B.; Gonzalez, B.; Losada, J.; Coord. Chem. Rev. (1999); 185-6; 53.

44. Balzani, V.; Campagna, S.; Denti, G.; Juris, A.; Serroni, S.; Venturi, M.; Acc. Chem. Res. (1998); 31; 26.

45. (a)Cuadrado, I.; Moran, M.; Casado, C. M.; Alonso, B.; Losada, J.; Coord. Chem. Rev. (1999); 193-5; 395. (b) Ong, W.; Gomez-Kaifer, M.; Kaifer, A.E.; Chem. Commun. (2004); 1677. (c) Kaifer, A. E.; Eur. J. Inorg. Chem. (2007); 5015.

46. (a) Oosterom, G. E.; Reek, J. N. H.; Kamer, P. C. J.; van Leeuwen, P. W. N. M.; Angew. Chem., Int. Ed. (2001); 40; 1828. (b) van Heerbeek, R.; Kamer, P. C. J.; van Leeuwen, P.

W. N. M.; Reek, J. N. H.; Chem. Rev. (2002); 102; 3717. (c) Kreiter, R.; Kleij, A. W.; Gebbink, R. J. M. K.; van Koten, G.; Top. Curr. Chem. (2001); 217; 163. (d) Astruc, D.; Chardac, F.; Chem. Rev. (2001); 101; 2991.

47. Fujigaya, T.; Jiang, D.-L.; Aida, T.; J. Am. Chem. Soc. (2005); 127; 5484.

48. (a) Sonar, P.; Grunert, C. M.; Wei, Y-L.; Kusz, J.; Gütlich, P.; Schlüter, A. D.; Eur. J. Inorg. Chem. (2008); 1613. (b) Wei, Y-L.; Sonar, P.; Grunert, M.; Kusz, J.; Schlüter, A. D.; Gütlich, P.; Eur. J. Inorg. Chem. (2010); 3930.

49. Aromí, G.; Brechin, E. K.; Struct. Bond. (2006); 122; 1.

50. Wang, X-Y.; Avendaño, C.; Dunbar, K. R.; *Chem. Soc. Rev.* (2011); **40**; 3213.

51. Caneschi, A.; Gatteschi, D.; Sessoli, R.; Barra, A.L.; Brunel, L.C.; Guillot, M.; *J. Am. Chem. Soc.* (1991); 113; 5873.

52. Lis, T.; Acta Cryst. Section B (1980); 36; 2042.

53. Aubin, S. M. J.; Wemple, M. W.; Adams, D. M.; Tsai, H-L.; Christou, G.; Hendrickson, D. N.; *J. Am. Chem. Soc.*, (1996); 118; 7746.

54. (a) Zhang, Y-Z.; Wernsdorfer, W.; Pan, F.; Wanga Z-M.; Gao, S.; Chem. Commun. (2006); 3302. (b) Jia, Q-X.; Tian, H.; Zhang, J-Y.; Gao, E-Q.; Chem. Eur. J. (2011); 17; 1040. (c) Tang, J.; Hewitt, I.; Madhu, N. T.; Chastanet, G.; Wernsdorfer, W.; Anson, C. E.; Benelli, C.; Sessoli, R.; Powell, A. K.; Angew. Chem. Int. Ed. (2006); 45; 1729.

55. Milios, C. J.; Vinslava, A.; Wernsdorfer, W.; Moggach, S.; Parsons, S.; Perlepes, S. P.; Christou, G.; Brechin, E. K.; J. Am. Chem. Soc. (2007); 129; 2754.

56. Tasiopoulos, A. T.; Vinslava, A.; Wernsdorfer, W.; Abboud, K .A.; Christou, G.; Angew. Chem. Int. Ed. (2004); 43; 2117.

57. Murugesu, M.; Habrych, M.; Wernsdorfer, W.; Abboud, K. A.; Christou, G.; J. Am. Chem. Soc. (2004); 126; 4766.

58. (a)Fernandez, J. F.; Luis, F.; Bartolome, J.; Phys. Rev. Lett. (1998); 80; 5659. (b) Bokacheva, L.; Kent, A. D.; Walters, M. A.; Polyhedron (2001); 20; 1717. (c) Wernsdorfer, W.; Bhaduri, S.; Tiron, R.; Hendrickson, D. N.; Christou, G.; Phys. Rev. Lett. (2002); 89; 197201.

59. Hendrickson, D. N.; Christou, G.; Ishimoto, H.; Yoo, J.; Brechin, E. K.; Yamaguchi, A.; Rumberger, E. M.; Aubin, S. M. J.; Sun, Z. M.; Aromí, G.; Polyhedron (2001); 20; 1479.

60. (a) Ishikawa, N.; Sugita, M.; Wernsdorfer, W.; J. Am. Chem. Soc. (2005); 127; 3650. (b) Jiang, S.-D.; Wang, B.-W.; Sun, H.-L.; Wang, Z.-M.; Gao, S.; J. Am. Chem. Soc. (2011); 133; 4730. (c) Li, D. P.; Wang, T. W.; Li, C. H.; Liu, D. S.; Li, Y. Z.; You, X. Z.; Chem. Commun. (2010); 46; 2929. (d) AlDamen, M. A.; Clemente-Juan, J. M.; Coronado, E.; Marti-Gastaldo, C.; Gaita-Arino, A.; J. Am. Chem. Soc. (2008); 130; 8874. (e) Rinehart, J. D.; Long, J. R.; J. Am. Chem. Soc. (2009); 131; 12558. (f) Jiang, S. D.; Wang, B. W.; Su, G.; Wang, Z. M.; Gao, S.; Angew. Chem. Int. Ed. (2010); 49; 7448. (g) Magnani, N.; Apostolidis, C.; Morgenstern, A.; Colineau, E.; Griveau, J.-C.; Bolvin, H.; Walter, O.;

Caciuffo, R.; Angew. Chem. Int. Ed. (2011); 50; 1696. (h) Rinehart, J. D.; Meihaus, K. R.; Long J. R.; J. Am. Chem. Soc. (2010); 132; 7572.

61. (a) Harman, W. H.; Harris, T. D.; Freedman, D. E.; Fong, H.; Chang, A; Rinehart, J. D.; Ozarowski, A.; Sougrati, M. T.; Grandjean, F.; Long, G. J.; Long, J. R.; Chang, C. J.; J. Am. Chem. Soc. (2010); 132; 18115. (b) Freedman, D. E.; Harman, W. H.; Harris, T. D.; Long, G. J.; Chang, C. J.; Long, J. R.; J. Am. Chem. Soc. (2010); 132; 1224.

62. Bedanta, S.; Kleemann, W.; J. Phys. D: Appl. Phys. (2009); 42; 13001.

63. Carlin, R. L.; Magnetochemistry (1986); Springer, Berlin.

64. Murrie, M.; Chem. Soc. Rev. (2010); 39; 1986.

65. Ako, M.; Hewitt, I. J.; Mereacre, V.; Clerac, R.; Wensdorfer, W.; Anson, C.E.; Powell, A.K.; Angew. Chem. Int. Ed. (2006); 45; 4926.

66. Krzystek, J.; Gregory, J. Y.; Park, J.-H.; Britt, R. D.; Weisel, M. W.; Brunel, L. C.; Telser, J.; Inorg. Chem. (2003); 42; 4610.

67. Cirera, J.; Ruiz, E.; Alvarez, S.; Neese, F.; Kortus, J.; Chem. Eur. J. (2009); 15; 4078.

68. Boca, R.; Coord. Chem. Rev. (2004); 248; 757.

69. Berreau, L. M.; Comm. Inorg. Chem. (2007); 28; 123.

70. Addison, A. W.; Rao, T. N.; Reedijk, J.; van Rijn, J.; Verschoor, G. C.; J. Chem. Soc. Dalton Trans. (1984); 1349.

71. Jolly, W. L.; The Synthesis and Characterization of Inorganic Compounds (1970); Waveland Press; Prospect Heights, IL.

72. (a) Vrieze, K.; van Koten, G.; Inorg. Chim. Acta (1985); 100; 79. (b) Knight, P. D.; Clarke, A. J.; Kimberley, B. S.; Jackson, R. A.; Scott, P.; Chem. Commun. (2002); 4; 352. (c) Clentsmith, G. K. B.; Gibson, V. C.; Hitchcock, P. H.; Kimberley, B. S.; Rees, C. W.; Chem. Commun. (2002); 14; 1498. (d) Sugiyama, H.; Gambarotta, S.; Yap, G. P. A.; Wilson, D. R.; Thiele, S. K.-H.; Organometallics (2004); 23; 5054. (e) Bruce, M.; Gibson, V. C.; Redshaw, C.; Solan, G. A.; White, A. J. P.; Williams, D. J.; Chem. Commun. (1998); 2523. (f) Nuckel, S.; Burger, P.; Organometallics (2001); 20; 4345. (g) Reardon, D.; Conan, F.; Gambarotta, S.; Yap, G.; Wang, Q.; J. Am. Chem. Soc. (1999); 121; 9318.

73. (a) Small, B. L.; Brookhart, M.; J. Am. Chem. Soc. (1998); 120; 7143. (b) Britovsek, G. J. P.; Gibson, V. C.; Kimberley, B. S.; Maddox, S. J.; Solan, G. A.; White, A. J. P.; Williams, D. J.; Chem. Commun. (1998); 849.

74. (a) Small, B. L.; Brookhart, M.; Bennett, A. M. A.; J. Am. Chem. Soc. (1998); 120; 4049. (b) Bennett, A. M. A.; DuPont; WO Patent (1998); 98/27124. (c) Britovsek, G. J. P.; Bruce, M.; Gibson, V. C.; Kimberley, B. S.; Maddox, P. J.; Mastroianni, S.; McTavish, S. J.; Redshaw, C.; Solan, G. A.; Strömberg, S.; White, A. J. P.; Williams, D. J.; J. Am. Chem. Soc. (1999); 121; 8728. (d) Britovsek, G. J. P.; Mastroianni, S.; Solan, G. A.; Baugh, S. P. D.; Redshaw, C.; Gibson, V. C.; White, A. J. P.; Williams, D. J.; Elsegood, M. R. J.; Chem. Eur. J. (2000); 6; 2221.

75. Bianchini, C.; Giambastiani, G.; Luconi, L.; Meli, A.; Coord. Chem. Rev. (2010); 254; 431.

76. (a) Jurca, T.; Korobkov, I.; Yap, G. P. A.; Gorelsky, S. I.; Richeson, D. S.; Inorg. Chem. (2010); 49; 10635 (b) Jurca, T.; Dawson, K.; Mallov, I.; Burchell, T.; Yap, G. P. A.; Richeson, D. S.; Dalton Trans. (2010); 39; 1266 (c) Jurca, T.; Lummis, J.; Burchell, T.; Gorlesky, S. I.; Richeson, D. S.; J. Am. Chem. Soc. (2009); 131; 4608.

77. (a) Bianchini, C.; Gatteschi, D.; Giambastiani, G.; Guerrero Rios, I.; Ienco, A.; Laschi, F.; Mealli, C.; Meli, A.; Sorace, L.; Toti, A.; Vizza, F.; Organometallics (2007); 26; 726. (b) Bianchini, C.; Mantovani, G.; Meli, A.; Migliacci, F.; Organometallics (2003); 22; 2545. (c) Sun, W.-H.; Tang, X.; Gao, T.; Wu, B.; Zhang, W.; Ma, H.; Organometallics (2004); 23; 5037. (d) Champouret, Y. D. M.; Fawcett, J.; Nodes, W. J.; Sing, K.; Solan, G. A.; Inorg. Chem. (2006); 45; 9890.(e) Barbaro, P.; Bianchini, C.; Giambastiani, G.; Guerrero Rios, I.; Meli, A.; Oberhauser, W.; Segarra, A. M.; Sorace, L.; Toti, A.; Organometallics (2007); 26; 4639. (f) Bianchini, C.; Giambastiani, G.; Guerrero Rios, I.; Meli, A.; Oberhauser, W.; Sorace, L.; Toti, A.; Organometallics (2007); 26; 5066.

78. APEX Software Suite v.2010; Bruker AXS: Madison, WI, 2005.

79. Bottaro, J. C.; Penwell, P. E.; Schmitt, R. J.; Synth. Comm. (1997); 27; 1465.

80. Pardin, C.; Roy, I.; Lubell, W. D.; Keillor, J. W.; Chem. Biol. Drug. Des. (2008); 72; 189.

81. Wu, P.; Feldman, A. K.; Nugent, A. K.; Hawker, C. J.; Scheel, A.; Voit, B.; Pyun, J.; Fréchet, J. M. J.; Sharpless, K. B.; Fokin, V. V.; Angew. Chem. Int. Ed. (2004); 43; 3928.

82. Feldman, A. K.; Colasson, B.; Fokin, V. V.; Org. Lett. (2004); 6; 3897.

83. Malkoch, M.; Schleicher, K.; Drockenmuller, E.; Hawker, C. J.; Russell, T. P.; Wu, P.; Fokin, V. V.; Macromolecules (2005); 38; 3663.

84. Baker, W.; Buggle, K. M.; McOmie, F. W.; Watkin; D. A. M.; J. Chem. Soc. (1958); 3594.

85. Canovese, L.; Chessa, G.; Marangoni, G.; Pitteri, B.; Uguagliati, P.; Visentin, F.; Inorganica Chimica Acta, (1991); 186; 79.

86. Fan, R.-Q.; Zhu, D.-S.; Mu, Y.; Li, G.-H.; Yang, Y.-L.; Su, Q.; Feng, S.-H.; Eur. J. Inorg. Chem. (2004); 4891.

87. Moses J. E.; Moorhouse, A. D.; Chem. Soc. Rev. (2007); 36; 1249.

88. Kolb, H. C.; Finn, M. G.; Sharpless, K. B.; Angew. Chem. Int. Ed. (2001); 40; 2004.

89. (a) Gokel, G.; Lüdke, G.; Ugi, I.; Isonitrile Chemistry (Ed.: I. Ugi); Academic Press, New York, (1971); pp. 145 -199; (b) Ugi, I.; Meyr, R.; Fetzer, U.; Steinbrückner, C.; Angew. Chem. (1959); 71; 386.

90. (a) Huisgen, R.; Angew. Chem. (1963); 75; 604; Angew. Chem. Int. Ed. Engl. (1963); 2; 565. (b) Huisgen, R.; Angew. Chem. (1963); 75; 742; Angew. Chem. Int. Ed. Engl. (1963); 2; 633.

91. (a) Rostovtsev, V. V.; Green, L. G.; Fokin, V. V.; Sharpless, K. B.; Angew. Chem. (2002); 114; 2708; Angew. Chem. Int. Ed. (2002); 41; 2596. (b) Tornoe, C. W.; Christensen, C.; Meldal, M.; J. Org. Chem. (2002); 67; 3057.

92. Binder, W. H.; Kluger, C.; Curr. Org. Chem. (2006); 10; 1791.

93. (a) Chan, T. R.; Hilgraf, R.; Sharpless, K. B.; Fokin, V. V.; Org. Lett. (2004); 6; 2853. (b) Candelon, N.; Lastécouères, D.; Diallo, A. K.; Aranzaes, J. R.; Astruc, D.; Vincent, J.-M.; Chem. Commun. (2008); 741.

94. Hawker, C. J.; Wooley, K. L.; Science (2005); 309; 1200.

95. Wu, P.; Feldman, A. K.; Nugent, A. K.; Hawker, C. J.; Scheel, A.; Voit, B.; Pyun, J.; Fréchet, J. M. J.; Sharpless, K. B.; Fokin, V. V.; Angew. Chem. (2004); 116; 4018; Angew. Chem. Int. Ed. (2004); 43; 3928.

96. (a) Diaz, D. D.; Punna, S.; Holzer, P.; McPherson, A. K.; Sharpless, K. B.; Fokin, V. V.; Finn, M. G.; J. Polym. Sci. Part A (2004); 42; 4392. (b) Helms, B.; Mynar, J. L.; Hawker, C. J.; Fréchet, J. M. J.; J. Am. Chem. Soc. (2004); 126; 15020. (c) Joralemon, M. J.; O'Reilly, R. K.; Hawker, C. J.; Wooley, K. L.; J. Am. Chem. Soc. (2005); 127; 16892. (d) Joralemon, M. J.; O'Reilly, R. K.; Matson, J. B.; Nugent, A. K.; Hawker, C. J.; Wooley, K. L.; Macromolecules (2005); 38; 5436. (e) Malkoch, M.; Schleicher, K.; Drockenmuller, E.; Hawker, C. J.; Russell, T. P.; Wu, P.; Fokin, V. V.; Macromolecules (2005); 38; 3663.

97. (a) van Steenis, D. J. V. C.; David, O. R. P.; van Strijdonck, G. P. F.; van Maarseveen, J. H.; Reek, J. N. H.; Chem. Commun. (2005); 4333. (b) Dichtel, W. R.; Miljanic, O. S.; Spruell, J. M.; Heath, J. R.; Stoddart, J. F.; J. Am. Chem. Soc. (2006); 128; 10388. (c) Zhu, Y.; Huang, Y.; Meng, W.-D.; Li, H.; Qing, F.-L.; Polymer (2006); 47; 6272.

98. (a) Astruc, D.; Ornelas, C; Ruiz, J.; Acc. Chem. Res. (2008); 41; 841. (b) Astruc, D.; Ornelas, C.; Aranzaes, J. R.; J. Inorg. Organomet. Polym. (2008); 18; 4.

99. (a) Klerman, Y.; Ben-Ari, E.; Yael Diskin-Posner, Y.; Leitus, G.; Shimon, L.; Ben-Davida, Y.; Milstein, D.; Dalton Trans. (2008); 3226. (b) Bassetti, M.; Capone, A.; Mastrofrancesco, L.; Salamone, M.; Organometallics (2003); 22; 2535. (c) Constable, E. C.; King, A. C.; Raithby, P. R.; Polyhedron (1998); 17; 4275.

100. Mabbs, F. E.; Machin, D. J.; Magnetism and Transition Metal Complexes (2008); Dover Publications.

101. Davidson, E. R.; MAGNET (1999); Indiana University: Bloomington, IN.

102. (a)Chirico, R. D.; Carlin, R. L.; Inorg. Chem. (1980); 19; 3031. (b) Hung, S.-W.; Yang, F.-A.; Chen, J.-H.; Wang, S.-S.; Tung, J.-Y.; Inorg. Chem. (2008); 47; 7202.

103. Luis, F.; Mettes, F.; Evangelisti, M.; Morello, A.; de Jongh, L. J.; J. Phys. Chem. Solids (2004); 65; 763.

104. (a) Wernsdorfer, W.; Bhaduri, S.; Boskovic, C.; Christou, G.; Hendrickson, D. N.; Phys. Rev. B (2002); 65; 180403. (b) Wernsdorfer, W.; Chakov, N. E.; Christou, G.; Phys. Rev. Lett. (2005); 95; 037203.

105. (a) Orbach, R.; Proc. R. Soc. London, Ser. A (1961); 264; 458. (b) Orbach, R.; Proc. R. Soc. London, Ser. A (1961); 264; 485.

106. Real, J. A.; Gaspara, A. B.; Munoz, M. C.; Dalton Trans. (2005); 2062.

107. Milios, C. J.; Piligkos, S.; Brechin, E. K.; Dalton Trans. (2008); 1809.